Remote sensing of Southern Ocean phytoplankton blooms in a warming world

Shinae Montie

Gateway Antarctica

College of Science

University of Canterbury

This thesis is submitted for the degree of Master of Antarctic Studies

February 2020

“With every drop of water you drink, every breath you take, you’re connected to the sea. No matter where on Earth you live.”

- Sylvia Earle, Oceanographer.

Declaration

This dissertation is the result of my own work and includes nothing, which is the outcome of work done in collaboration except where specifically indicated in the text. It has not been previously submitted, in part or whole, to any university of institution for any degree, diploma, or other qualification.

Signed: 

Date: 17/02/2020

Shinae Montie

Abstract

Marine phytoplankton are important ubiquitous phototrophs that play an essential role in biogeochemical cycles, mediate global climate, are at the base of food webs and fuel fisheries worldwide. Since 2006, ca. 60-90% of the increase in global ocean heat, associated with the burning of fossil fuels has occurred in the Southern Ocean (SO) alone. Being unicellular, short-lived and fast growing, phytoplankton can respond rapidly to changes in sea surface temperature (SST). Concurrent with long-term small increases in average SST, according to the latest IPCC Special Report on the Oceans and Cryosphere (2019), the more dramatic increases in short term warming events, that is marine heatwaves (MHWs), are very likely to also be attributable to global warming. Little is known about how oceanic warming coupled with MHWs will affect phytoplankton distribution and abundances in the SO. This research aims to address this research gap by quantifying the effects of SST anomalies and MHWs on chlorophyll-a (chl-a) concentrations, a proxy for phytoplankton biomass, using satellite measurements of ocean colour and remote sensing applications.

First, I correlated SST and chl-a anomalies on a pixel-by-pixel scale for the entire Ross Sea region of the SO over 20 years. The Ross Sea is the most productive region in Antarctica's coastal zone, accounting for ~30% of total annual primary production. Therefore, a recent observed decrease in chl-a in this region warranted further research scrutiny. Both positive and negative correlations between SST and chl-a anomalies were found. Based on Anova and post hoc Tukey tests, I found that correlations for different zones varied systematically across monthly, seasonal and annual timescales. Highly significant differences occurred between months and seasons, more specifically, between March and December, and autumn and summer, representing the coldest and warmest periods in the year accounted for during this study.

Second, I identified all extreme summer MHW events across the SO over a 16 year time period, and correlated the associated temperature anomalies to chl-a concentrations using a 'control vs. impact' experimental design. A relatively new MHW identification procedure, based on Hobday et al. (2016), was used to identify 19 events that could be analysed from remote sensing images. MHWs were here defined as anomalously warm events during which temperatures exceed the 90th percentile and persisted for >5 days, although my study focused only on 'extreme' summer MHWs where temperatures were four times higher than the 90th percentile of the climatological SST. Based on Anova and correlation analyses, I found that these extreme summer MHWs increased chl-a in the SO, and that this increase was stronger in regions that had lower sea surface temperatures and higher cover of winter ice.

The results outlined here suggest that a focus on average changes over long periods and over wide areas could overlook ecologically important short-term changes associated with anomalously short-term warming events, such as MHWs. These short-term events, superimposed on long-term climate changes, may eventually reach a tipping point in the SO with large-scale shifts to entire communities at the base of the food web. Therefore, it remains a fundamental challenge to understand and model variability in phytoplankton abundances and community structure. Furthermore, it is important that future research from the SO adopt this relatively new MHW approach to study phytoplankton dynamics and to ensure consistency within this rapidly expanding literature.

Acknowledgements

Since embarking on a career in polar science, the support that I have received has been incredible.

I would first like to thank Dr. Wolfgang Rack for allowing me to pursue a thesis driven solely by my passion for the Southern Ocean marine environment. Your technical support and countless hours spent discussing marine phytoplankton, despite our contrasting interests and backgrounds, has been invaluable. Thank you for making this project come to life and advancing my skills in remote sensing.

A huge thank you to Dr. Mads Thomsen for his continuous support, teaching and enthusiasm. I will forever be grateful that you came on board and supported me through such an exciting interdisciplinary project. Your knowledge of the marine environment, coupled with your willingness to provide feedback on all my writing has been second to none. Aside from your consistent academic support, you have been an excellent mentor during my undergraduate studies and time working for MERG. I look forward to our future collaborations.

I would like to thank Dr. Paul Broady for your insight into Southern Ocean processes and marine phytoplankton. Your level of enthusiasm, knowledge and support has unquestionably enhanced my learning. Thank you for being such a crucial element to the supervisory team.

Thank you to Dr. Matt Pinkerton for your advice and support during the first data chapter of this thesis. The data you made readily available, your expertise and the time you set aside since the Antarctic Science Conference has been greatly appreciated. I feel very privileged to have collaborated on this study and have hopes to work together in the future.

I am incredibly grateful of Dr. Mia Wege for her support during my statistical analyses. Your coding skills, patience and mentoring enhanced my understanding of basic R skills. It was a pleasure to work with you this year.

Thank you to Dr. Paul South for taking the time to read through the second data chapter of this thesis. Your constructive comments and suggestions were extremely helpful. I look forward to working together in the future.

I would like to thank the Ministry of Foreign Affairs and Trade for their generous scholarship support through the Gateway Antarctica's Ministry of Foreign Affairs and Trade Scholarship in Antarctic and Southern Ocean Studies.

To my former PCAS 2018/19 group, thank you for your friendship and support during this year. You were an incredible group to travel down to the ice with, those memories I will treasure forever. During my transition into the MASt you all maintained a high morale and constantly reminded me of my passion and why we do polar science!

Gateway Antarctica has been an extraordinary environment to work in. Thank you to all of my office mates, who have provided such a lively space to learn and work. To the staff of Gateway – Adrian, Andrea C., Andrea H., Carey, Daniela, Michelle L., Michelle R. F., Ursula and fellow students – Adele, Gabriela, Gemma, Rodrigo, Rose, Shanelle and Usama – You have all been incredible friends and colleagues.

On a more personal note, thank you to Liam, who has been the most supportive partner I could have ever wished for. Thank you for fuelling my passion to study, motivating me during the hard times, providing endless emotional support and constantly putting up with my science jargon. Your relentless love and loyalty has not gone unnoticed.

Finally to my family, Mum, Dad, Grandad and Ben – I could not have achieved any of this without your help. Thank you for your endless love, support and interest in my goals and passions.

Table of Contents

List of Tables

List of Figures

Figure 5.1. Comparison of the spatial and temporal resolution for data sets used in chapters three and four.

List of Abbreviations and Acronyms

ACC	Antarctic Circumpolar Current
AIC	Akaike Information Criterion
AMSR-E	Advanced Microwave Scanning Radiometer on the Earth observing system
AVHRR	Advanced Very High Resolution Radiometer
chl-a	Chlorophyll-a
chlor_a	MODIS Chlorophyll-a Concentration data product
CI	Hu Colour Index
CZ	Coastal zone
ENSO	El Niño Southern Oscillation
EPOC	ENVI Plugin for Ocean Colour
HDF	Hierarchical Data Format
IPCC	Intergovernmental Panel on Climate Change
MERIS	Medium-spectral Resolution Imaging Spectroradiometer
MHW	Marine heatwave
MIZ	Marginal Ice zone
Mod0	Null model
Mod1	Treatment model
MODIS	Moderate Resolution Imaging Spectroradiometer
Net CDF	Network Common Data Format
NIWA	National Institute of Water and Atmospheric Research
NOAA	National Oceanic and Atmospheric Administration
OCx	O'Reilly band ratio algorithm
OSSIT	Optimum Interpolation Sea Surface Temperature
POOZ	Permanently Open Ocean zone
ROI	Region of interest
RRS	Remote sensing reflectance

Rsr	Radiance reflectance
SAM	Southern Annular Mode
SAZ	Sub-Antarctic zone
SeaWiFS	Sea Wide Field-of-view
SO	Southern Ocean
SOCCOM	Southern Ocean Carbon, Climate Observations and Modelling
SSIZ	Seasonal Sea Ice Zone
SST	Sea surface temperature
WAP	West Antarctic Peninsula

List of Appendices

Chapter One

Introduction

The Earth's oceans are inhabited by more than two million species (Mora et al., 2011) represented by charismatic megafauna to microscopic unicellular algae. Unicellular algae are ubiquitous photoautotrophs of particular importance because they play an essential role in biogeochemical cycles and are at the base of food webs. Phytoplankton use light harvesting pigments such as chlorophyll-a for photosynthesis and, despite amounting to ~1% of global standing photosynthetic biomass, are responsible for ca. 50% of global primary productivity (Boyce, Lewis, & Worm, 2010; Cavicchioli et al., 2019; Frenger, Münnich, & Gruber, 2018; Marinov, Doney, & Lima, 2010; Petrou et al., 2016; Thomas, Kremer, Klausmeier, & Litchman, 2012; Worden et al., 2015).

Phytoplankton are vital in that they fuel fisheries worldwide (Dutkiewicz et al., 2019; Frenger et al., 2018). They also play a pivotal role in key biogeochemical processes such as the global carbon cycle (Mann & Lazier, 2006) as they fix inorganic carbon during photosynthesis (Marinov et al., 2010). For example, ca. 25-30% of anthropogenic CO_2 is taken up by oceans (Deppeler & Davidson, 2017). A proportion of the algae sink to the deep ocean and this drives the 'biological carbon pump'. This pump consists of export production from the photic zone to the deeper ocean and has the effect of reducing CO_2 concentration in surface waters and the atmosphere (Behrenfeld et al., 2006; Marchant, Davidson, & Wright, 2001). In deep water, organic carbon is re-mineralised into inorganic forms, which eventually return to the surface through upwelling processes. A small fraction of carbon bound in sinking phytoplankton and other detritus can become deeply buried in sediments and is then removed from the carbon-cycle for millions of years (Williams & Follows, 2011).

The Southern Ocean (SO) is ca. 20% of the area of the global ocean, but has a disproportional high amount of CO_2 uptake, accounting for ca. 40% (Arrigo et al., 2008). The SO also plays an important role in global ocean circulation, biogeochemical cycling of nutrients, climate regulation (Arrigo et al., 2008; Petrou et al., 2016) and in supporting a large biomass of phytoplankton, with strong spring and summer blooms (Llort, Lévy, Sallée, & Tagliabue, 2015).

The composition, functioning and structure of the SO marine ecosystem are strongly influenced by physical and climatic variability. Changes in sea surface temperature (SST), surface winds, light and nutrient availability are the main physical variables which influence biological processes (Alvain et al., 2013). Being short-lived and fast growing, phytoplankton can respond rapidly to any changes in the physical and chemical characteristics of their habitat (Feng et al., 2015; Maranón, Cermeno, Latasa, & Tadonléké, 2012; Trainer et al., 2019). It remains a fundamental challenge to understand variability in phytoplankton biomass on a regional scale and to relate changes in biomass to specific types of environmental

forcing, such as nutrient levels, salinity, grazing pressure and sea surface temperature (SST) (Behrenfeld et al., 2006).

It is widely known that SST and phytoplankton biomass are particularly strongly linked (Dunstan et al., 2018). Warming of the surface ocean is therefore likely to affect phytoplankton primary production both directly, by changing metabolic rates, and/or indirectly, for example by changing stratification and the mixed layer depth (Arrigo et al., 2008). In high latitude regions, where SST generally is below 14°C, the positive effects of increased SST on phytoplankton growth and biomass can often exceed negative effects (Feng et al., 2015) as also documented from the Arctic region (IPCC, 2019). Increased SST may therefore be of particular importance in regulating phytoplankton biomass and production in the SO.

Since 2006, it has been estimated that 60-90% of the increase in global ocean heat, associated with the burning of fossil fuels ('global warming'), has occurred in the SO alone (Deppeler & Davidson, 2017). The surface waters of the SO within and north of the Antarctic Circumpolar Current are warming at a rate of 0.1° – 0.2°C per decade. Surface waters south of this region are not warming at such a dramatic rate and some regions have been shown to be cooling (Sallée, 2018). The warming of most of the SO is likely to have profound impacts on microbial systems, with cascading effects on higher trophic level consumers, commercial fisheries and marine mammals and birds. Concurrent with these long term increases in average SST, more dramatic increases in short term warming, that is marine heatwaves (MHWs) and warm SST anomalies, are "very likely" (IPCC, 2019) to also be attributed to anthropogenic global warming. More specifically, MHWs have become more frequent, extensive and more intense over the last century (Frölicher, Fischer, & Gruber, 2018; Oliver et al., 2018; Smale et al., 2019). If phytoplankton abundance in the SO is not monitored, analysed and predicted in relation to short-term MHWs, the SO ecosystem and Antarctic marine living resources are at increasing risk of becoming compromised (Deppeler & Davidson, 2017).

Satellite measurements of ocean colour are indispensable remote sensing techniques for quantification of the abundance of phytoplankton (with correlations to primary productivity) on large scales. Satellite images can be used to correlate abundance with environmental conditions (Behrenfeld et al., 2006). Sensors aboard satellites, such as the Sea-Viewing Wide Field-of-View Sensor (SeaWiFS) and the Moderate Resolution Imaging Spectroradiometer (MODIS), have been particularly important in measurement of the concentration of chlorophyll-a (chl-a) and other algal pigments (Alvain, Moulin, Dandonneau, & Bréon, 2005). The blue-to-green ratio of water leaving radiance is used to estimate chl-a concentration using bio-optical algorithms and atmospheric correction methods (Alvain, Moulin, Dandonneau, & Loisel, 2008). Chl-a is the most important proxy for phytoplankton biomass because this pigment is present in all phytoplankton species (Alvain et al., 2005; Alvain et al., 2008). Due to the much higher spatial and temporal capabilities of satellites compared to the complexities of gathering *in situ* data from ships (Brewin et al., 2014), remote sensing of ocean colour is the principle source of data for assessing changes to phytoplankton biomass. Furthermore, sensors such as the Optimum Interpolation Sea Surface

Temperature (OISST) can estimate SST which can then be linked to changes in phytoplankton biomass and production (Volpe, Nardelli, Cipollini, Santoleri, & Robinson, 2012).

1.1. Aims, objectives and structure of this thesis

Surprisingly little is known about how ocean warming and increases in warm SST anomalies and/or MHWs will affect phytoplankton distribution and biomass in the SO. My research aims to address this research gap by quantifying the effects of SST anomalies on chl-a concentration using remote sensing techniques. First, I use an analytical approach by correlating SST and chl-a anomalies on a pixel-by-pixel scale for the entire Ross Sea region. In a second analysis, I identified all extreme summer MHW events (Hobday et al., 2018) in the SO over a 16 year period, and correlated the associated temperature anomalies to chl-a signals using a 'control vs. impact' experimental design.

More specifically, this project addresses five research questions:

1) Do monthly SST anomalies from 1998-2018 in the Ross Sea region correlate with chlorophyll-a concentration anomalies?
2) Do correlation levels vary between regions; more specifically between the coastal (>75°S), the transition (75°S - 70°S) and open ocean (70°S - 60°S) zones?
3) Do correlations for different zones vary systematically across monthly, seasonal and annual time scales and between El Niño and non-El Niño years?
4) Do extreme MHWs have an effect on chlorophyll-a concentration in the SO?
5) Do varying regions characterised by different sea surface temperatures and levels of winter ice cover modify the effect of extreme MHWs in the SO on chl-a concentrations?

The overall structure of the remainder of this thesis is as follows:

Chapter Two: *"Literature review"* reviews the literature on phytoplankton dynamics in the SO in the context of global warming, and highlights the expected increase in frequency and intensity of MHWs.

Chapter Three: *"Correlation analysis of sea surface temperature and chlorophyll-a concentration anomalies in the Ross Sea"* tests research questions 1-3.

Chapter Four: *"Marine heatwave remote sensing analysis in the Southern Ocean"* test research questions 4-5.

Chapter Five: *"Synthesis and conclusions"* compares and contrasts findings from chapters three and four within the context of the chapter two, the literature review.

Chapter Two

Phytoplankton, physical forces, climate change and oceanic heatwaves

Here I review phytoplankton biomass dynamics in the Southern Ocean. First, I describe 1) typical species and community composition, 2) ecosystem services and influence on SO biogeochemical cycling, and 3) the importance of phytoplankton in the SO food web. Second, the influence of physical variables on SO phytoplankton is addressed, including: 1) large scale climatic events, 2) upwelling, 3) fronts, gyres and currents, and 4) mesoscale eddies. Third, I describe the observed long-term effects of anthropogenic climate change on the SO and predicted ecological implications within four major zones in the SO; the sub-Antarctic zone (SAZ), the permanently open ocean zone (POOZ), the seasonal sea ice zone (SSIZ), and the coastal zone (CZ). Finally, I describe marine heatwaves and discuss impacts of these and climate changes on phytoplankton species and community composition in the SO.

2.1. Southern Ocean primary productivity

The SO is largely oligotrophic, i.e. with low biomass and productivity of phytoplankton (Smith, 1990). The oligotrophic status of the SO is typically attributed to light limitation caused by sea ice cover, and a constant dark winter, iron scarcity and high grazing pressure (Arrigo et al., 2008; Boyd et al., 2000; Coale et al., 2004; Martin et al., 2013). Nevertheless, large scale, but spatio-temporally patchy, phytoplankton blooms (Garrison, 2005; Smith, 1990) can extend over hundreds of square kilometres (Deacon, 1984; Llort et al., 2015; Sallée, Llort, Tagliabue, & Lévy, 2015; Smetacek & Nicol, 2005).

A recurrent seasonal phytoplankton bloom is typically initiated in spring when thermal stratification (i.e. followed by upwelling of nutrient rich waters) and daily irradiance increase. These changes typically occur when sea ice is lost through melting and/ or advection (Arrigo et al., 2008; Ji, Edwards, MacKas, Runge, & Thomas, 2010). SO phytoplankton species have evolved life history and behavioural strategies to exploit these favourable growth periods (Ji et al., 2010). Most phytoplankton species have rapid growth rates and large scale phytoplankton blooms can therefore develop in a few weeks (Antoine, Morel, Gordon, Banzon, & Evans, 2005). Concentrations of chl-a, a proxy for phytoplankton biomass, are often detected at low levels in September, with slow increases in early spring (October) (Arrigo & van Dijken, 2003; Cape, Vernet, Kahru, & Spreen, 2014) reaching peak concentrations in summer months and declining again to pre-bloom concentrations in March/April (Arrigo & van Dijken, 2003; Arrigo et al., 2008). The seasonal decline is caused by the formation of new sea ice, increased winds and storm intensity, reduced nutrient levels (nitrogen, phosphorus, iron and silicon for diatoms) and eventually, low light levels as the Antarctic winter approaches (Arrigo et al., 2008).

However, the described above seasonal changes to SO phytoplankton can vary between spatial zones. The highest concentrations of chl-a in the SO are associated with the coastal zone (CZ), 'polynyas' and the retreating sea ice margin. Polynyas are areas of open water surrounded by ice cover, which can be caused by latent heat (katabatic winds blowing in a persistent direction to push ice away from a barrier) or sensible heat (thermodynamically driven by upwelling of warm water keeping the surface water above freezing point). Polynyas are characterised by nutrient-enriched upwelled upper circumpolar deep water (Arrigo & van Dijken, 2003; Arrigo et al., 2008; Marchant et al., 2001; Smith & Barber; Stonehouse, 2002). Rates of primary productivity increase as much as ten-fold during the month of December in the CZ creating biological hotspots. By comparison, the lowest concentrations of chl-a are associated with pelagic waters north of the seasonal sea ice zone (SSIZ). The reason for this stark contrast can be attributed to elevated nutrient inputs, especially iron, from the Antarctic continental shelves and upwelling of circumpolar deep water in the CZ allowing for accumulation of phytoplankton biomass (Arrigo et al., 2008; Mann & Lazier, 2006).

2.1.1. Southern Ocean phytoplankton species and community composition

Phytoplankton are often grouped according to their cell size: picoplankton (0.2-2.0 μm), nanoplankton (2.0-20 μm), microplankton (20-200 μm), and mesoplankton (0.2-20mm) (Knox, 2007). SST is the most fundamental driver of phytoplankton metabolic processes that determine their biogeographical boundaries (Boyd et al., 2013). In the SO, picoplankton and nanoplankton compromise 10-20% and 25-75%, respectively, of the entire plankton communities (Hewes, 2009). Large-scale spring blooms are dominated by microplankton, including many diatoms, dinoflagellates, silicoflagellates and *Phaeocystis antarctica* (a haptophyte) (Alvain et al., 2005; Alvain et al., 2008; Knox, 2007). Dominant species include the diatoms *Nitzschia cylindricus* and *N. pseudonana,* although >100 species of diatoms and >60 species of dinoflagellates and silicoflagellates have been recorded from the SO (Knox, 2007; Stonehouse, 2002).

During the seasonal cycle there is a succession of phytoplankton species. *P. antarctica* contributes 20% of total chl-a in November and December as this species dominate in deep mixed-layers and the newly open CZ. However, when the surface waters become more stratified, diatoms become more dominant across the majority of the SO, contributing 50% of total chl-a in December and January (Alvain et al., 2008; Rohr, Long, Kavanaugh, Lindsay, & Doney, 2017; Tortell et al., 2008). Highest concentrations are found between the Polar Front and south of the Antarctic Circumpolar Current Front (see Figure 2.1) (Landry et al., 2002). Diatoms are generally 'r-strategists' exploiting high nutrient environments in the spring surface ocean (Marinov et al., 2010; Tréguer et al., 2018; Williams & Follows, 2011). Diatoms have several functional traits which favour them over the smaller size classes and enable large-scale blooms, including their high maximal nutrient uptake rate, ability to accumulate excess nutrients (Maranón et al., 2012), larger sizes that protect them against krill grazing (Maranón et al., 2012; Marinov et al., 2010), storage of fatty acids and oils enabling them to float in the water column (Garrison, Ellis, & National Geographic, 2018) and fast growth rates through asexual reproduction (Dutkiewicz, Scott, &

Follows, 2013; Townsend, 2012). Furthermore, their large size and dense silicon cell wall frustules facilitates high sinking rates and export of organic matter into deep water and eventually to accumulate in sediments more efficiently than any other size class. This plays an important role in various biogeochemical cycles (Alvain et al., 2013; Alvain et al., 2005).

2.1.2. Ecosystem services and influence on Southern Ocean biogeochemical cycling

Microbes make up 90% of marine biomass (Cavicchioli et al., 2019), support various ecosystem services and are vital for biogeochemical cycling of elements such as nitrogen, phosphorus, iron, zinc and copper (Alvain et al., 2005; Boyd et al., 2013). Globally, more than 100 million tons of carbon are fixed by phytoplankton each day (Behrenfeld et al., 2006). The sinking of this fixed carbon into the deep ocean and sediments is a fundamental mechanism for sequestering excess anthropogenic CO_2 from the atmosphere (Cape et al., 2014; Cavicchioli et al., 2019; Worden et al., 2015). However, there is little to no evidence that global productivity of phytoplankton and export into the deep ocean has increased over the last century. If the oceans continue to warm, phytoplankton productivity and export to deep water could be further restricted and less of the excess CO_2 will diffuse from the atmosphere to the ocean. The SO, in particular, can modify global climate mediation over glacial-interglacial cycles (Deppeler & Davidson, 2017; Tortell et al., 2008). Without the ~40% of CO_2 uptake that occurs in the SO alone, it is predicted that the concentration of atmospheric CO_2 would be ~50% greater than it currently is (Deppeler & Davidson, 2017). However, more recently Witze (2019) highlighted that certain areas within the SO could be net-sources of CO_2 particular during dark and cold winters

The efficiency of the Biological Carbon Pump is largely dependent on community composition and size of phytoplankton cells (Alvain et al., 2008). For example, large diatoms are more efficient at carbon transfer and export than smaller phytoplankton (Alvain et al., 2005). Diatom dominance in the SO during blooms, in part, explain why this region has a disproportionate effect on global conditions. Shifts in species and community composition is likely vulnerable to future climate change, and will in turn affect biogeochemical cycles (Alvain et al., 2013; Alvain et al., 2005). Given SO phytoplankton species play a pivotal role in oceanic, atmospheric and tropic processes, understanding their variability under a changing climate is essential (McClain, 2009; Petrou et al., 2016).

2.1.3. Phytoplankton and the Southern Ocean food-web

Phytoplankton form the base of the SO food-web which ultimately sustains highly diverse and iconic wildlife of Antarctica, including krill, penguins, seabirds, seals and whales (Deppeler & Davidson, 2017; Doney, 2010). Conceptually, two communities consume SO phytoplankton: 1) the microbial loop and 2) the classic “diatom-to-krill-to-whales” food chain (Hewes, 2009) (Figure 2.2). In part of the microbial loop dissolved organic carbon released from phytoplankton fuels the growth of archaea and bacteria, which are then consumed by protists, that through leaking and excretions, return carbon to the microbial food web (Deppeler & Davidson, 2017). The more classic “diatom-to-krill-to-whales” food

chain occurs throughout the entire SO with large spatial and temporal variability. At each transfer between trophic levels 80-90% of potential energy is lost as heat. The food chain begins with primary production (phytoplankton) which is consumed by grazing herbivores (primary consumers, e.g. copepods and krill), then eaten by carnivores (secondary consumers, like whales or small fish) and finally different types of apex predators (like birds, bigger fish, seals, sealions and dolphins) (Knox, 2007). More specifically, in the Ross Sea, blooms of diatoms dominated by *N. cylindricus* and *N. pseudonana* and *P. antarctica* is consumed by Crystal Krill, *Euphausia crystallorophias* and the Antarctic Silverfish, *Pleuragramma antarcticum* (Deppeler & Davidson, 2017). Antarctic krill species, such as *E. crystallorophias* and *E. superba* are versatile organisms that can withstand harsh environmental conditions. A range of predators from seals and whales, to fish and seabirds depend on krill as a food source (Smetacek & Nicol, 2005). Ultimately, phytoplankton that is not consumed by grazers or re-mineralised by bacteria sinks through the water column. These biogenic aggregates of often dead cells transport carbon to the deep ocean, where they can become buried and thereby removed from the carbon cycle (Deppeler & Davidson, 2017).

Climate change is increasingly affecting oceanic life. It is important to consider this "unseen majority" in climate change research, because microorganisms provide a direct food source or trophic linkages and modify biogeochemical cycling (Cavicchioli et al., 2019). Any change in community composition, species type, phenology of blooms and the ecological boundaries of SO phytoplankton will therefore affect higher trophic levels (Dutkiewicz et al., 2019; Li, Ji, Jenouvrier, Jin, & Stroeve, 2016). For example, the size structure of phytoplankton communities can affect the organisation of the pelagic ecosystem, and enhance organic matter production, and increase biological CO_2 drawdown. These changes can occur because larger cells absorb more light per unit of chlorophyll and have a higher sinking velocity compared to small cells (Maranón et al., 2012). Changes at the base of the food web attributed to climate change should therefore be studied further to understand the oceanic status in a warming world.

2.2. Influence of physical variables on phytoplankton

Physical variables unique to the SO result in regional responses that differ from global phytoplankton trends. The polar waters surrounding Antarctica can be extreme with regard to temperature, light levels, nutrient variability and presence of ice. However, many phytoplankton species have evolved physiological mechanisms to withstand these conditions (Boyd, 2019; Doney, 2010). Physical variables within the SO are influential on the distribution and concentration of phytoplankton. Large scale climatic variables, such as the Southern Annular Mode (SAM) and El Niño events, can trigger physical changes that affect phytoplankton dynamics (Alvain et al., 2013; Arrigo et al., 2008; Behrenfeld et al., 2006; Deppeler & Davidson, 2017; Petrou et al., 2016; Zhang et al., 2014). Furthermore, oceanographic and physical variables in the SO, such as upwelling (Boyce et al., 2010; Mann & Lazier, 2006; Moore & Abbott, 2000; Sokolov, 2008; Townsend, 2012), polar fronts and currents (Arrigo et al., 2008; Boyd et al., 2000; Garrison et al., 2018; Knox, 2007; Landry et al., 2002; Mann & Lazier, 2006; Moore & Abbott, 2000; Sokolov, 2008; D. N. Thomas, 2017; Townsend, 2012; Tréguer et al., 2018; Williams & Follows, 2011), and mesoscale

eddies and gyres (Deppeler & Davidson, 2017; Frenger et al., 2018; Garrison et al., 2018; Knox, 2007; Mann & Lazier, 2006; Williams & Follows, 2011) all affects phytoplankton ecology in the SO.

2.2.1. Large scale climatic variables: Southern Annular Mode and El Niño

The dominant climate pattern in the SO is the Southern Annular Mode (SAM). SAM is characterised by a north-south atmospheric pressure gradient and westerly winds. During SAMs 'positive' phase, pressures are low over Antarctica and high over Australia and New Zealand. Strong wind anomalies intensify divergence near the Antarctic Polar Front to increase upwelling of cooler, nutrient rich deep water (Arrigo et al., 2008). During the past 50 years, the SO has seen an increase in the positive phase of SAM, at least in part attributed to the depletion of the ozone layer over Antarctica and increased concentrations of greenhouse gases (Alvain et al., 2013; Deppeler & Davidson, 2017; Petrou et al., 2016). It has been suggested that the positive phase of SAM will continue to increase and the summer mixed layer deepen and cloud cover increase, and hereby result in a decline in phytoplankton biomass in the POOZ (Deppeler & Davidson, 2017). In contrast, as the westerly wind belt intensifies and moves south, enhanced upwelling at the Antarctic Slope Front will increase phytoplankton biomass in the SAZ (Deppeler & Davidson, 2017). A significant relationship also exists between the positive phase of SAM and decreased SO SST, particularly in the Ross Sea region (Arrigo et al., 2008). Furthermore, a positive SAM facilitate the dominance of large diatom species over smaller phytoplankton due to enhanced nutrient concentrations and upwelling induced by stronger and poleward shifted winds (Alvain et al., 2013).

El Niño events are another large-scale climatic variable that influences phytoplankton dynamics in the SO. El Niño events are characterised by warming of SST in the eastern tropical Pacific. The coupling between ocean and atmosphere is referred to as the El Niño Southern Oscillation (ENSO) (Liu et al., 2019). Phytoplankton growth rates and community composition in the SO is closely related to sustained periods of above average temperatures, conditions typical of El Niño events. Furthermore, El Niño transitions correlate with monthly anomalies of chl-a, that is, above average phytoplankton production, in part because upwelling with nutrient rich waters are more common (Behrenfeld et al., 2006; Hobday et al., 2018; Liu et al., 2019; Zhang et al., 2014).

2.2.2. Upwelling

Upwelling is a type of vertical current, typically characterized by high nutrient concentrations, that can facilitate high phytoplankton production (Boyce et al., 2010). Upwelling can be wind driven coastal Ekman processes or occur at oceanographic divergence zones (Townsend, 2012). Both types of upwelling occur in the SO. Upwelling zones are a source of nutrient rich, cooler, deep water that enters the epipelagic photic zone, and is therefore sometimes referred to as "the heart of the oceans productivity" (Townsend, 2012). These periods of high productivity are analogous to spring phytoplankton blooms. Upwelling provides ideal growth conditions when followed by calm high-light periods. During the calm

period, stratification in the water column develop due to warming of the surface waters and, if sea ice is melting, reduced salinity. This process facilitates phytoplankton growth and biomass accumulation within the shallow stratified upper layer. Upwelling can also, in some regions, be induced by complex topography that generate eddies and mesoscale activity, again causing plankton blooms that can extend for hundreds of kilometres downstream from the initial high topographic complexity (Mann & Lazier, 2006; Sokolov, 2008).

Coastal Ekman upwelling occurs when waves are generated by strong winds and the water is dragged along the surface as a current. This current is affected by the Coriolis force, resulting in net movement of surface water at right angles to the wind (Knox, 2007; Mann & Lazier, 2006). During Ekman transport, there is transfer of momentum between layers of moving water. The coriolis force deflects each successively deeper layer farther to the left (in the Southern Hemisphere), creating an Ekman spiral (Mann & Lazier, 2006; Townsend, 2012). When this process occurs away from a coast, surface waters move off-shore and are replaced by nutrient rich, cooler, deeper water. Thus, upwelling at the Antarctic Divergence is caused by Ekman drift driven by both easterly and westerly winds. Easterly winds close to the coast of the continent result in the 'East Wind Drift' current. The Coriolis force deflects this easterly current southwards towards the coast where it 'down wells'. Further north, westerly winds drive the Antarctic Circumpolar Current which is deflected towards the north (Knox, 2007). However, upwelling occurs where these two currents diverge, extending as far north as the Polar Front (Mann & Lazier, 2006).

2.2.3. Fronts and currents

The physics of the SO is strongly coupled with the distribution of blooms and dominant phytoplankton species (Tréguer et al., 2018). Oceanographic fronts are defined as the boundaries between regions of water largely characterised by their temperature and salinity conditions. The SO has several circumpolar fronts (Boyd et al., 2000). North of the SSIZ, frontal waters support higher rates of primary production than generally found in the SO. More specifically, phytoplankton blooms are typically facilitated where fronts interact with topography and when the divergence of currents brings nutrient rich water to the surface (Arrigo et al., 2008; Moore & Abbott, 2000). For example, the Polar Front (Figure 2.1), divides the SO into a sub- and full-Antarctic region, where its southern front is characterised by a sharp decline in SST that affect ecological boundaries of phytoplankton communities and prevents poleward introductions (Boyd, 2019; Knox, 2007; Stonehouse, 2002). The SO encompasses the Antarctic circumpolar current (ACC), one of the largest currents worldwide. The ACC is the only zonal current worldwide unobstructed by land, encircling the globe between 50° to 70° latitude (Knox, 2007). Although the surface speed of the ACC is weaker than western boundary currents, it is wider and less intensified at the surface (Williams & Follows, 2011). Importantly, the ACC is characterized by nutrient rich, cold, deep water upwelling to the photic zone and thereby stimulates high phytoplankton production, particularly in summer months when polar light conditions are optimal.

2.2.4. Mesoscale eddies and gyres

Mesoscale eddies dominate the kinetic energy spectrum in the oceans. These eddies have major effects on phytoplankton dynamics and are recognised as one of the most important drivers due to their spatio-temporal variance. In the Southern Hemisphere eddies can be anticyclonic, and these eddies cause upwelling of nutrient rich waters, enhance stratification, and create ideal conditions for phytoplankton blooms. Alternatively, eddies can also be cyclonic resulting in downwelling in their core. This type of eddy transports cool, low salinity water across the Polar Front and the Sub-Antarctic Front into the SAZ where intermediate waters forms and contribute to cooler and fresher SAZ waters (Deppeler & Davidson, 2017; Frenger et al., 2018). Local rates of growth and loss of phytoplankton biomass are strongly affected by these processes (Frenger et al., 2018). More specifically, an eddy is formed when currents of water adopt a circular or swirling motion. This is a general pattern of ocean flow, at the mesoscale they can be hundreds to thousands of kilometres wide, with a surface velocity of more than 30 cm per second (Knox, 2007; Williams & Follows, 2011). For example, western boundary currents in the SO can meander as they flow poleward, ultimately forming 'turbulent rings'. This turbulent motion can stimulate phytoplankton bloom formation, dominated by diatoms, because the turbulence counteracts the tendency for their dense silica cell wall to sink out of the photic zone (Mann & Lazier, 2006).

Similarly, gyres are larger system of circulating currents around the periphery of the ocean basins. Gyres are caused by wind patterns and the Coriolis Effect, planetary velocity along with vertical and horizontal friction (Knox, 2007). Gyres circulate water around the entire planet and are essential in regulating SST and nutrient concentrations. More specifically, two gyres circulate above the continental shelf in the SO; the Weddell Sea and Ross Sea gyres (Townsend, 2012; Williams & Follows, 2011). Although the ACC is a closed circuit, it is not technically a gyre because it does not flow around the periphery of an ocean basin. However, the ACC joins the southern-most extent of the major oceanic gyres of the South Atlantic, South Indian and South Pacific (Garrison et al., 2018; Knox, 2007).

2.3. Southern Ocean Climate Change

As greenhouse gasses continue to be released into the atmosphere, climate induced warming are expected to affect the SO ecosystems in the near-future (Petrou et al., 2016). For example, surface waters of the SO are predicted to become warmer, but also fresher, more stratified as sea ice thickness declines and more acidic as CO_2 concentrations increase (Tortell et al., 2008). These, often spatially heterogeneous, changes will differentially affect SST, salinity, irradiance and nutrient concentrations and will likely alter the function and structure of SO phytoplankton communities (Cavicchioli et al., 2019; Deppeler & Davidson, 2017; Petrou et al., 2016). Predicting the response of phytoplankton to climate change is further complicated because growth rates depend on multiple physical and environmental variables (Kirchman, Morán, & Ducklow, 2009; Marinov et al., 2010). Importantly, SST is likely the single strongest predictor of climate related changes to chl-a and phytoplankton productivity (Boyce et al., 2010), but its impact in the SO is yet to be determined. Globally in some

regions SST and phytoplankton productivity have been shown to correlate positively, whereas in other regions negative correlations have been found (Dunstan et al., 2018).

Several studies have discussed potential responses of SO phytoplankton to increased SST and possible cascading effects. There is general consensus among models that in the SO surface stratification is likely to increase. This will suppress vertical exchange of nutrients from the deep ocean and reduce mixed layer depths, resulting in reduced phytoplankton productivity (Arrigo et al., 2008; Bach, Riebesell, Sett, & Schulz, 2018; Behrenfeld et al., 2006; Ortiz-Ahumada, Álvarez-Borrego, & Gómez-Valdés, 2018). This will reduce the efficiency of the biological pump and removal of CO_2 from the atmosphere (Deppeler & Davidson, 2017). In a study by Boyce (2010) high latitude areas, south of 60 degrees, have shown the greatest decline in phytoplankton productivity (Boyce, 2010) with an estimated decline of -0.015 +/- 0.0016 mg/m^{-3} yr^{-1}. However, further work is needed to understand the complex oceanographic drivers of phytoplankton trends in the SO, because ocean warming has also been predicted to enhance phytoplankton growth in the SO region (Boyce, 2010).

Trends of increased SST enhancing phytoplankton productivity have already been reported from the Arctic Ocean. In polar waters the possible negative effects on phytoplankton growth are thought to be outweighed by the positive effects because growth is significantly constrained by light availability and deep mixing (Boyce et al., 2010; Rohr et al., 2017). Despite the fact increased SST can lead to lower nutrient concentrations and enhanced stratification, it can also lead to increased light availability and an extended growing season due to lower sea ice concentrations (Behrenfeld et al., 2006; Kirchman et al., 2009). This trend is evident in the southern West Antarctic Peninsula (WAP). The WAP has already experienced a transition from a cold-dry polar climate to a warmer maritime climate (Montes-Hugo et al., 2009). The ocean in the WAP has become warmer due to an increased supply of heat from the Upper Circumpolar Deep Water which is fed by the ACC. Consequently, sea ice retreat has occurred in areas previously covered all year round and this has produced more favourable conditions for phytoplankton growth in the southern region. Conversely, in the northern region of the WAP, waters are more open to the effects of strong winds and deep mixing, as they are mostly ice free in the summer. This has resulted in decreased productivity and shifted the community to a microbial food web (Montes-Hugo et al., 2009). Because phytoplankton growth and production can differ on regional scales future research should focus on these specific scales to gain greater understanding of phytoplankton dynamics.

2.3.1. Potential ecological implications in different Southern Ocean zones

It is important to consider regional variation associated with effects of climate change and increased SST in the SO. I have split the SO into four spatial zones as typically done in other studies (Deppeler & Davidson, 2017; Petrou et al., 2016); the Sub-Antarctic zone, permanently open ocean zone, seasonal sea ice zone and coastal zone. It is crucial to consider the primary physical constraints and typical community composition in accordance with each region whilst evaluating the effects of a warming SO on phytoplankton. The predicted effects

within and between each zone vary considerably, highlighting the need for more research in this area.

2.3.1.1. The sub-Antarctic zone (SAZ)

The Sub-Antarctic zone (SAZ) covers more than half of the SO. The SAZ includes the Polar Front, Sub-Antarctic Front and the Sub-Tropical Front (Figure 2.1) and forms a transitional boundary between the dominance of cocolithophores (that construct carbonate shells) to the north, and diatoms (with silicate tests) to the south (Deppeler & Davidson, 2017). It is predicted that waters of the SAZ will become warmer, more acidic and fresher and that storms and precipitation will increase in intensity and frequency (Deppeler & Davidson, 2017). Subsequently, the buoyancy of surface water is expected to increase stratification and reduce the depth of the mixed layer. These changes could reduce upwelling and transport of nutrient rich waters and thereby favour smaller phyto-flagellates and reduce primary production (Figure 2.3). However, alternatively, increases in SST and iron concentration in the SAZ (associated with more frequent and intense storms) could increase phytoplankton productivity and favour diatom species (if and where iron is the main limiting growth factor) (Hutchins & Boyd, 2016).

2.3.1.2. The permanently open ocean zone (POOZ)

The permanently open ocean zone (POOZ) is found between the Polar Front and the northern winter sea ice limit where it separates the warmer SAZ and cooler Antarctic waters. This region displays strong seasonality in biological production and contains a low phytoplankton biomass dominated by diatoms, nano-flagellates and pico-flagellates. Low production rates in this region are a result of deep mixing, low sun angles and nutrient limitation (Arrigo et al., 2008; Deppeler & Davidson, 2017). Climate change will likely cause a shift in the location and area of the POOZ. Its northern limit has shifted 60 km south from 1992 – 2017 (Deppeler & Davidson, 2017). Furthermore, the increased positive phase in SAM is likely to deepen the mixed layer over summer and increase cloud cover in this region. These changes may result in decreased light availability and therefore reduced productivity and biomass in the expanding POOZ (Figure 2.3). Alternatively, strong winds induced by positive SAM could bring nutrient-rich water to the surface. When light is not limited, high nutrient concentrations, coupled with incursions of warm core eddies from the Polar Front could result in localised phytoplankton blooms and favour large diatoms (Deppeler & Davidson, 2017).

2.3.1.3. The seasonal sea ice zone (SSIZ)

The seasonal sea ice zone (SSIZ) is defined as the region between the summer minimum and winter maximum of sea ice cover. This region has large seasonal changes in sea ice extent and concentration. Climate induced changes in the retreat and expanse of sea ice will strongly affect productivity in this region. While ice algae are not major contributors to SO primary production, changes to their blooms may restrict the availability of essential food sources for grazers such as krill and further modify the community composition in this

region (Deppeler & Davidson, 2017). The SSIZ also contains the highly productive marginal ice zone (MIZ), where pack ice transitions into open water. During early spring, the MIZ support large phytoplankton blooms, although changes in nutrient availability, temperatures and grazing rates will complicate predictions (Figure 2.3). Furthermore, phytoplankton dynamics are strongly associated with geographic differences in receding sea ice in the SSIZ (Montes-Hugo et al., 2009) so that expansion of the POOZ into the SSIZ will most likely alter the magnitude, duration and timing of phytoplankton blooms in this zone (Deppeler & Davidson, 2017).

2.3.1.4. The coastal zone (CZ)

The coastal zone (CZ) borders the Antarctic continent. The CZ is the smallest zone but also the most productive per unit area. The high productivity in the CZ is related to high nutrient concentrations, including iron enrichment from coastal sediments, and enhanced light availability in polynyas (Deppeler & Davidson, 2017; Feng et al., 2015; Petrou et al., 2016). Climate change is expected to slightly increase SST and productivity in this zone. However, melting ice shelves and lowered surface salinity could result in increased stratification and therefore faster nutrient depletions. Furthermore, localised shifts in community composition could result in a shift from large to small cells in more northern CZs such as the northern WAP, potentially decreasing carbon export to the deeper ocean (Deppeler & Davidson, 2017) (Figure 2.3).

2.4. The most extreme marine heatwaves

Global warming causes slow increases in average temperature around the world, including the SO. However, superimposed on slow long-term increases in mean temperature, are more dramatic short-term and more localized increases in temperature (= warm anomalies = marine heatwaves; MHWs). Without the assessment of such short-term MHWs, many changes to phytoplankton communities on regional and local scales could be overlooked (Dunstan et al., 2018). More specifically, MHWs are defined as anomalously warm events during which temperatures exceed the 90^{th} percentile of the 30 year climatic mean and persist for >5 days. Periods between MHWs of <2 days are considered a continuous event (Frölicher et al., 2018; Hobday et al., 2016; Hobday et al., 2018; Jones et al., 2019; Smale et al., 2019; Thomsen et al., 2019). This qualitative definition does not assume any particular drivers or impacts and accounts for specific regional and local ranges of SST. Multiples of this difference define four categories of extremity based on the intensity of a MHW event: 1) moderate (1-2 x 90^{th} percentile), 2) strong (2-3 x 90^{th} percentile), 3) severe (3-4 x 90^{th} percentile) and 4) extreme (>4 x 90^{th} percentile). This classification system uses the maximum and cumulative intensity to categorise the overall event after a MHW event has subsided, as done for tropical cyclones and earthquakes (Figure 2.4) (Hobday et al., 2018). Today, 87% of MHWs have been attributed to anthropogenic climate change and there is strong evidence to suggest that MHWs will become more frequent, extensive and intense (Frölicher et al., 2018; Hobday et al., 2016; Hobday et al., 2018; Oliver et al., 2018; Smale et al., 2019). For example, MHW intensity in the world's oceans has increased by 65% from 1982-2016 (Figure 2.4) (Oliver et al., 2018). In comparison to heatwaves on land, we know

much less about their formation in the ocean and their impact on marine life (Frölicher et al., 2018).

MHWs can have major consequences for ecosystems, species ranges, cause local extinctions, and affect biodiversity and regional fisheries (Frölicher et al., 2018; Hobday et al., 2016; Holbrook et al., 2019; Smale et al., 2019). More specifically, MHWs have resulted in sustained loss of kelp forests (Thomsen et al., 2019; Wernberg et al., 2016), coral bleaching (Hughes et al., 2017), reduced concentrations of surface chl-a (Bond, Cronin, Freeland, & Mantua, 2015; Gómez-Ocampo, Gaxiola-Castro, Durazo, & Beier, 2018; Hobday et al., 2018), mass mortality of invertebrates through heat stress (Garrabou et al., 2009; Oliver et al., 2017), species range shifts and changes to community composition (Cavole et al., 2016; Oliver et al., 2017; Wernberg et al., 2016), closure of fisheries (Caputi et al., 2016; Cavole et al., 2016; Oliver et al., 2017) and intensified economic tensions (Oliver et al., 2018). Such dramatic effects typically occur when species living near their upper thermal tolerance levels are exposed to MHWs – where they may respond to elevated temperatures after as little as a few days. These impacts will often last beyond the duration of the MHW event. Some of the most intense ecosystem changes have been attributed to 'extreme' MHWs (Oliver et al., 2018).

MHWs at higher latitudes such as in the SO are characterised by shifts in warmer ocean currents, ocean – atmosphere interactions and mesoscale eddy activity (Holbrook et al., 2019). These impacts have been suggested to alter phytoplankton dynamics and growth in the SO. Although surface waters in the SO are projected to remain relatively cool and the frequency of MHWs may actually decrease at times poleward of 50° South, it is nevertheless important to study MHWs in the SO (Frölicher et al., 2018; Oliver et al., 2018) because short term extreme events, superimposed on incremental global warming have the capacity to reach a tipping point with community wide phase shifts.

2.4.1. Impacts on Southern Ocean phytoplankton species and community composition

Phytoplankton in the SO are psychrophilic, that is, they are cold adapted species that grow and reproduce at low temperatures. Surface waters in the SO vary from -1.8°C in northern regions but can increase to 4°C in the summer months (Cavicchioli, 2016; Knox, 2007). It has been predicted that the average SST in the SO, by 2100, will increase by 1.5°C (Boyd, 2019). However, short term (extreme) MHWs in the SO can be of similar magnitudes (see Chapter 4), on average increasing SST by 2.61°C and, in some cases, lasting for >100 days. I identified 28 research papers that have linked MHWs to phytoplankton production (Barber & Chavez, 1983; Barber et al., 1996; Bond et al., 2015; Chavez et al., 1999; De Bernardi, Ziveri, Erba, & Thunell, 2005; Fiedler, Methot, & Hewitt, 1986; Furnas, 2007; Gómez-Ocampo et al., 2018; González, Ortiz, & Sobarzo, 2000; González, Sobarzo, Figueroa, & Nöthig, 2000; N. M. González et al., 2000; Harris, Varela, Whitney, & Harrison, 2009; Hereu, Lavaniegos, Gaxiola-Castro, & Ohman, 2006; Iriarte & González, 2004; Jacox et al., 2016; Jiménez-Quiroz et al., 2019; Kahru & Mitchell, 2000, 2002; Lipsen, Crawford,

Gower, & Harrison, 2007; Macfarlane, Ralston, Royer, & Norton, 2005; Ortiz-Ahumada et al., 2018; Peterson, Keister, & Feinberg, 2002; Piontkovski et al., 2010; Putt & Prézelin, 1985; Torres-Moye & Alvarez-Borrego, 1987; Yang, Emerson, & Peña, 2018). However, although MHWs are clearly emerging as a strong driver of phytoplankton production, all these analyses were done in tropical and temporal to cold waters (Figure 2.5). Or, in other words, no research has, to my knowledge, yet quantified impacts from MHWs on polar phytoplankton communities and primary production (i.e., >60° latitude, see Figure 2.5)

Temperature change is a principal physical driver in the SO and has been found to cause species-specific increases and/or decreases in growth rates and shifts in community composition. Temperature change may thereby modify competitive interactions, with consequences for the entire SO food web (Marchant et al., 2001). Monitoring changes to SO phytoplankton dynamics in a warming world is vital, because phytoplankton provide the base of the marine food web and they regulate climate regulation, biogeochemical cycling and support commercial fisheries (Bach et al., 2018; Dutkiewicz et al., 2013). However, complex interactions and feedback mechanisms in the marine environment make quantifying ecosystem change extremely challenging (Petrou et al., 2016). For example, warmer, more stratified waters will allow new phytoplankton species to colonise and outcompete those that are currently abundant. Furthermore, species ranges may increase, decrease and/or shift poleward (Dutkiewicz et al., 2019; Dutkiewicz et al., 2013; Thomas et al., 2012). For example, in the southern sub-region of the WAP there has been a poleward shift of large-celled diatom species, in part because the summer sea ice extent has decreased. By comparison, the northern sub-region of the WAP has experienced a decline in local species ranges and dominance has shifted to a microbial food-web (Montes-Hugo et al., 2009). The outcome of a 1.5°C increase in average temperatures by 2100, is expected to increase dominance warmer water species over much of SO (Boyd, 2019), whilst restricting currently dominant species to the most southern waters (Petrou et al., 2016). Warmer waters will likely also increase dispersal and colonization of warmer-water grazer communities, with unknown effect on the SO food web (Deppeler & Davidson, 2017).

Several studies have incorporated remote sensing, modelling and laboratory experiments on SO phytoplankton to better understand how increasing temperature will affect plankton communities in the future. Most of these studies suggest that the SO will experience increased phytoplankton production and diatom biomass (Bach et al., 2018; Boyd et al., 2013; Montes-Hugo et al., 2009; Petrou et al., 2016; Tréguer et al., 2018). Two studies have, in particular, focused on temperature effects on SO diatoms (Boyd et al., 2019; Petrou et al., 2016). For example, a 3°C increase in ambient temperature resulted in a 25% increase in growth of *Proboscia inermis* whereas higher temperatures caused a rapid decline in productivity. This suggests that at least some polar diatoms have low maximum temperature tolerances, and highlights a lack of oceanic refugia in a future warmer. Thermal tolerance curves have also been measured under laboratory conditions for five bloom-forming polar phytoplankton species that are common in the SO (the diatoms *Chaetoceros neglectus, Pseudonitzschia* sp., *Proboscia* sp. and *Nitzschia stellata,* and the picoplankton species *P. Antarctica*) (Boyd, 2019). In this study all tests species would grow faster in warmer waters

(Figure 2.6) although some researchers argue that thermal preference curves and temperature–dependent growth rates can be misleading (Cavicchioli, 2016; Cavicchioli et al., 2019). For example, the upper temperature limit (Tmax) and optimal limit (Topt) for growth is typically interpreted as the 'best' temperature for an organism, even though other studies questions if maximum growth necessarily reflect optimal competitive ability (in part because other factors affect competitive ability) (Cavicchioli, 2016; Cavicchioli et al., 2019). Thus, little is known about which phytoplankton species may replace current species in the SO, although it is likely that entire groups, such as cocolithophores, will decrease in abundance south of 60° when SST drops below 4°C. Overall, an increase in SST of 1.5°C by 2100 in the SO, combined with superimposed more frequent and stronger MHWs, will likely have dramatic impact on phytoplankton dynamics with shifts in community composition and cascading impacts on food webs and biogeochemical fluxes in the SO (Boyd et al., 2013; Marchant et al., 2001).

2.4.2. Implications for the Southern Ocean food-web

Climate change may result in warmer ocean temperatures and more frequent and intense MHWs. Consequently, poleward range shifts and change in community composition at the bottom of the SO food web are expected, with likely cascading impacts on the entire ecosystem. First, changes to phytoplankton community structure through southward relocation and increased cell size will likely affect the coupling between production and heterotrophic microorganisms, as well as, the biogeography of microbial species (Kirchman et al., 2009; Montes-Hugo et al., 2009). The change in cell size is also predicted to affect grazing by herbivores, such as krill, that primarily feed on nano- and microplankton (Wright et al., 2009). In addition, the recruitment success of krill depend on the synchronisation of seasonally pulsed phytoplankton production (Ji et al., 2010). Krill are a crucial link to higher trophic levels, including fish, seals, whales, penguins and other seabirds, and any changes to their abundances would have dramatic impact on higher trophic levels (Jones et al., 2019; Montes-Hugo et al., 2009; Schofield et al., 2010). For example, in the northern sub-region of the WAP, biogeographic shifts has been driven by changes at the base of the food web (Montes-Hugo et al., 2009). More specifically, local environmental drivers, in particular increased SST, have caused southward relocation of krill and reduced local biomass in the more northern region. This change was followed by salps replacing krill species in the northern WAP and reduced the populations of *Pleuragramma antarctica* (silverfish) and *Pygoscelis adeliae* (Adélie penguins), yet has favoured other species such as *Electrona antarctica* (lanternfish)*, P. papua* (Gentoo penguin) and *P. antarcticus* (Chinstrap penguin). Overall, this example highlights that effect of climate change will be complex and in turn will produce both new "winners and losers" at the regional level.

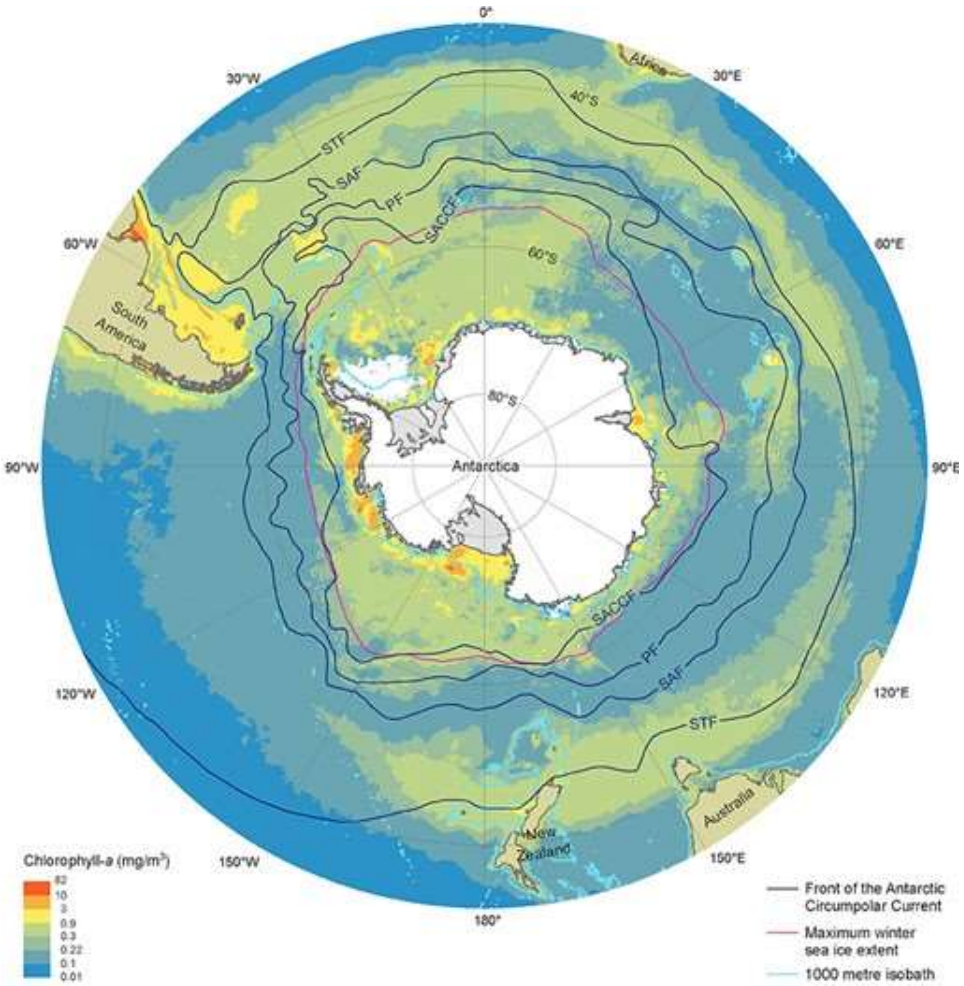

Figure 2.1. Map of the Southern Ocean outlining key fronts and the maximum winter sea ice extent. The blue lines indicate the four fronts: Sub-Tropical (STF), Sub-Antarctic (SAF), Polar (PF) and Southern Antarctic Circumpolar Current (SACCF). The pink line indicates the winter sea ice maximum. Figure derived from Deppeler & Davidson (2017), permission granted under the Creative Common License see: https://creativecommons.org/licenses/by/4.0/.

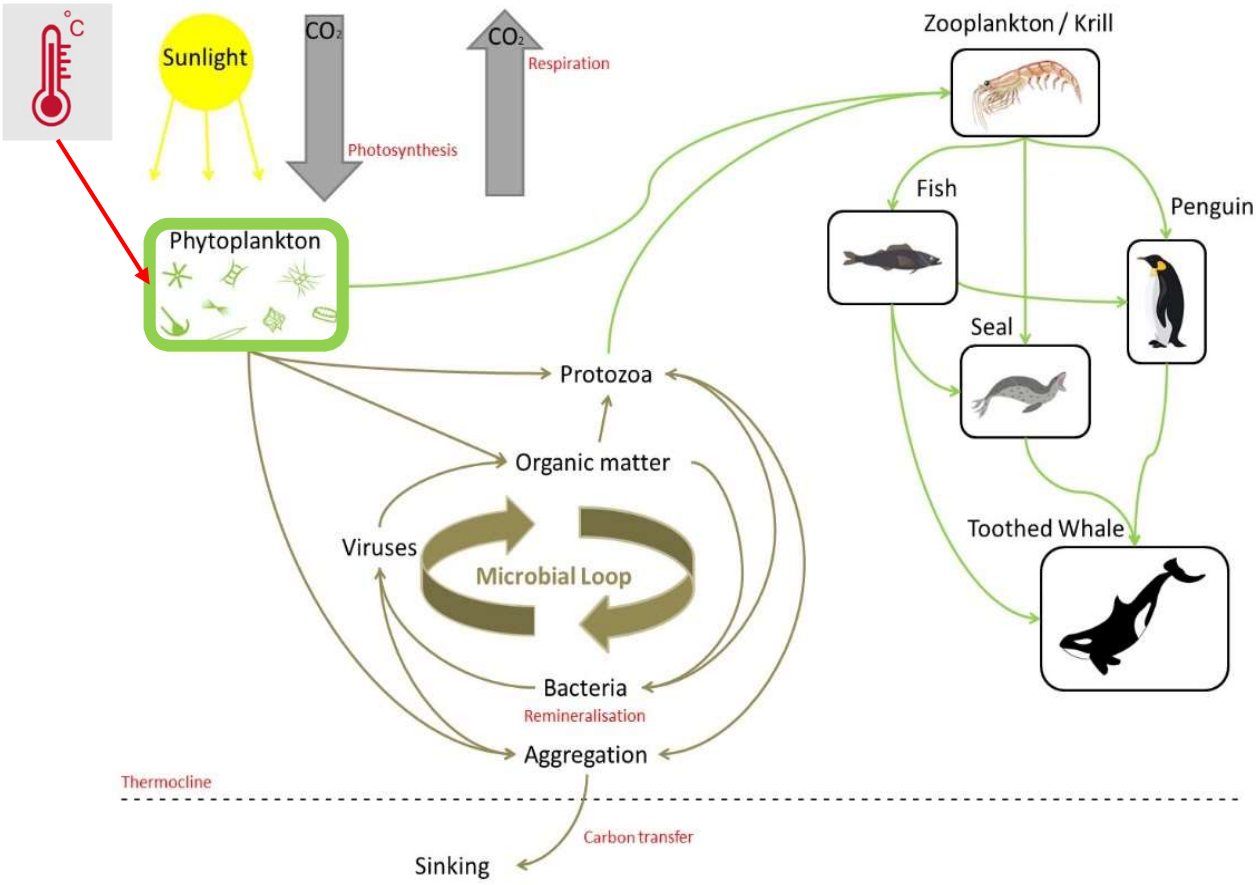

Figure 2.2. Diagram showing how phytoplankton control both (a) the microbial loop community (brown lines) and (b) the 'classic' Southern Ocean food-chain (green lines) with zooplankton, krill, fish, penguins, seals and toothed whales. Processes driving carbon transfer to the atmosphere, higher trophic levels and flux to the deep ocean are in red.

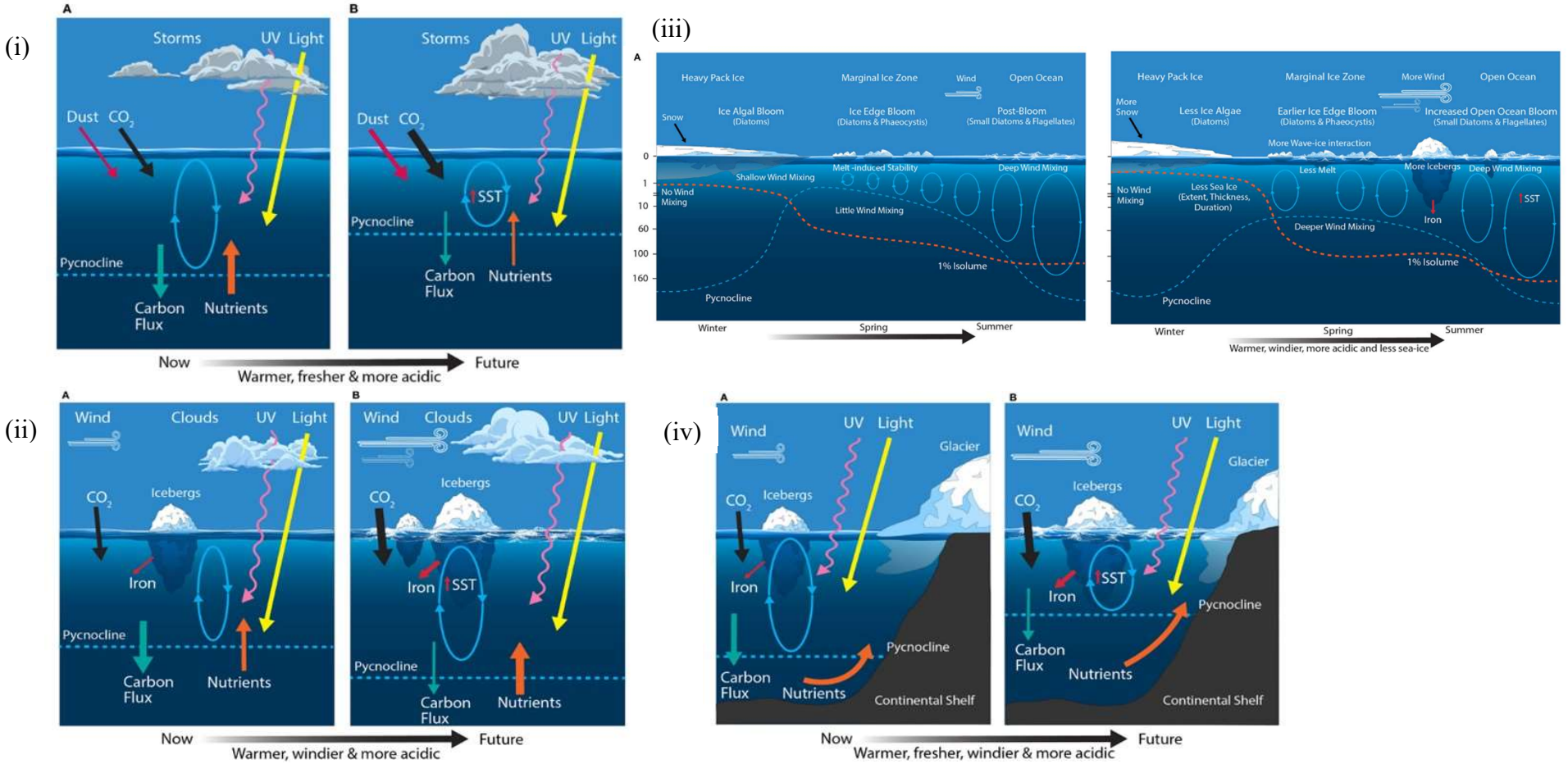

Figure 2.3. The primary physical constraints on phytoplankton in (i) the Sub-Antarctic Zone (SAZ), (ii) the Permanently Open Ocean Zone (POOZ), (iii) in the Seasonal Sea Ice and Marginal Ice Zones (SSIZ and MIZ), and (iv) in the Continental Shelf Zone (CSZ), before (A) and after (B) climate changes. Ovals represent the depth of mixing and arrow thickness reflects relative rates of flux. SST denotes sea surface temperature. The blue dashed line shows the location of the pycnocline. The red dashed line shows the depth for 1% surface irradiance. SST, sea surface temperature. Schematic from Deppeler & Davidson (2017), permission granted under the Creative Common License see: https://creativecommons.org/licenses/by/4.0/

(a)

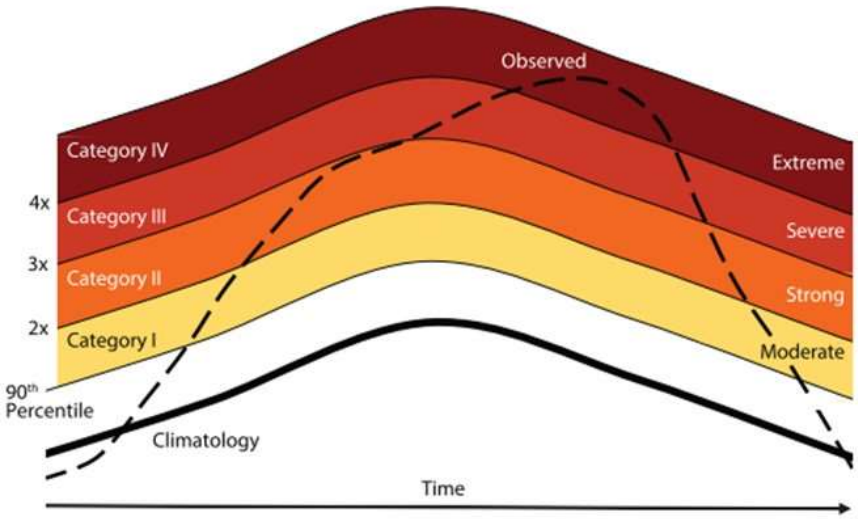

(b)

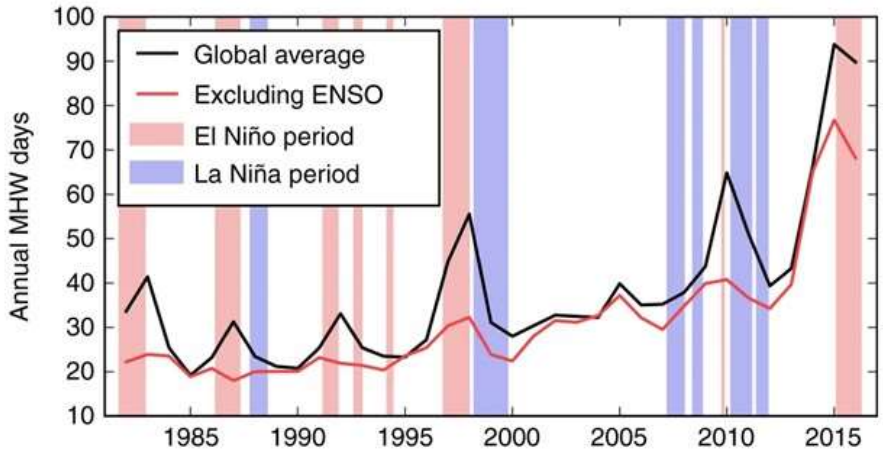

Figure 2.4. (a) Categorisation of MHWs. The dashed line depicts the observed temperature time series, the bold line depicts the long-term regional climatology and the thin lines depict the 90th percentile climatology. Multiples of the difference between the climatology and 90th percentile (2x, 3x and 4x) define each of the categories (moderate, strong, severe and extreme). This example shows an event that peaks as an extreme MHW. Taken from Hobday et al. (2018), copyright permission requested and pending. (b) How MHWs have changed over time using a global averaged time series of total MHWs from 1982 – 2016 derived from the NOAA OISST data product. The black line depicts the averaged time series and the red line depicts the metric after removing the effect of ENSO. Red shading indicates periods of El Niño and blue shading indicates periods of La Niña. Figure derived from Oliver et al. (2018), copyright permission requested and pending.

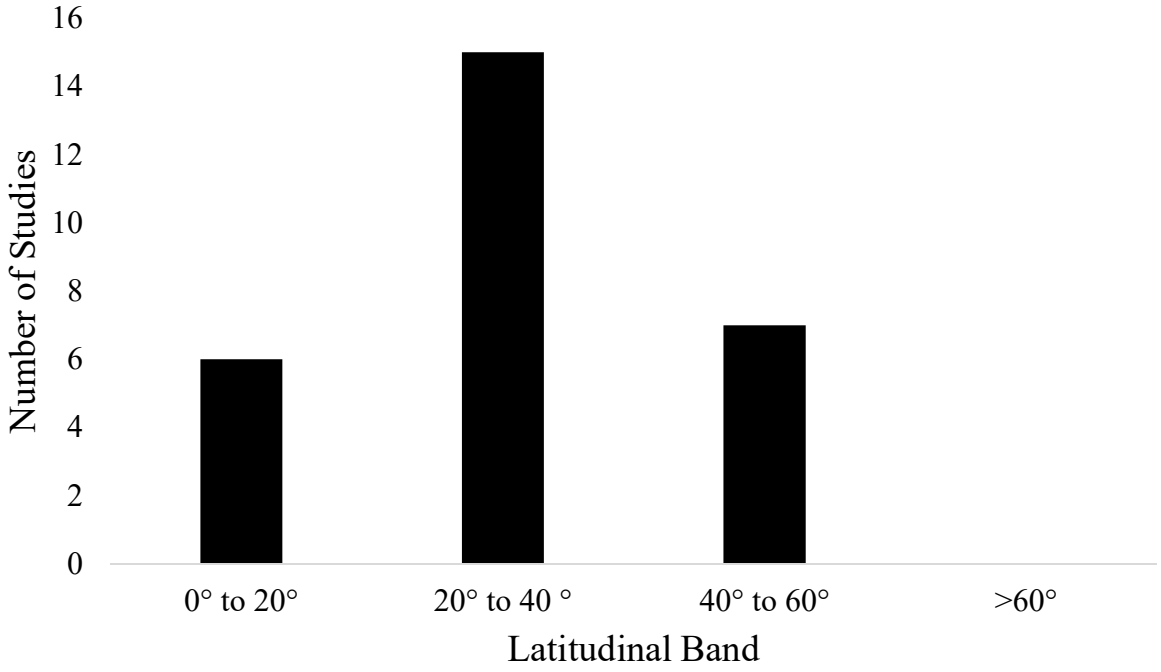

Figure 2.5. Documented effects between MHWs and phytoplankton and/or chlorophyll-a concentration in 28 peer reviewed research papers, found using Scopus (provided by Elsevier), grouped into 4 latitudinal bands. Note the absence of data from polar regions (>60°).

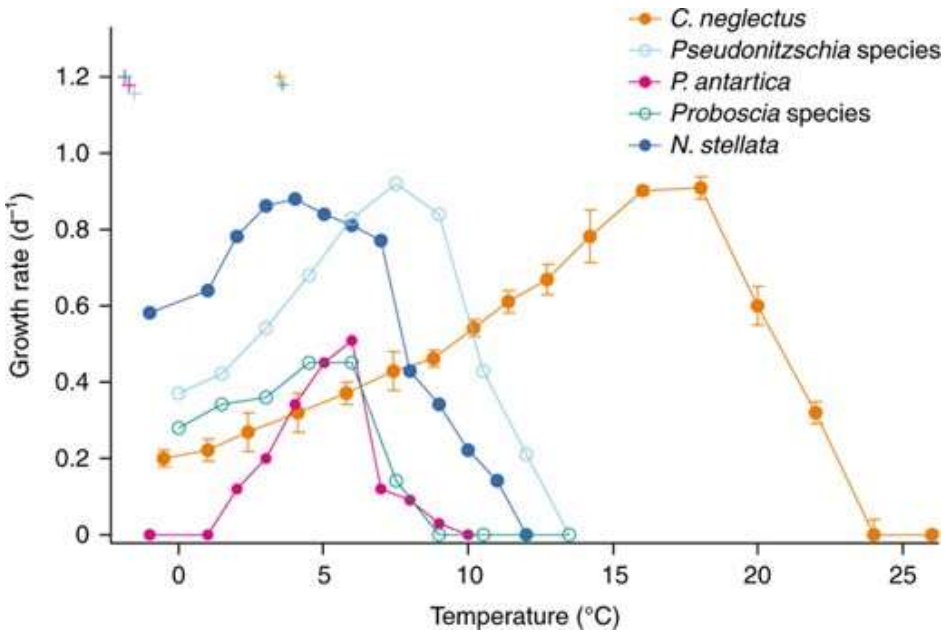

Figure 2.6. Thermal performance curves for five common diatom species; *C. neglectus, Pseudonitzschia sp., Proboscia sp. and N. stellate* and for *P. antarctica* (*P.* antarctica in the figure key). The x axis is scaled to − 1.8 °C, i.e., the temperature at which seawater freezes. Symbols in the top left-hand corner denote the ocean temperature at which each strain was collected (each being above − 1 °C). Note that all species except *P. antarctica* grew at sub-zero temperatures. Zero growth rates denote the inability to grow at a temperature (and hence define upper or lower bounds). Figure derived from Boyd (2019), permission granted under the Creative Common License see: https://creativecommons.org/licenses/by/4.0/.

References (Chapters 1 and 2)

Alvain, S., Le Quéré, C., Bopp, L., Racault, M. F., Beaugrand, G., Dessailly, D., & Buitenhuis, E. T. (2013). Rapid climatic driven shifts of diatoms at high latitudes. *Remote Sensing of Environment, 132*, 195-201. https://doi.org/10.1016/j.rse.2013.01.014

Alvain, S., Moulin, C., Dandonneau, Y., & Bréon, F. M. (2005). Remote sensing of phytoplankton groups in case 1 waters from global SeaWiFS imagery. *Deep-Sea Research Part I: Oceanographic Research Papers, 52*(11), 1989-2004. https://doi.org/10.1016/j.dsr.2005.06.015

Alvain, S., Moulin, C., Dandonneau, Y., & Loisel, H. (2008). Seasonal distribution and succession of dominant phytoplankton groups in the global ocean: A satellite view. *Global Biogeochemical Cycles, 22*(3). https://doi.org/10.1029/2007GB003154

Antoine, D., Morel, A., Gordon, H. R., Banzon, V. F., & Evans, R. H. (2005). Bridging ocean color observations of the 1980s and 2000s in search of long-term trends. *Journal of Geophysical Research: Oceans, 110*(6), 1-22. https://doi.org/10.1029/2004JC002620

Arrigo, K. R., & van Dijken, G. L. (2003). Phytoplankton dynamics within 37 Antarctic coastal polynya systems. *Journal of Geophysical Research C: Oceans, 108*(8), 27-21.

Arrigo, K. R., van Dijken, G. L., & Bushinsky, S. (2008). Primary production in the Southern Ocean, 1997-2006. *Journal of Geophysical Research: Oceans, 113*(8). https://doi.org/10.1029/2007JC004551

Bach, L. T., Riebesell, U., Sett, S., & Schulz, K. G. (2018). Shift towards larger diatoms in a natural phytoplankton assemblage under combined high-CO2 and warming conditions. *Journal of Plankton Research, 40*(4), 391-406. https://doi.org/10.1093/plankt/fby018

Barber, R. T., & Chavez, F. P. (1983). Biological consequences of El Niño. *Science, 222*(4629), 1203-1210. https://doi.org/10.1126/science.222.4629.1203

Barber, R. T., Sanderson, M. P., Lindley, S. T., Chai, F., Newton, J., Trees, C. C., . . . Chavez, F. P. (1996). Primary productivity and its regulation in the equatorial pacific during and following the 1991-1992 El Nino. *Deep-Sea Research Part II: Topical Studies in Oceanography, 43*(4-6), 933-969. https://doi.org/10.1016/0967-0645(96)00035-5

Behrenfeld, M. J., O'Malley, R. T., Siegel, D. A., McClain, C. R., Sarmiento, J. L., Feldman, G. C., . . . Boss, E. S. (2006). Climate-driven trends in contemporary ocean productivity. *Nature, 444*(7120), 752-755. https://doi.org/10.1038/nature05317

Bond, N. A., Cronin, M. F., Freeland, H., & Mantua, N. (2015). Causes and impacts of the 2014 warm anomaly in the NE Pacific. *Geophysical Research Letters, 42*(9), 3414-3420. https://doi.org/doi:10.1002/2015GL063306

Boyce, D. G., Lewis, M. R., & Worm, B. (2010). Global phytoplankton decline over the past century. *Nature, 466*(7306), 591-596. https://doi.org/10.1038/nature09268

Boyd, P. W. (2019). Physiology and iron modulate diverse responses of diatoms to a warming Southern Ocean. *Nature Climate Change, 9*(2), 148-152. https://doi.org/10.1038/s41558-018-0389-1

Boyd, P. W., Rynearson, T. A., Armstrong, E. A., Fu, F., Hayashi, K., Hu, Z., . . . Thomas, M. K. (2013). Marine phytoplankton temperature versus growth responses from polar to tropical waters--outcome of a scientific community-wide study. *PloS one, 8*(5), e63091. https://doi.org/10.1371/journal.pone.0063091

Boyd, P. W., Watson, A. J., Law, C. S., Abraham, E. R., Trull, T., Murdoch, R., . . . Zeldis, J. (2000). A mesoscale phytoplankton bloom in the polar Southern Ocean stimulated by iron fertilization. *Nature, 407*(6805), 695-702. https://doi.org/10.1038/35037500

Brewin, R. J. W., Mélin, F., Sathyendranath, S., Steinmetz, F., Chuprin, A., & Grant, M. (2014). On the temporal consistency of chlorophyll products derived from three ocean-colour sensors. *ISPRS Journal of Photogrammetry and Remote Sensing, 97*, 171-184. https://doi.org/10.1016/j.isprsjprs.2014.08.013

Cape, M. R., Vernet, M., Kahru, M., & Spreen, G. (2014). Polynya dynamics drive primary production in the Larsen A and B embayments following ice shelf collapse. *Journal of Geophysical Research: Oceans, 119*(1), 572-594. https://doi.org/10.1002/2013JC009441

Caputi, N., Kangas, M., Denham, A., Feng, M., Pearce, A., Hetzel, Y., & Chandrapavan, A. (2016, Jun). Management adaptation of invertebrate fisheries to an extreme marine heat wave event at a global warming hot spot. *Ecology and evolution, 6*(11), 3583-3593. https://doi.org/10.1002/ece3.2137

Cavicchioli, R. (2016). On the concept of a psychrophile. *The ISME journal, 10*(4), 793-795. https://doi.org/10.1038/ismej.2015.160

Cavicchioli, R., Ripple, W. J., Timmis, K. N., Azam, F., Bakken, L. R., Baylis, M., . . . Webster, N. S. (2019, 2019/06/18). Scientists' warning to humanity: microorganisms and climate change. *Nature Reviews Microbiology*. https://doi.org/10.1038/s41579-019-0222-5

Cavole, L. M., Demko, A. M., Diner, R. E., Giddings, A., Koester, I., Pagniello, C. M. L. S., . . . Franks, P. J. S. (2016). Biological Impacts of the 2013–2015 Warm-Water Anomaly in the Northeast Pacific Winners, Losers, and the Future. *Oceanography, 29*(2), 273-285.

Chavez, F. P., Strutton, P. G., Friederich, G. E., Feely, R. A., Feldman, G. C., Foley, D. G., & McPhaden, M. J. (1999). Biological and chemical response of the equatorial Pacific Ocean to the 1997-98 El Nino. *Science, 286*(5447), 2126-2131. https://doi.org/10.1126/science.286.5447.2126

Coale, K. H., Johnson, K. S., Chavez, F. P., Buesseler, K. O., Barber, R. T., Brzezinski, M. A., . . . Johnson, Z. I. (2004). Southern Ocean Iron Enrichment Experiment: Carbon Cycling in High- and Low-Si Waters. *Science, 304*(5669), 408-414. https://doi.org/10.1126/science.1089778

De Bernardi, B., Ziveri, P., Erba, E., & Thunell, R. C. (2005). Coccolithophore export production during the 1997-1998 El Niño event in Santa Barbara Basin (California). *Marine Micropaleontology, 55*(1-2), 107-125. https://doi.org/10.1016/j.marmicro.2005.02.003

Deacon, G. E. R. S. (1984). *The Antarctic circumpolar ocean*. London;New York;: Cambridge University Press.

Deppeler, S. L., & Davidson, A. T. (2017). Southern Ocean phytoplankton in a changing climate. *Frontiers in Marine Science, 4*(FEB). https://doi.org/10.3389/fmars.2017.00040

Doney, S. C. (2010). The growing human footprint on coastal and open-Ocean biogeochemistry. *Science, 328*(5985), 1512-1516. https://doi.org/10.1126/science.1185198

Dunstan, P. K., Foster, S. D., King, E., Risbey, J., O'Kane, T. J., Monselesan, D., . . . Thompson, P. A. (2018, 2018/10/02). Global patterns of change and variation in sea surface temperature and chlorophyll a. *Scientific Reports, 8*(1), 14624. https://doi.org/10.1038/s41598-018-33057-y

Dutkiewicz, S., Hickman, A. E., Jahn, O., Henson, S., Beaulieu, C., & Monier, E. (2019). Ocean colour signature of climate change. *Nature Communications, 10*(1). https://doi.org/10.1038/s41467-019-08457-x

Dutkiewicz, S., Scott, J. R., & Follows, M. J. (2013). Winners and losers: Ecological and biogeochemical changes in a warming ocean. *Global Biogeochemical Cycles, 27*(2), 463-477. https://doi.org/10.1002/gbc.20042

Feng, J., Durant, J. M., Stige, L. C., Hessen, D. O., Hjermann, D. Ø., Zhu, L., . . . Stenseth, N. C. (2015). Contrasting correlation patterns between environmental factors and chlorophyll levels in the global ocean. *Global Biogeochemical Cycles, 29*(12), 2095-2107. https://doi.org/10.1002/2015gb005216

Fiedler, P. C., Methot, R. D., & Hewitt, R. P. (1986). Effects of California El Nino 1982-1984 on the northern anchovy. *Journal of Marine Research, 44*(2), 317-338. https://doi.org/10.1357/002224086788405365

Frenger, I., Münnich, M., & Gruber, N. (2018). Imprint of Southern Ocean mesoscale eddies on chlorophyll. *Biogeosciences, 15*(15), 4781-4798. https://doi.org/10.5194/bg-15-4781-2018

Frölicher, T. L., Fischer, E. M., & Gruber, N. (2018). Marine heatwaves under global warming. *Nature, 560*(7718), 360-364. https://doi.org/10.1038/s41586-018-0383-9

Furnas, M. (2007). Intra-seasonal and inter-annual variations in phytoplankton biomass, primary production and bacterial production at North West Cape, Western Australia: Links to the 1997-1998 El Niño event. *Continental Shelf Research, 27*(7), 958-980. https://doi.org/10.1016/j.csr.2007.01.002

Garrabou, J., Coma, R., Bensoussan, N., Bally, M., Chevaldonne, P., Cigliano, M., . . . Cerrano, C. (2009). Mass mortality in Northwestern Mediterranean rocky benthic communities: effects of the 2003 heat wave. *Global Change Biology, 15*(5), 1090-1103. https://doi.org/10.1111/j.1365-2486.2008.01823.x

Garrison, T., Ellis, R., & National Geographic, L. (2018). *Essentials of oceanography* (Eighth ed.). Independence, KY;United Kingdom;Boston, MA;Australia;: Cengage Learning.

Gómez-Ocampo, E., Gaxiola-Castro, G., Durazo, R., & Beier, E. (2018). Effects of the 2013-2016 warm anomalies on the California Current phytoplankton. *Deep-Sea Research Part II: Topical Studies in Oceanography, 151*, 64-76. https://doi.org/10.1016/j.dsr2.2017.01.005

González, H. E., Ortiz, V. C., & Sobarzo, M. (2000). The role of faecal material in the particulate organic carbon flux in the northern Humboldt Current, Chile (23°S), before and during the 1997-1998 El Nino. *Journal of Plankton Research, 22*(3), 499-529.

González, H. E., Sobarzo, M., Figueroa, D., & Nöthig, E. M. (2000). Composition, biomass and potential grazing impact of the crustacean and pelagic tunicates in the northern Humboldt Current area off Chile: Differences between El Nino and non-El Nino years. *Marine Ecology Progress Series, 195*, 201-220. https://doi.org/10.3354/meps195201

González, N. M., Müller-Karger, F. E., Estrada, S. C., De Los Reyes, R. P., Del Río, I. V., Pérez, P. C., & Arenal, I. M. (2000). Near-surface phytoplankton distribution in the western Intra-Americas Sea: The influence of El Niño and weather events. *Journal of Geophysical Research: Oceans, 105*(C6), 14029-14043.

Harris, S. L., Varela, D. E., Whitney, F. W., & Harrison, P. J. (2009). Nutrient and phytoplankton dynamics off the west coast of Vancouver Island during the 1997/98 ENSO event. *Deep-Sea Research Part II: Topical Studies in Oceanography, 56*(24), 2487-2502. https://doi.org/10.1016/j.dsr2.2009.02.009

Hereu, C. M., Lavaniegos, B. E., Gaxiola-Castro, G., & Ohman, M. D. (2006). Composition and potential grazing impact of salp assemblages off Baja California during the 1997-1999 El Niño and La Niña. *Marine Ecology Progress Series, 318*, 123-140. https://doi.org/10.3354/meps318123

Hewes, C. D. (2009). Cell size of Antarctic phytoplankton as a biogeochemical condition. *Antarctic Science, 21*(5), 457-470. https://doi.org/10.1017/S0954102009990125

Hobday, A. J., Alexander, L. V., Perkins, S. E., Smale, D. A., Straub, S. C., Oliver, E. C. J., . . . Wernberg, T. (2016). A hierarchical approach to defining marine heatwaves. *Progress in Oceanography, 141*, 227-238. https://doi.org/10.1016/j.pocean.2015.12.014

Hobday, A. J., Oliver, E. C. J., Gupta, A. S., Benthuysen, J. A., Burrows, M. T., Donat, M. G., . . . Smale, D. A. (2018). Categorizing and naming marine heatwaves. *Oceanography, 31*(2 Special Issue), 162-173. https://doi.org/10.5670/oceanog.2018.205

Holbrook, N. J., Scannell, H. A., Sen Gupta, A., Benthuysen, J. A., Feng, M., Oliver, E. C. J., . . . Wernberg, T. (2019, 2019/06/14). A global assessment of marine heatwaves and their drivers. *Nature Communications, 10*(1), 2624. https://doi.org/10.1038/s41467-019-10206-z

Hoppenrath, M., Elbrächter, M., & Drebes, G. (2009). Marine phytoplankton.

Hughes, T. P., Kerry, J. T., Álvarez-Noriega, M., Álvarez-Romero, J. G., Anderson, K. D., Baird, A. H., . . . Wilson, S. K. (2017, 03/15/online). Global warming and recurrent mass bleaching of corals. *Nature, 543*, 373. https://doi.org/10.1038/nature21707

Hutchins, D. A., & Boyd, P. W. (2016, 11/24/online). Marine phytoplankton and the changing ocean iron cycle. *Nature Climate Change, 6*, 1072. https://doi.org/10.1038/nclimate3147 https://www.nature.com/articles/nclimate3147#supplementary-information

IPCC, 2019: IPCC Special Report on the Ocean and Cryosphere in a Changing Climate [H.-O. Pörtner, D.C. Roberts, V. Masson-Delmotte, P. Zhai, M. Tignor, E. Poloczanska, K. Mintenbeck, A. Alegría, M. Nicolai, A. Okem, J. Petzold, B. Rama, N.M. Weyer (eds.)]. In press.

Iriarte, J. L., & González, H. E. (2004). Phytoplankton size structure during and after the 1997/98 El Niño in a coastal up welling area of the northern Humboldt Current System. *Marine Ecology Progress Series, 269*, 83-90. https://doi.org/10.3354/meps269083

Jacox, M. G., Hazen, E. L., Zaba, K. D., Rudnick, D. L., Edwards, C. A., Moore, A. M., & Bograd, S. J. (2016). Impacts of the 2015–2016 El Niño on the California Current System: Early assessment and comparison to past events. *Geophysical Research Letters, 43*(13), 7072-7080. https://doi.org/doi:10.1002/2016GL069716

Ji, R., Edwards, M., MacKas, D. L., Runge, J. A., & Thomas, A. C. (2010). Marine plankton phenology and life history in a changing climate: Current research and future directions. *Journal of Plankton Research, 32*(10), 1355-1368. https://doi.org/10.1093/plankt/fbq062

Jiménez-Quiroz, M. d. C., Cervantes-Duarte, R., Funes-Rodríguez, R., Barón-Campis, S. A., García-Romero, F. d. J., Hernández-Trujillo, S., . . . Barrón-Barraza, F. J. (2019, 2019-February-07). Impact of "The Blob" and "El Niño" in the SW Baja California Peninsula: Plankton and Environmental Variability of Bahia Magdalena. *Frontiers in Marine Science, 6*(25). https://doi.org/10.3389/fmars.2019.00025

Jones, T., Divine, L. M., Renner, H., Knowles, S., Lefebvre, K. A., Burgess, H. K., . . . Parrish, J. K. (2019). Unusual mortality of Tufted puffins (Fratercula cirrhata) in the eastern Bering Sea. *PloS one, 14*(5), e0216532. https://doi.org/10.1371/journal.pone.0216532

Kahru, M., & Mitchell, B. G. (2000). Influence of the 1997-98 El Niño on the surface chlorophyll in the California current. *Geophysical Research Letters, 27*(18), 2937-2940. https://doi.org/10.1029/2000GL011486

Kahru, M., & Mitchell, B. G. (2002). Influence of the El Niño-La Niña cycle on satellite-derived primary production in the California Current. *Geophysical Research Letters, 29*(17), 27-21.

Kirchman, D., Morán, X. A., & Ducklow, H. (2009). *Kirchman DL, Moran XAG, Ducklow H.. Microbial growth in the polar oceans: role of temperature and potential impact of climate change. Nat Rev Micro 7: 451-459* (Vol. 7).

Knox, G. A. (2007). *Biology of the Southern Ocean* (2nd ed.). Boca Raton: CRC Press/Taylor & Francis.

Landry, M. R., Selph, K. E., Brown, S. L., Abbott, M. R., Measures, C. I., Vink, S., . . . Nolla, H. (2002, 2002/01/01/). Seasonal dynamics of phytoplankton in the Antarctic Polar Front region at 170°W. *Deep Sea Research Part II: Topical Studies in Oceanography, 49*(9), 1843-1865. https://doi.org/https://doi.org/10.1016/S0967-0645(02)00015-2

Li, Y., Ji, R., Jenouvrier, S., Jin, M., & Stroeve, J. (2016). Synchronicity between ice retreat and phytoplankton bloom in circum-Antarctic polynyas. *Geophysical Research Letters, 43*(5), 2086-2093. https://doi.org/10.1002/2016GL067937

Lipsen, M. S., Crawford, D. W., Gower, J., & Harrison, P. J. (2007). Spatial and temporal variability in coccolithophore abundance and production of PIC and POC in the NE subarctic Pacific during El Niño (1998), La Niña (1999) and 2000. *Progress in Oceanography, 75*(2), 304-325. https://doi.org/10.1016/j.pocean.2007.08.004

Liu, C., Sun, Q., Xing, Q., Wang, S., Tang, D., Zhu, D., & Xing, X. (2019). Variability in phytoplankton biomass and effects of sea surface temperature based on satellite data from the Yellow Sea, China. *PloS one, 14*(8), e0220058-e0220058. https://doi.org/10.1371/journal.pone.0220058

Llort, J., Lévy, M., Sallée, J.-B., & Tagliabue, A. (2015). Onset, intensification, and decline of phytoplankton blooms in the Southern Ocean. *ICES Journal of Marine Science, 72*(6), 1971-1984. https://doi.org/10.1093/icesjms/fsv053

Macfarlane, R. B., Ralston, S., Royer, C., & Norton, E. C. (2005). Juvenile chinook salmon (Oncorhynchus tshawytscha) growth on the central California coast during the 1998 El Niño and 1999 La Niña. *Fisheries Oceanography, 14*(5), 321-332. https://doi.org/10.1111/j.1365-2419.2005.00338.x

Mann, K. H., & Lazier, J. R. N. (2006). *Dynamics of marine ecosystems: biological-physical interactions in the oceans* (3rd ed.). Malden, MA: Blackwell Pub.

Maranón, E., Cermeno, P., Latasa, M., & Tadonléké, R. D. (2012). Temperature, resources, and phytoplankton size structure in the ocean. *Limnology and Oceanography, 57*(5), 1266-1278.

Marchant, H. J., Davidson, A. T., & Wright, S. W. (2001). Antarctic marine microorganisms and climate change: Impacts and feedbacks. *Ocean and Polar Research, 23*(4), 401-410.

Marinov, I., Doney, S. C., & Lima, I. D. (2010). Response of ocean phytoplankton community structure to climate change over the 21st century: Partitioning the effects of nutrients, temperature and light. *Biogeosciences, 7*(12), 3941-3959. https://doi.org/10.5194/bg-7-3941-2010

Martin, P., Van Der Loeff, M. R., Cassar, N., Vandromme, P., D'Ovidio, F., Stemmann, L., . . . Naqvi, S. W. A. (2013). Iron fertilization enhanced net community production but not

downward particle flux during the Southern Ocean iron fertilization experiment LOHAFEX. *Global Biogeochemical Cycles, 27*(3), 871-881. https://doi.org/10.1002/gbc.20077

McClain, C. R. (2009). A decade of satellite ocean color observations. *Annual Review of Marine Science, 1*, 19-42. https://doi.org/10.1146/annurev.marine.010908.163650

Montes-Hugo, M., Doney, S. C., Ducklow, H. W., Fraser, W., Martinson, D., Stammerjohn, S. E., & Schofield, O. (2009). Recent changes in phytoplankton communities associated with rapid regional climate change along the western Antarctic Peninsula. *Science, 323*(5920), 1470-1473. https://doi.org/10.1126/science.1164533

Moore, J. K., & Abbott, M. R. (2000). Phytoplankton chlorophyll distributions and primary production in the Southern Ocean. *Journal of Geophysical Research: Oceans, 105*(C12), 28709-28722.

National Oceanic and Atmospheric Administration (NOAA). (July, 2017). NOAA Ocean Service Education. Retrieved October 17, 2019, from https://oceanservice.noaa.gov/education/tutorial_currents/welcome.html

Oliver, E. C. J., Benthuysen, J. A., Bindoff, N. L., Hobday, A. J., Holbrook, N. J., Mundy, C. N., & Perkins-Kirkpatrick, S. E. (2017). The unprecedented 2015/16 Tasman Sea marine heatwave. *Nature Communications, 8*. https://doi.org/10.1038/ncomms16101

Oliver, E. C. J., Donat, M. G., Burrows, M. T., Moore, P. J., Smale, D. A., Alexander, L. V., . . . Wernberg, T. (2018). Longer and more frequent marine heatwaves over the past century. *Nature Communications, 9*(1). https://doi.org/10.1038/s41467-018-03732-9

Ortiz-Ahumada, J. C., Álvarez-Borrego, S., & Gómez-Valdés, J. (2018). Effects of seasonal and interannual events on satellite-derived phytoplankton biomass and production in the southernmost part of the California Current System during 2003-2016. *Ciencias Marinas, 44*(1), 1-20. https://doi.org/10.7773/cm.v44i1.2743

Peterson, W. T., Keister, J. E., & Feinberg, L. R. (2002). The effects of the 1997-99 El Niño/La Niña events on hydrography and zooplankton off the central Oregon coast. *Progress in Oceanography, 54*(1-4), 381-398. https://doi.org/10.1016/S0079-6611(02)00059-9

Petrou, K., Kranz, S. A., Trimborn, S., Hassler, C. S., Ameijeiras, S. B., Sackett, O., . . . Davidson, A. T. (2016, 2016/09/20/). Southern Ocean phytoplankton physiology in a changing climate. *Journal of Plant Physiology, 203*, 135-150. https://doi.org/https://doi.org/10.1016/j.jplph.2016.05.004

Piontkovski, S., Fonda-Umani, S., Olita, A., Alessandra, D., Stemmann, L., C.G, R., . . . Altukhov, D. (2010). *The 2003 heat wave and marine plankton communities*.

Putt, M., & Prézelin, B. B. (1985). Observations of diet patterns of photosynthesis in cyanobacteria and nanoplankton in the Santa Barbara channel during 'el niño'. *Journal of Plankton Research, 7*(6), 779-790. https://doi.org/10.1093/plankt/7.6.779

Rohr, T., Long, M. C., Kavanaugh, M. T., Lindsay, K., & Doney, S. C. (2017). Variability in the mechanisms controlling Southern Ocean phytoplankton bloom phenology in an ocean

model and satellite observations. *Global Biogeochemical Cycles, 31*(5), 922-940. https://doi.org/10.1002/2016gb005615

Sallée, J.-B., Llort, J., Tagliabue, A., & Lévy, M. (2015). Characterization of distinct bloom phenology regimes in the Southern Ocean. *ICES Journal of Marine Science, 72*(6), 1985-1998. https://doi.org/10.1093/icesjms/fsv069

Schofield, O., Ducklow, H. W., Martinson, D. G., Meredith, M. P., Moline, M. A., & Fraser, W. R. (2010). How do polar marine ecosystems respond to rapid climate change? *Science, 328*(5985), 1520-1523. https://doi.org/10.1126/science.1185779

Smale, D. A., Wernberg, T., Oliver, E. C. J., Thomsen, M., Harvey, B. P., Straub, S. C., . . . Moore, P. J. (2019, 2019/03/04). Marine heatwaves threaten global biodiversity and the provision of ecosystem services. *Nature Climate Change*. https://doi.org/10.1038/s41558-019-0412-1

Smetacek, V., & Nicol, S. (2005). Polar ocean ecosystems in a changing world. *Nature, 437*(7057), 362-368. https://doi.org/10.1038/nature04161

Smith, W. O. (1990). *Polar oceanography*. San Diego: Academic Press.

Smith, W. O., & Barber, D. G. (2007). *Polynyas: windows to the world*, Amsterdam;Boston;.

Sokolov, S. (2008). Chlorophyll blooms in the Antarctic Zone south of Australia and New Zealand in reference to the Antarctic Circumpolar Current fronts and sea ice forcing. *Journal of Geophysical Research: Oceans, 113*(3). https://doi.org/10.1029/2007JC004329

Stonehouse, B. (2002). *Encyclopedia of Antarctica and the southern oceans*. New York: J. Wiley.

Thomas M. K., Kremer, C. T., Klausmeier, C. A., & Litchman, E. (2012). A global pattern of thermal adaptation in marine phytoplankton. *Science, 338*(6110), 1085-1088. https://doi.org/10.1126/science.1224836

Thomas, D. N. (2017). *Sea ice* (Third ed.). Chichester, UK;Hoboken, NJ;: John Wiley & Sons.

Thomsen, M. S., Mondardini, L., Alestra, T., Gerrity, S., Tait, L., South, P. M., . . . Schiel, D. R. (2019, 2019-March-06). Local Extinction of Bull Kelp (Durvillaea spp.) Due to a Marine Heatwave. *Frontiers in Marine Science, 6*(84). https://doi.org/10.3389/fmars.2019.00084

Torres-Moye, G., & Alvarez-Borrego, S. (1987). Effects of the 1984 El Nino on the summer phytoplankton of a Baja California upwelling zone. *Journal of Geophysical Research, 92*(C13), 14,383-"314,386".

Tortell, P. D., Payne, C. D., Li, Y., Trimborn, S., Rost, B., Smith, W. O., . . . DiTullio, G. R. (2008). CO<inf>2</inf> sensitivity of Southern Ocean phytoplankton. *Geophysical Research Letters, 35*(4). https://doi.org/10.1029/2007GL032583

Townsend, D. W. (2012). *Oceanography and marine biology: an introduction to marine science*. Sunderland, Mass: Sinauer Associates.

Trainer, V. L., Moore, S. K., Hallegraeff, G., Kudela, R. M., Clement, A., Mardones, J. I., & Cochlan, W. P. (2019, 2019/05/03/). Pelagic harmful algal blooms and climate change: Lessons from nature's experiments with extremes. *Harmful Algae*. https://doi.org/https://doi.org/10.1016/j.hal.2019.03.009

Tréguer, P., Bowler, C., Moriceau, B., Dutkiewicz, S., Gehlen, M., Aumont, O., . . . Pondaven, P. (2018). Influence of diatom diversity on the ocean biological carbon pump. *Nature Geoscience, 11*(1), 27-37. https://doi.org/10.1038/s41561-017-0028-x

Volpe, G., Nardelli, B. B., Cipollini, P., Santoleri, R., & Robinson, I. S. (2012). Seasonal to interannual phytoplankton response to physical processes in the Mediterranean Sea from satellite observations. *Remote Sensing of Environment, 117*, 223-235. https://doi.org/10.1016/j.rse.2011.09.020

Wernberg, T., Bennett, S., Babcock, R., de Bettignies, T., Cure, K., Depczynski, M., . . . Wilson, S. (2016, 07/08). Climate-driven regime shift of a temperate marine ecosystem. *Science, 353*, 169-172. https://doi.org/10.1126/science.aad8745

Williams, R. G., & Follows, M. J. (2011). *Ocean dynamics and the carbon cycle: principles and mechanisms*. Cambridge, UK;New York;: Cambridge University Press.

Witze, A. (2019, June 8). Southern Ocean — friend or foe? The waters surrounding Antarctica may not be absorbing as much carbon as expected. Retrieved October 29, 2019, from https://www.sciencenews.org

Worden, A. Z., Follows, M. J., Giovannoni, S. J., Wilken, S., Zimmerman, A. E., & Keeling, P. J. (2015). Rethinking the marine carbon cycle: Factoring in the multifarious lifestyles of microbes. *Science, 347*(6223). https://doi.org/10.1126/science.1257594

Wright, S. W., Ishikawa, A., Marchant, H. J., Davidson, A. T., Van Den Enden, R. L., & Nash, G. V. (2009). Composition and significance of picophytoplankton in Antarctic waters. *Polar Biology, 32*(5), 797-808. https://doi.org/10.1007/s00300-009-0582-9

Yang, B., Emerson, S. R., & Peña, M. A. (2018). The effect of the 2013–2016 high temperature anomaly in the subarctic Northeast Pacific (the "Blob") on net community production. *Biogeosciences, 15*(21), 6747-6759. https://doi.org/10.5194/bg-15-6747-2018

Zhang, H., Han, Z., Zhao, J., Yu, P., Hu, C., Sun, W., . . . Vetter, W. (2014, December 01). Phytoplankton and chlorophyll a relationships with ENSO in Prydz Bay, East Antarctica. *Science China Earth Sciences, 57*(12), 3073-3083. https://doi.org/10.1007/s11430-014-4939-8

Chapter Three

Correlation Analysis of Sea Surface Temperature and Chlorophyll-a Concentration Anomalies in the Ross Sea

3.1. Introduction

Chlorophyll-a (chl-a) is the most important proxy for phytoplankton biomass because this pigment is present in all phytoplankton species (Alvain, Moulin, Dandonneau, & Bréon, 2005; Alvain, Moulin, Dandonneau, & Loisel, 2008). Chl-a is estimated by the blue-to-green ratio of water reflected radiance and uses bio-optical algorithms and atmospheric correction methods in the infrared spectrum (Alvain et al., 2008). A recent analysis of chl-a concentration demonstrated an increase from 1981 to 2019 across the entire Southern Ocean (Pinkerton, 2019). However, to better understand impacts of climate change on specific ecosystems, it is important to also quantify changes on smaller more regional scales. For example, in the same study Pinkerton (2019) also found that chl-a concentrations have decreased in the Ross Sea region. The Ross Sea region is the most productive region in Antarctica's coastal zone, accounting for ~30% of total annual primary production, therefore this decrease in chl-a warranted further research scrutiny (Deppeler & Davidson, 2017).

Phytoplankton productivity fluctuates at seasonal and inter-annual time scales due to changes in species composition, population dynamics, predator-prey interactions, biogeochemistry and physical drivers, in particular sea surface temperature (SST) (Feng et al., 2015). This relationship between SST and chl-a is complex. For example, warming of the surface ocean can affect phytoplankton primary production both directly, by changing metabolic rates, and/or indirectly, by changing stratification and the mixed layer depth (Arrigo, van Dijken, & Bushinsky, 2008). Furthermore, in high latitude polar regions, sea ice plays an important role in both SST and phytoplankton bloom dynamics (Knox, 2007). In high latitude regions, where SST generally is below 14°C, the positive effects of increased SST on phytoplankton growth and biomass can often exceed negative effects (Feng et al., 2015). There has therefore been recent research on identifying correlation patterns between chl-a and SST at regional scales, albeit largely focused on temperate, sub-tropical and tropical latitudes (Behrenfeld et al., 2006; Kitsiou & Topouzelis, 2014; Li et al., 2018; Liu et al., 2019; Macias, Stips, Garcia-Gorriz, & Dosio, 2018; Xue, Dong, & Fan, 2014) (but see Arrigo et al., 2008 for a rare case study from the Southern Ocean). In this chapter I build on the research by Arrigo et al. (2008) and Pinkerton (2019) by performing a pixel by pixel correlation analysis between monthly SST and chl-a concentration anomalies for each month from January 1998 to December 2018 in the Ross Sea region in the Southern Ocean. More specifically, I address the following three key questions:

1) Do monthly SST anomalies from 1998-2018 in the Ross Sea region correlate with chlorophyll-a concentration anomalies?
2) Do correlation levels vary between regions; more specifically between the coastal (>75°S), the transition (75°S - 70°S) and open ocean (70°S - 60°S) zones?
3) Do correlations for different zones vary systematically across monthly, seasonal and annual time scales and between El Niño and non-El Niño years?

The expected lifetime of satellites (ca. 10 years) is too short for multi-decadal analysis, therefore, careful integration across several satellite sensors was required for this study (Pinkerton, 2019). Previous research has shown that chl-a data from SeaWiFS can be combined with data from MODIS-Aqua sensors for use in long term trend analysis (Brewin et al., 2014). For example, Kitsiou & Topouzelis (2014) merged MERIS, MODIS and SeaWiFS sensors to obtain a long term dataset showing a negative correlation between chl-a and SST in the Mediterranean Sea (Atlantic Ocean). Similarly, Xue et al (2014) and Liu (2019) found negative correlations between chl-a and SST in the North-Western Pacific Ocean and Yellow Sea (western Pacific Ocean) respectively. Finally, Li (2018) found that anomalies of chl-a were negatively correlated with positive SST anomalies in the Red Sea (Indian Ocean). These results from sub-tropical and tropical latitudes are likely to reflect indirect negative effects of increased SST. By contrast, in colder high-latitude regions positive effects of increased SST may surpass and compensate for the negative effects (Feng et al., 2015). Similarly, Brewin et al. (2014) found negative correlations between SST and chl-a in the low latitudes (<40°), but positive correlations at high latitudes (>40°). This result was also consistent with Arrigo et al (2008) and Zhang et al. (2014) who both found strong positive correlations between annual primary production and annual SST in the Ross Sea and Prydz Bay (Zhang et al., 2014), respectively.

I therefore hypothesise that in the Ross Sea, I will also find a positive correlation between SST and chl-a. Importantly, my analysis will differ from past analyses by (a) including a longer time series of 20 years, over a larger spatial region and (b) by focusing on monthly anomalies of SST and chl-a concentration rather than annual trends (to represent impacts of shorter more intense events). Note however, that on these shorter time scales variables not accounted for here, like sea ice, nutrient concentrations, salinity levels, grazing pressure, areas of upwelling, location of fronts and the movement of currents, may have stronger impact and thereby suppress the temperature signal.

3.2. Methods and materials

Two decades of satellite imagery was used for correlation analysis between SST anomalies (°C) and chl-a concentration (mg/m^{-3}) anomalies in the Ross Sea region.

3.2.1. SeaWiFS, MODIS and OISST satellite data

I analysed monthly satellite imagery from the Southern Ocean from 1998 to 2018, with a spatial resolution of 9 km. Monthly anomalies were calculated by subtracting the climatological monthly mean from the observation in a given month for each pixel (higher values than the climatological mean results in positive anomalies and lower values results in negative anomalies). In other words, each pixel was assigned a positive or negative value if SST (or chl-a concentration) was higher or lower than the monthly climatological average, respectively.

The 20 year dataset is a combination of SeaWiFS and Aqua MODIS satellite data stitched together. The SeaWiFS instrument on board the OrbView-2 Satellite was optimised for ocean colour measurements. It launched in August 1997, became operational in September 1997 and covered routine operations through to December 2010. The satellite and sensor The OrbView-2 Satellite orbit had an equator crossing time at local noon, low

polarisation sensitivity and tilt capability (NASA Ocean Colour Web, n.d.). Ocean colour reflectance was acquired in 8 spectral bands from 412 to 865 nm with a resolution of 1 km. The Aqua satellite was launched on 4th May 2002 and is still functioning. The Moderate Resolution Imaging Spectroradiometer (MODIS) is a key sensor on board the Aqua satellite. The Aqua satellite passes south to north over the equator in the afternoon and covers the entire Earth's surface every 1-2 days, acquiring data in 36 wavelength bands with a resolution of 250 m (bands 1-2), 500 m (bands 3-7) and 1 km (bands 8-36) (NASA Ocean Colour Web, n.d. These spectral bands can be used to determine chl-a concentration of surface waters in cloud- and ice-free areas.

SST data was obtained based on satellite measurements by the Advanced Very High Resolution Radiometer series, operated by the National Oceanic and Atmosphere Administration (NOAA). The data set is the Optimum Interpolation Sea Surface Temperature (OISST) and spans the period from 1981 to August 2018. Daily OISST is a composite analysis constructed by combining data from satellites, ships and buoys, on a global grid. Interpolation methods create a spatially complete sea surface temperature map with a minimum resolution of 0.25 of a degree.

Ocean colour data is obtained from cloud free satellite scenes, therefore to provide clearest possible images, the satellite data was composited in time and space. In order to stitch together SeaWiFS and MODIS data sets, 8-day composite images were used (this was necessary because SeaWiFS and MODIS pass overhead at different times in the day). If cloud cover varied between these times, sensors will pick up information on different parts of the ocean surface leading to a temporal mismatch. Using a short compositing period reduces this discrepancy. The satellite sensors had an overlap period between 2002 and 2010. There are some additional discrepancies to note between measurements of chl-a concentration as a result of the different satellite sensors: 1) sensor design (spectral bands used from SeaWiFS and MODIS are slightly different in terms of band-width, spatial resolution, polarization sensitivity and signal to noise ratio), 2) chl-a retrieval algorithms, 3) atmospheric correction methods and 4) general sensor degradation.

Information regarding the SeaWiFS sensor, Aqua MODIS sensor and the daily OSSIT product were accessed from the NASA Ocean Colour Web Website (https://oceancolor.gsfc.nasa.gov/data/seawifs/), the NASA MODIS website (https://modis.gsfc.nasa.gov/) and the NOAA website (https://www.ncdc.noaa.gov/oisst), respectively.

3.2.2. Image processing

Processing of the combined SeaWiFS and MODIS satellite imagery was done in ENVI 5.5 and ArcGIS.

The chl-a concentration and corresponding SST anomaly image for January 1998 was imported as GeoTiff files in Polar Stereographic projection covering the entire Southern Ocean. The gridlines layer was created using the Australian Antarctic 1998 Geographic Coordinate System. To visualise SST anomalies I reversed the colour table and modified the histogram to a minimum value of 0 (so that positive SST anomalies were shown with red colour). For chl-a concentration anomalies I applied the same colour table and used the default histogram values (to contrast location of positive and negative anomalies). The Ross

Sea region was defined as the area between 160°W and 160°E with a northern limit of 60°S, outlined with the vector layers tool. Because this is a spatially extensive region I further divided it into three sub-zones; a coastal zone (>75°S), a transition zone (75°S to 70°S) and an open water zone (70°S to 60°S). Because the three zones were defined by latitude, arrangement of vectors was consistent and accurate for all replicates. Figure 3.1 shows final SST and chl-a images for January 1998 used for correlation analysis (this process was repeated for each month through to December 2018).

Following the initial image processing, SST and chl-a anomaly raster images were combined using the layer stacking tool in ENVI 5.5. Since the two images are in the same geographic projection with similar spatial resolution no resampling was required. The final output was a new multiband file containing the two georeferenced images. The individual sub-zone of the Ross Sea was saved as its own GeoTiff file using the new multiband image. First, the coastal zone was used as a mask on the final image (the area contained within the red vector layer) (Figure 3.1a and 3.1b). Data values of -9999 were ignored as they represent pixels which contain land, ice or cloud. This processes was repeated for the transition and open water zones. See Figure 3.2a for an outlined of the entire analytical process in ENVI 5.5.

Subsequent data processing was done in ArcGIS ArcMap 10.6. Monthly GeoTiff files of the coastal, transition and open water zones were imported into ArcMap 10.6 for correlation analysis. The Band Collection Statistics tool was used to calculate the covariance matrix and correlation coefficient for the two input bands (i.e. with a single correlation coefficient per month and per regional zone) Furthermore, the statistical tool also report the minimum, maximum, mean and standard deviation values for both the SST and chl-a concentration anomalies. See Figure 3.2b for a flow diagram over the entire data analytical process in ENVI 5.5 ArcMap 10.6.

3.2.3. Visualisation of correlation coefficients

First, a Shapiro-Wilks test for normality was performed in R-Studio on correlation coefficients to see whether the data was normally distributed. Categorical Anova analyses were performed to determine if there was a stronger dependence of chl-a on positive SST anomalies between monthly, seasonal and annual time scales. Followed by post hoc Tukey tests to determine specific months, seasons and years that were significantly different from another. Additionally, average correlation coefficients for the different zones were tested whether they varied systematically between El Niño vs non El Niño years. This is because growth rates and community composition in the SO are closely related to sustained periods of above average temperatures, conditions typical of El Niño events (Boyd, 2019). Furthermore, El Niño transitions significantly correspond to monthly anomalies of chl-a (higher than normal phytoplankton production). Significant interactions and individual effects were confirmed at alpha = 0.05 and spatial variation was accounted for in all analyses by including zones in each of the graphs and analysis.

Average correlation coefficient values and mean values of SST and chl-a anomalies are outlined in Table 3.1. Mean values are the average temperature and chl-a concentration respectively, which deviate from the climatological mean (making it an anomaly) for all pixels within the analysis. Correlations were averaged between seasons (summer, autumn and

spring), spatial zones (coastal, transition and open ocean) and months (all excluding June, July and August). No values were obtained in the winter season (June, July and August) because high cloud and ice cover preventing satellite observations. For the same reasons, gaps in the data set are also present for one or more zones in April, May, September and October.

3.3. Results

Correlation patterns between SST and chl-a anomalies were analysed for the Ross Sea region between 1998 and 2018 to test if correlations vary (a) spatially, i.e., between the Southern coastal (>75°S), transition (75°S - 70°S) and open ocean (70°S - 60°S) zones, and (b) temporally, i.e., between months, seasons, years and between El Niño vs non El Niño years.

The largest positive correlation was found within the summer month of December for the coastal (0.090) and the transition (0.084) zones. The largest negative correlation was found within the autumn month of March in the open ocean zone (-0.043). Additionally, line graphs were created for exploratory data analysis. Graphs (Fig. 5.1-5.4) show the average correlation coefficient value for the coastal, transition and open ocean zones for different temporal resolutions.

3.3.1. Monthly analysis

The average monthly correlation coefficients were analysed to test if correlation trends varied over a time period of one year (Figure 3.3). I hypothesised that positive correlations would be observed during the warmer months of January, February, November and December for all zones. In contrast, I hypothesised no or negative correlations between positive SST anomalies and chl-a anomalies for the remaining cooler months. I expected these correlation trends because within warmer months increased SST, light and nutrient availability, and stability in the upper mixed layer stimulates phytoplankton growth. Coupled with the added influence of an SST anomaly significant positive effects may be observed. Whereas in the cooler months, decreased SST, sea ice cover and constant darkness prevents photosynthesis which could make the effect of an SST anomaly not significant.

The Anova analysis (Table 3.2) showed no interaction effect between month and zone ($p = 0.897$) and no effect of zone ($p = 0.067$). However, there was a significant difference in correlation coefficients between months ($p = <0.001$). More specifically, a post-hoc Tukey test found a significant difference between the months of March and December ($p = <0.001$). Overall, positive correlation values peaked during the summer months of January and December, with the highest positive correlation of 0.090 documented in the coastal zone, followed by 0.084 in the transition zone, in December. This suggests that as SST anomalies increase, so does chl-a anomalies, or chl-a anomalies do occur in the same location. However, these correlation values remain extremely low (< +0.1). During February, correlations begin to decline and reach negative values for all zones in March. During March and April, average correlation coefficients alternate to a negative correlation, meaning as SST anomalies increase, the chl-a anomalies decrease or do not occur in the same location. Again, correlation coefficients were extremely low (< -0.1). During October and November there is a steep incline in positive correlation values. Once again, the open ocean zone remains

negatively correlated and demonstrates a more gradual increase into the summer months (Figure 3.3).

3.3.2. Seasonal analysis

The average correlation coefficients per season were analysed between SST and chl-a anomalies in the Ross Sea region from 1998 to 2018 (Figure 3.4). It was hypothesised that positive correlations would be observed in all zones during summer and in the coastal and transition zone during spring. It was also hypothesised that no correlation, or negative correlations would be observed in autumn and winter between positive SST anomalies and chl-a anomalies. These correlation trends were expected because different conditions characterise each season in the SO. For example, in the autumn and winter cooler ocean temperatures, less frequent SST anomalies and sea ice cover were predicted to inhibit any significant positive effects. By comparison, in summer and spring elevated SST, sea ice retreat, enhanced light penetration, stability of the upper mixed layer and an influx of nutrients from the deep ocean were predicted to have a positive effect on phytoplankton dynamics.

The Anova analysis (Table 3.3) showed no interaction effect between season and zone ($p = 0.476$) and no effect of zone ($p = 0.070$). However, there was a significant difference in correlation coefficients between seasons ($p = <0.001$). More specifically, a post-hoc Tukey test found a significant difference between the summer and autumn season ($p = 0.0117$). The summer season was characterised by a correlation of >0.04 for all zones. In autumn, correlations switched from positive to negative for all zones. Correlation values of -0.031 and -0.034 are shown for the transition and open ocean zones respectively. The coastal zone had a correlation of -0.021 following the cooler seasons, spring was characterised by a rapid shift from negative correlations to positive for the coastal and transition zone. Values are similar to that of the summer season being >0.04. However, the open ocean zone remains negatively correlated in spring and demonstrates a more gradual positive increase into the summer season.

3.3.3. Annual analysis

Average correlation coefficients were plotted inter-annually from 1998 to 2018 (Figure 3.5). I hypothesised that average correlations would vary between years, with different zones demonstrating different trends. Slow increases in CO_2 in the atmosphere and associated climate changes would have resulted in years with enhanced SST anomalies and corresponding chl-a anomalies compared to other years. However, I hypothesise that the length of this time series is not sufficient to detect any general increase or decrease in correlation trends associated with climate change.

A linear regression analysis between years vs. correlation coefficients, demonstrated very low R^2 values for all zones (i.e. the coastal, transition and open ocean zones were 0.079, 0.031 and 0.020, respectively). However, the Anova analysis (Table 3.4) showed an interaction effect between year and zone ($p = 0.030$) as well as an individual effect of year ($p = 0.035$). There was no significant difference in correlation coefficients between zones ($p = 0.060$).

There were specific years where correlations had both positive and negative spikes. However, these spikes occur across different years for each of the three zones (except 2012). The effect of SST anomalies on chl-a anomalies and chl-a concentrations may be constrained or elevated within different zones because of other physical drivers influencing phytoplankton dynamics at that time. The highest positive correlation of 0.20 was observed in 2003 within the transition zone. The lowest negative correlation of -0.13 was observed in 1998, also within the transition zone. However, these positive and negative correlations still remain low. Overall, the correlation values for all zones throughout the 20 year period were highly variable with an overall mean close to zero. Therefore, there is no evidence to suggest correlations between SST and chl-a anomalies in the Ross Sea has changed systematically over this 20-year data set.

3.3.4. El Niño analysis

Finally, I tested if average correlation coefficients for different zones varied between El Niño vs non El Niño years. More specifically, I hypothesised that correlation values will vary during El Niño years compared to non-El Niño years. There is robust evidence to suggest that during El Niño events, impacts on phytoplankton appear throughout the world's oceans, however, they are greatest in the tropics and subtropics (Racault et al., 2017). An El Niño event is characterised by warmer than average SST (Behrenfeld et al., 2016), furthermore, the transition into an El Niño year corresponds to more significant monthly anomalies of chl-a compared to non- El Niño years (Behrenfeld et al., 2006; Hobday et al., 2016; Liu et al., 2019; Zhang et al., 2014). El Niño years during this study period were 1998, 2003, 2005, 2007, 2010, 2014, 2015 and 2016 (El Niño, n.d., para. 3)

The Anova analysis (Table 3.5) showed no interaction effects between El Niño year, zone and season ($p > 0.1$) or any individual effect of El Niño year (0.602) or zone (0.0703). However, there was, again, a significant difference in correlation coefficients between seasons (<0.001). Again, the post-hoc Tukey test found a significant difference between the summer and autumn season for both El Niño (0.00549) and non- El Niño years (0.0187).

Figure 3.6 show the average correlation coefficients for El Niño years and non-El Niño years for the coastal, transition and open ocean zone in the Ross Sea. Positive correlations are observed in the coastal zone for both El Niño years and non-El Niño years, 0.036 and 0.035, respectively. Positive correlations were also observed in the transition zone for both El Niño years and non-El Niño years, 0.034 and 0.036, respectively. In both cases these values are extremely similar and therefore suggest no difference between the two types of years. Finally, in the open ocean average correlation coefficients during non-El Niño years were also positive (0.011), however, during El Niño they were negative (-0.05). Again, these values are extremely similar with significant overlap of standard error, therefore suggesting no difference between the two types of years.

3.4. Discussion

The Ross Sea region is the most productive region for phytoplankton in Antarctica's coastal zone (Deppeler & Davidson, 2017). Despite an increase in chl-a from 1981 to 2019 across the entire SO (Pinkerton, 2019) it is important to better understand a possible link to climate change on the regional scale. Considering Pinkerton (2019) found the highly

productive Ross Sea region to be decreasing in chl-a compared to the SO as a whole, I set out to test correlation patterns between chl-a and SST at the regional scale. I used Arrigo et al. (2008) as a framework study to perform a pixel by pixel correlation analysis between monthly SST and chl-a concentration anomalies for each month from January 1998 to December 2018 in the Ross Sea region to address the following three key questions:

1) Do monthly SST anomalies from 1998-2018 in the Ross Sea region correlate with chlorophyll-a concentration anomalies?
2) Do correlation levels vary between the Southern coastal zone (>75°S), transition zone (75°S - 70°S) and Open Ocean (70°S - 60°S) of the Ross Sea?
3) Do correlations for different zones vary systematically across different time-scales, including monthly, seasonal, annual and between El Niño vs non El Niño years?

3.4.1. Correlation between SST and chl-a concentration anomalies

Correlation coefficients between monthly anomalies of SST and chl-a from 1998-2018 in the Ross Sea region were analysed. The results showed both positive and negative correlation patterns, albeit small. The largest positive correlation was found within the summer month of December for the coastal zone (0.090) and the largest negative correlation was found within the autumn month of March in the open ocean zone (-0.043). These low correlation patterns are to be expected because the analysis did not control for any other influential variables on chl-a in the Ross Sea. The use of satellite remote sensing and lack of *in situ* observations in this research prevented additional influences such as nutrient concentrations, salinity levels, grazing pressure from herbivores, areas of upwelling, location of fronts, movement of currents and impacts of mesoscale eddies to be considered. However, the aim of this research was to solely focus on the impact of SST anomalies on chl-a concentrations in the Ross Sea region, therefore, these variables were not essential in answering the first key question.

Similar low but significant correlation patterns were found in a study by Macias et al. (2018) in the Mediterranean Sea. Modelled SST and chl-a anomaly maps under different scenarios showed no coherent spatial correlation, but a rather widespread scattered response between variables. Ultimately, the anomalies in this study and the modelled anomalies in Macias et al. (2018) were limited in terms of spatial and temporal resolution. This could have severely impacted the level of correlation between the two variables. More specifically, the SST and chl-a anomalies used in this study had a spatial resolution of 9km and a temporal resolution of one month. This level of temporal resolution could mask the intense short term spikes in temperature if balanced out by subsequent drops in SST during the same month (Hobday et al., 2016). Since phytoplankton are unicellular, short-lived and fast growing, they can respond rapidly to any changes in the physical characteristics of their habitat, for example, SST (Feng et al., 2015; Maranón, Cermeno, Latasa, & Tadonléké, 2012; Trainer et al., 2019). Therefore, a spike in local SST could likely influence a spike in local chl-a concentration. However, by working on a monthly timescale short term information is missed and due to the high spatio-temporal variability of chl-a, monthly climatology is not appropriate (Frenger, Münnich, & Gruber, 2018).

3.4.2. Zonal effect

The second key question was to see whether correlation values varied between different spatial zones in the Ross Sea. These three sub-zones; a coastal zone (>75°S), a transition zone (75°S to 70°S) and an open water zone (70°S to 60°S) were defined by latitude so the arrangement of vectors was consistent and accurate for all replicates. The results from all Anova analyses however showed that there was no significant effect of zone. Therefore, correlation levels did not significantly vary between the coastal zone (>75°S), transition zone (75°S - 70°S) and Open Ocean (70°S - 60°S) of the Ross Sea. Although a significant result could not be confirmed in this study, it has been previously documented in the literature that zones within a region can exhibit different relationships when correlating SST and chl-a anomalies. For example, significant positive relationships between SST and chl-a anomalies have indicated a larger importance of the physiological control of growth rates by temperature in coastal zones within the Mediterranean Sea. However, in open water zones significant negative relationships were found and linked to freshwater flow modification in that region (Macias, Stips, Garcia-Gorriz, & Dosio, 2018). Their contrasting result suggests that this study requires more depth than zone allocation by latitude (See section 3.4.5). My Anova results for the independent effect of zone showed p values <0.1 for all analyses. However, a more definitive allocation of boundaries beyond the simplistic coastal, transition and open ocean model could see a significant effect (<0.05).

3.4.3. Timescale and environmental forcing effect

I tested whether correlations for different zones varied systematically across different time-scales, including monthly, seasonal, annual and between El Niño vs non El Niño years. The results varied for each time scale and, similar to Liu (2018) in China's Yellow Sea, correlation coefficients remained low, yet significant effects were confirmed in some cases. A highly significant difference in correlation coefficients occurred between months ($p = <0.001$), i.e., more specifically, between March and December, representing the coldest and warmest months in the year. This result, coupled with the interchange of positive correlations in the warmer months and negative correlations in the cooler months, confirmed my hypothesis and showed that correlations varied across monthly time scales. Unfortunately, due to the large gap in the data set (from May to August) these monthly results provide limited information for the analysis of long term trends over inter-annual to decadal time scales.

Another highly significant difference in correlation coefficients occurred between seasons ($p = <0.001$), i.e. between autumn and summer, again representing the coldest and warmest seasons in the year. This result, coupled with the interchange of positive correlation trends in spring and summer and negative correlations in winter, confirmed my hypothesis and showed that correlations varied across seasonal time scales.

On the annual time scale, there was an interaction effect found between zone and years ($p = 0.030$) as well as a single factor effect of year ($p = 0.035$). These results confirmed my hypothesis that average correlations would vary between years, with different zones demonstrating different trends. However, the results from the linear regression analysis demonstrated very low R^2 values for the coastal, transition and open ocean zones (0.079,

0.031 and 0.020, respectively). This result supports my additional hypothesis that a 20 year data set is not sufficient to detect general increases or decreases in correlation trends associated with climate change.

Finally, regarding correlation patterns between El Niño vs non-El Niño years my hypothesis was rejected. In all zones average correlation coefficients remained similar even though El Niño events previously have been shown to affect phytoplankton productivity throughout the world's oceans (Racault et al., 2017). This effect does not appear to be as significant in the SO Ross Sea region compared to other sub-tropical and tropical regions.

3.4.4. Remote sensing limitations

Satellite measurements of SST and chl-a are useful remote sensing techniques to quantify the temporal and spatial aspect of anomalies on large scales. Due to the much higher spatial and temporal capabilities of satellites compared to the complexities of gathering *in situ* data from ships (Brewin et al., 2014), remote sensing is the principle source of data for assessing changes to phytoplankton biomass, especially in the SO However, it is important to note the types of limitations associated with this type of data analysis.

First, although this study involved the careful integration SeaWiFS and Aqua MODIS satellite data to create a 20 year long data set, the time series is not sufficient to capture a general increase or decrease in correlation trends between SST and chl-a anomalies associated with climate change. Either alternative methods are adopted for this type of research or we wait for an advancement in satellite observations as currently, individual satellites only have a planned lifetime of ca. 10 years (Pinkerton, 2019).

Second, the temporal resolution of the data set (one month) could have masked any intense short term spikes in temperature if balanced out by subsequent drops in SST during the same month (Hobday et al., 2016). This limitation suggests that the more traditional approach of correlating SST anomalies and chl-a on a pixel-by-pixel scale for the Ross Sea lacked depth. Quite often in remote sensing applications data is limited to certain capabilities, in this case, data with higher spatial and temporal resolutions could have seen larger correlation patterns emerge for specific regions or timescales.

Furthermore, high quality validation data was absent in this study and can result in a decrease in the level of certainty in data sets (Yang et al., 2013). For example, the OISST product uses a combination of platform observations, including satellites, ships and buoys, on a global grid. Interpolation methods are also used to create a spatially complete SST map. However, in the SO a key limitation is that these *in situ* observations are sparse. Data are less reliable when interpolated or worse, extrapolated. Therefore, it should be stressed that while the SO remains an influential region for climate research and a knowledge gap in subsequent ocean colour research, more effort should be placed on satellite validation and *in situ* observations.

3.4.5. Future research

This study worked towards a baseline to better understand a possible impact of climate change in the Ross Sea region. More specifically, this research sought out to test

correlation patterns between chl-a and SST at the regional scale following results from Pinkerton (2019) which found the highly productive Ross Sea region to be decreasing in chl-a compared to the SO as a whole. Therefore, it is important that future research build upon these findings and take into consideration the suggestions and limitations outlined. First, the definition I used for an anomaly was problematic with respect to the spatial and temporal resolution of the data set. A more qualitative definition which accounts for specific regional, local and temporal ranges of SST should have been applied. In accordance with Dunstan et al. (2018), this would ensure that average SST and chl-a concentrations on even smaller scales were not smoothed out. Moving forward, it is important that a clear definition of anomalously warm events is adopted in future comparable SO studies to ensure consistency within the literature. Second, for a first attempt analysis, latitude was an effective way to reliably assign zones to the Ross Sea region. However, a future analysis should create more dynamic zonal boundaries by defining the location of fronts (boundaries between regions of water characterised by temperature and salinity) and sea ice extents, as they are known to influence SO phytoplankton dynamics (Boyd et al., 2000; Knox, 2007).

3.4.6. Conclusions

A recent analysis by Pinkerton (2019) demonstrated an increase in chl-a concentrations from 1981 to 2019 across the entire SO. However, in the same study chl-a concentrations were also found to have decreased in the Ross Sea region. My study aimed to better understand impacts of climate change in this particular region by building on the research by Arrigo et al. (2008). More specifically, I performed a pixel by pixel correlation analysis between monthly SST and chl-a concentration anomalies for each month from January 1998 to December 2018 in the Ross Sea region.

This analysis addressed three research questions. First, I asked if monthly SST anomalies correlate with chl-a concentration anomalies? Here, I found evidence of both positive and negative correlation patterns between monthly SST and chl-a anomalies in the Ross Sea between 1998 and 2018. These correlations were small and potentially impacted by the spatial and temporal resolution of the data set. Secondly, I asked if these correlation levels varied between spatial zones? Anova analyses showed no significant differences amongst the coastal zone (>75°S), transition zone (75°S - 70°S) and Open Ocean (70°S - 60°S) in the Ross Sea. However, a future analysis with zones allocated by physical forces in the SO, such as fronts, currents and sea ice extent, could see different results if regional SST anomalies continue to occur with anthropogenic climate change. Finally, I asked if correlations for different zones vary systematically across different time-scales and between El Niño vs non-El Niño years? Here I found a highly significant difference in correlation coefficients between both months and seasons. Additionally, there was a significant interaction effect between zone and year as well as a significant single factor effect of year. However, there was no significant difference in correlations between El Niño versus non-El Niño years.

Ultimately this research has identified significant correlations, albeit with low coefficients, between chl-a and SST anomalies in the Ross Sea. Other research has largely focused on temperate, sub-tropical and tropical latitudes (Behrenfeld et al., 2006; Kitsiou & Topouzelis, 2014; Li et al., 2018; Liu et al., 2019; Macias et al., 2018; Xue et al., 2014). Therefore, it is fundamental that future research aim to better understand the effects of SST

anomalies on phytoplankton dynamics at the regional scale in the SO and to fill this knowledge gap.

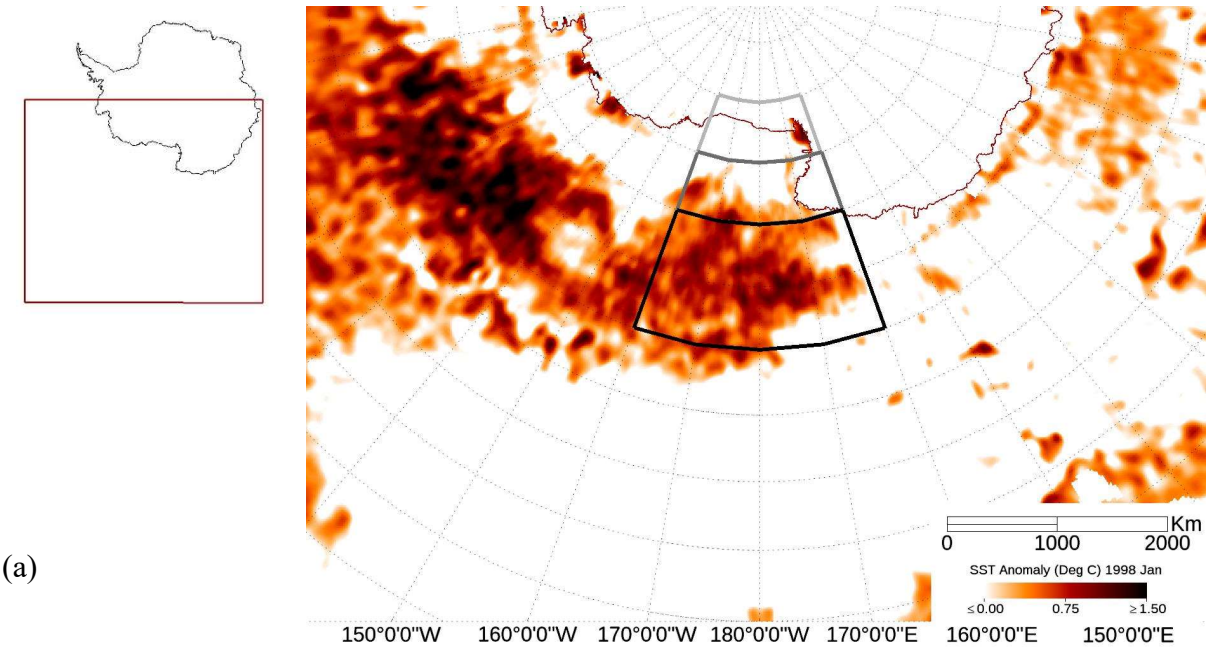

(a)

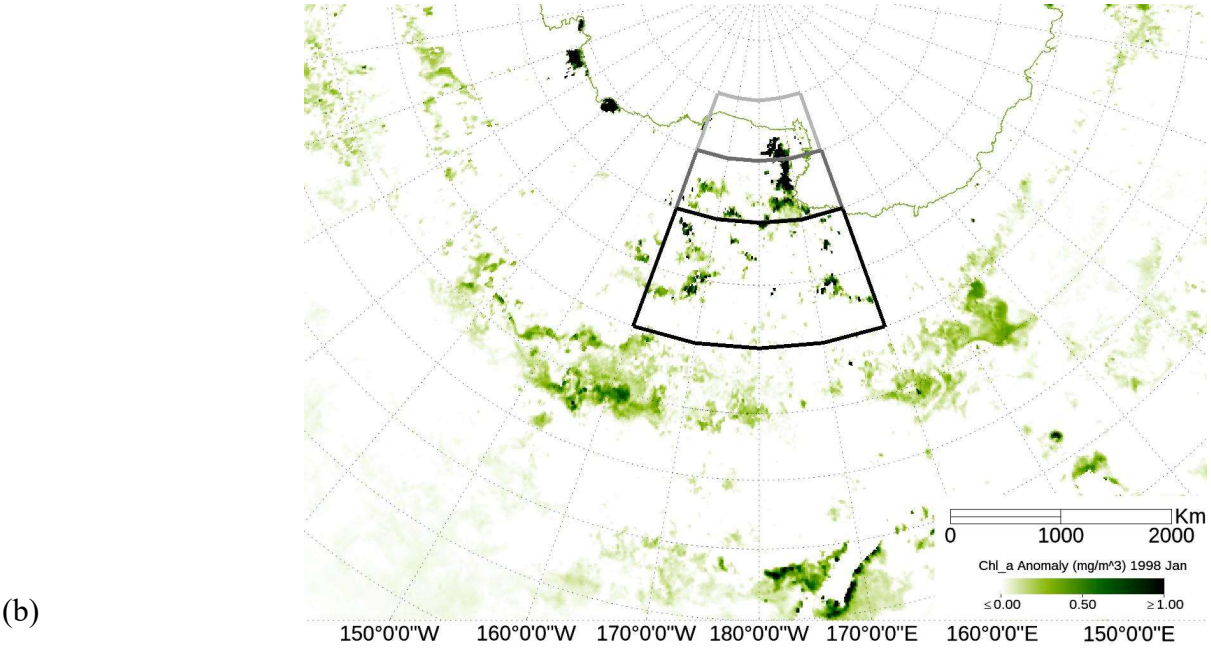

(b)

Figure 3.1. Satellite image products from January 1998. The gridlines layer shows lines of latitude in intervals of 5 degrees and longitude in intervals of 10 degrees. The Ross Sea region is considered the area of water between 160 degrees West and 160 degrees East with a northern limit of 60 degrees South. The light grey vector layer outlines the coastal zone (>75°S), the dark grey vector layer outlines the transition zone (75-70°S) and the black vector layer outlines the open water zone (70-60°S). **a)** SST anomaly image. Positive SST anomalies vary in colour from white to deep red. White indicates either no SST anomaly, a negative anomaly or land. **b)** Chlorophyll-a anomaly image. Chlorophyll-a anomalies vary in colour from white to deep green. White indicates either no chlorophyll-a anomaly, a negative anomaly or land.

(a)

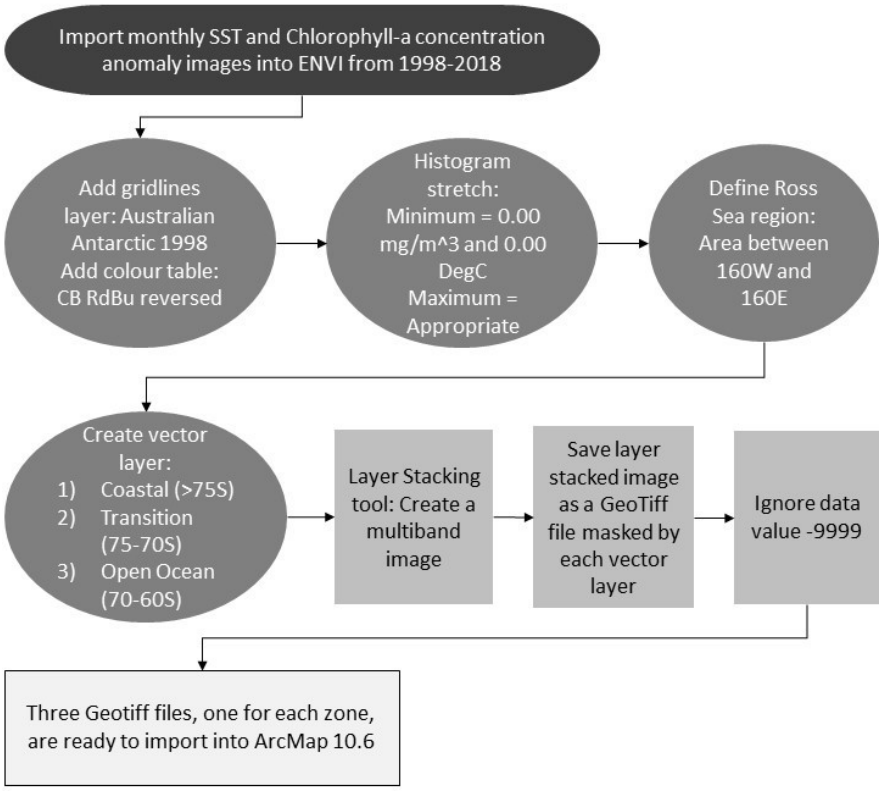

(b)

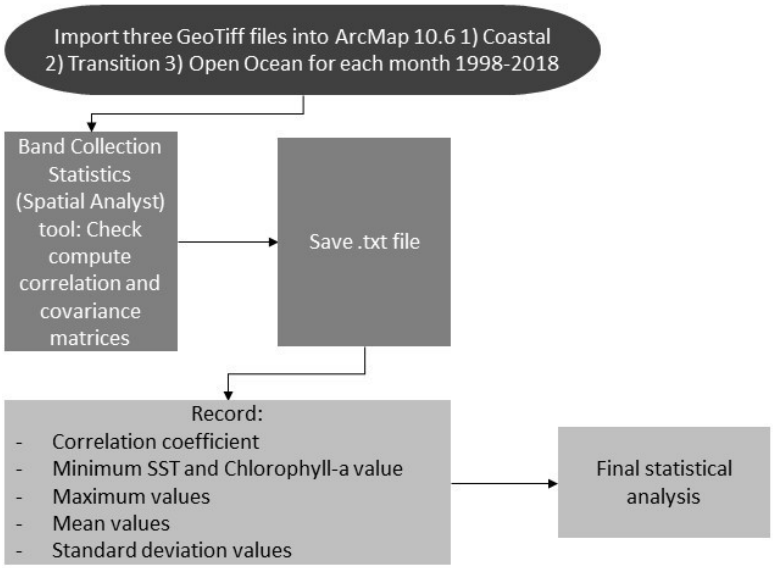

Figure 3.2 (a) Processing summary for analysis in ENVI 5.5. Including image input (oval), image modification (circles) and the use of the vector tool, layer stacking tool and masking process (squares). The result is three multiband GeoTiff files containing the SST and Chlorophyll-a concentration anomaly images, masked different zones (rectangles). (b) Processing summary for analysis in ArcMap10.6. Including input of images (oval), use of the band collection statistics/ spatial analyst tool (squares) and appropriate data collection for the final statistical analysis (rectangles).

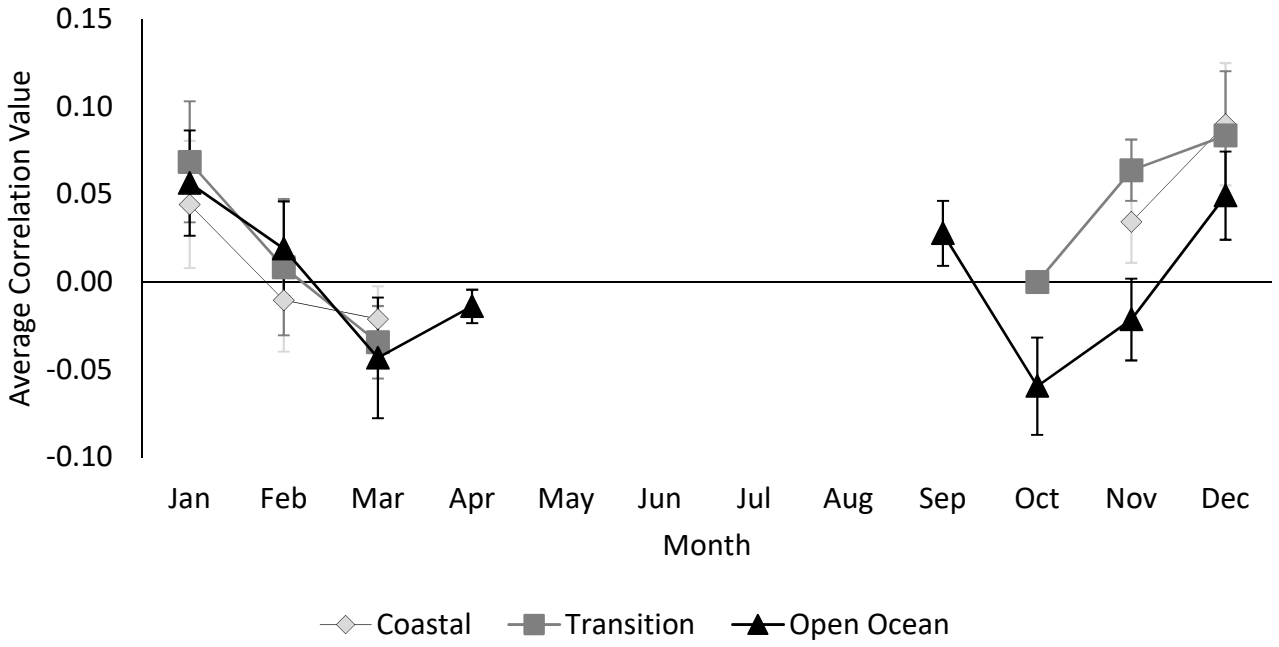

Figure 3.3 Average monthly correlation coefficients per month between SST and chl-a anomalies in the Ross Sea region from 1998 to 2018 for the coastal (white), transition (grey) and open ocean (black) zone (± SE). Positive and negative correlation values reflect that as SST anomalies increases, chl-a anomalies increase or decrease, respectively. Missing winter data reflect months with high cloud and ice cover.

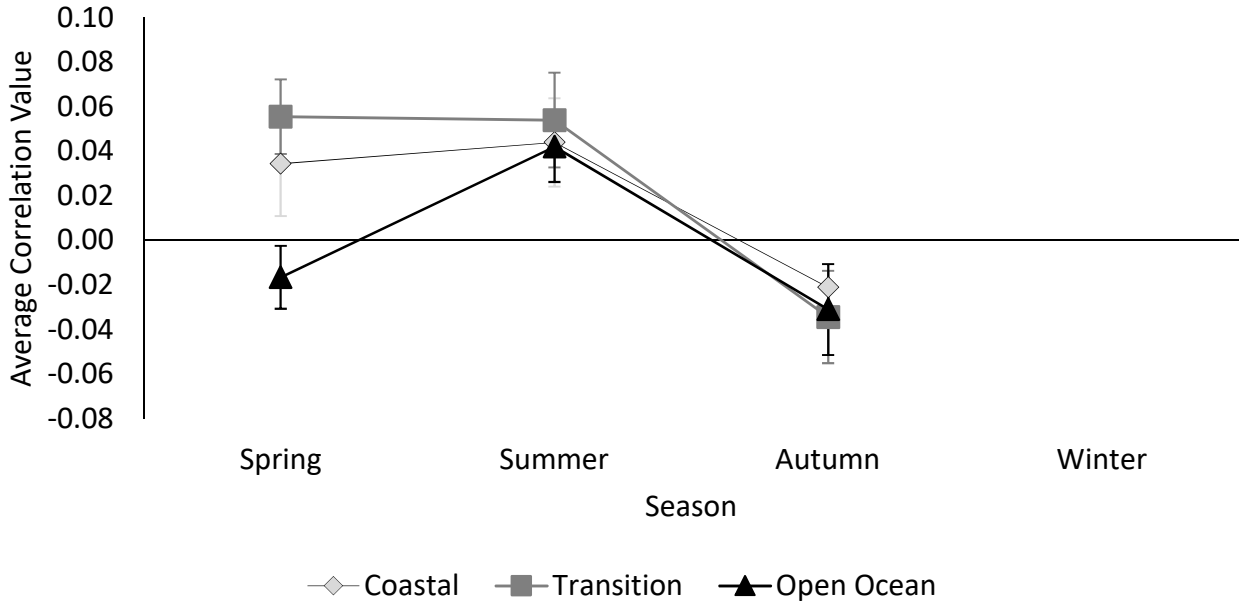

Figure 3.4. Average seasonal correlation coefficients between SST and chl-a anomalies in the Ross Sea region from 1998 to 2018 (± SE) for spring, summer, and autumn for the coastal (white), transition (grey) and open ocean (black) zone. Positive and negative correlation values reflect that as SST anomalies increases, chl-a anomalies increase or decrease, respectively. Missing winter data reflect high cloud and ice cover.

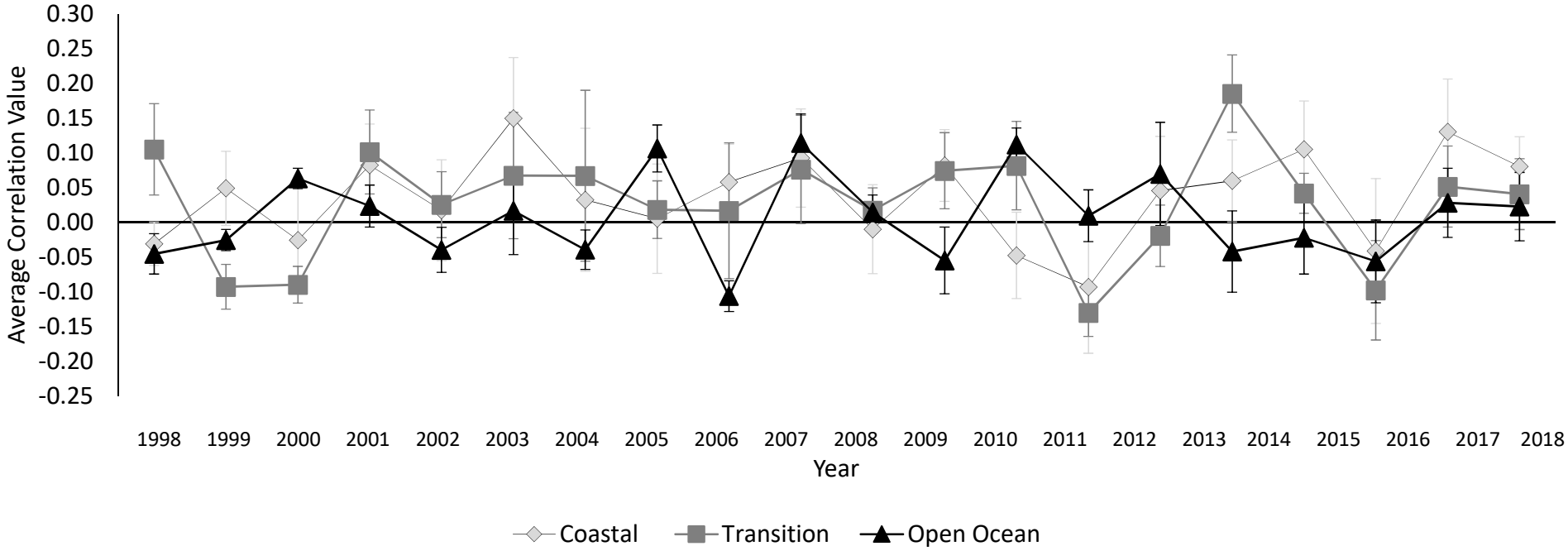

Figure 3.5. Average yearly correlation coefficients (1998-2018) between SST and chl-a anomalies in the Ross Sea region (± SE) for the coastal (white), transition (grey) and open ocean (black) zones. Positive and negative correlation values reflect that as SST anomalies increases, chl-a anomalies increase or decrease, respectively.

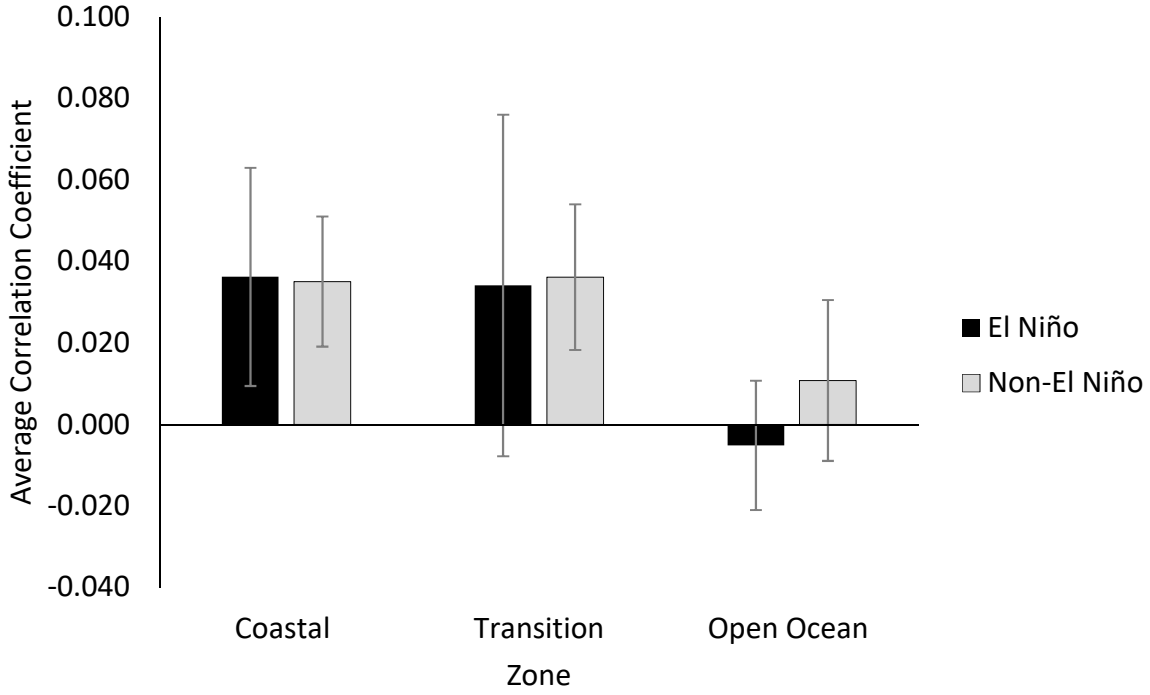

Figure 3.6. Average correlation coefficients between SST and chl-a anomalies in the Ross Sea region (± SE) for El Niño (black) and non-El Niño (white) years for the coastal, transition and open ocean zones. Positive and negative correlation values reflect that as SST anomalies increases, the chl-a anomalies increase or decrease, respectively.

Table 3.1 Correlation results and average values for anomalies of SST and chl-a concentration in the Ross Sea between 1998 and 2018.

Season/ Zone / Month	Average correlation	Mean SST anomalies	Mean chl-a anomalies	Number of observations
		°C	mg/m-3	
Spring	**0.008**			
Coastal	*0.042*	*-0.025*	*0.044*	*21*
September				
October				
November	0.042	-0.025	0.044	21
Open Ocean	*-0.018*	*-0.081*	*-0.012*	*63*
September	0.028	-0.065	-0.002	21
October	-0.059	-0.096	-0.001	21
November	-0.021	-0.081	-0.032	21
Transition	*0.056*	*-0.031*	*-0.024*	*16*
September				
October	0.000	0.035	0.000	1
November	0.059	-0.035	-0.026	15
Summer	**0.046**			
Coastal	*0.041*	*-0.073*	*-0.070*	*63*
December	0.090	-0.027	-0.183	21
February	-0.010	-0.024	0.047	21
January	0.044	-0.168	-0.075	21
Open Ocean	*0.042*	*-0.099*	*-0.008*	*62*
December	0.051	-0.106	-0.013	21
February	0.019	-0.129	-0.006	20
January	0.057	-0.065	-0.006	21
Transition	0.054	-0.032	-0.051	63
December	0.084	-0.024	-0.111	21
February	0.009	-0.017	-0.010	21
January	0.069	-0.054	-0.031	21
Autumn	**-0.028**			
Coastal	*-0.021*	*-0.015*	*0.075*	*6*
March	-0.021	-0.015	0.075	6
April				
May				
Open Ocean	*-0.031*	*-0.109*	*-0.004*	*36*
March	-0.043	-0.104	-0.005	21
April	-0.014	-0.117	-0.002	15
May				
Transition	*-0.034*	*-0.010*	*-0.034*	*21*
March	-0.034	-0.010	-0.034	21
April				
May				
Total Averages	**0.021**	**-0.066**	**-0.025**	

Table 3.2 Anova: Variation of correlation trends between SST and chl-a anomalies at monthly and three spatial scales (Zone: coastal, transition, open ocean).

Significant factors (P < 0.05) are shown in bold

Test	Treatment	s.s.	d.f.	F	P
Monthly	Zone	0.094	2	2.724	0.067
	Month	0.524	7	4.32	**<0.001**
	Zone X Month	0.073	9	0.466	0.897
	Error	5.750	332		

Table 3.3 Anova: Variation of correlation trends between SST and chl-a anomalies at seasonal and three spatial scales (Zone: coastal, transition, open ocean).

Significant factors (P < 0.05) are shown in bold

Test	Treatment	s.s.	d.f.	F	P
Seasonal	Zone	0.094	2	2.676	0.070
	Season	0.254	2	7.211	**<0.001**
	Zone X Season	0.062	4	0.881	0.476
	Error	6.030	342		

Table 3.4 Anova: Variation of correlation trends between SST and chl-a anomalies at annual and three spatial scales (Zone: coastal, transition, open ocean).

Significant factors (P < 0.05) are shown in bold

Test	Treatment	s.s.	d.f.	F	P
Annual	Zone	0.094	2	2.841	0.060
	Year	0.56	20	1.686	**0.035**
	Zone X Year	1.005	40	1.513	**0.030**
	Error	4.782	288		

Table 3.5 Anova: Variation of correlation trends between SST and chl-a anomalies for El Niño years, at seasonal and three spatial scales (Zone: coastal, transition, open ocean).

Significant factors (P < 0.05) are shown in bold

Test	Treatment	s.s.	d.f.	F	P
El Niño	Zone	0.094	2	2.65	0.072
	El Niño Year	0.005	1	0.273	0.602
	Season	0.255	2	7.151	**<0.001**
	Zone X El Niño Year	0.003	2	0.074	0.929
	Zone X Season	0.062	4	0.874	0.480
	El Niño Year X Season	0.069	2	1.935	0.146
	Zone X El Niño Year X Season	0.026	4	0.366	0.833
	Error	5.928	333		

References

Alvain, S., Moulin, C., Dandonneau, Y., & Loisel, H. (2008). Seasonal distribution and succession of dominant phytoplankton groups in the global ocean: A satellite view. *Global Biogeochemical Cycles, 22*(3). https://doi.org/10.1029/2007GB003154

Arrigo, K. R., van Dijken, G. L., & Bushinsky, S. (2008). Primary production in the Southern Ocean, 1997-2006. *Journal of Geophysical Research: Oceans, 113*(8). https://doi.org/10.1029/2007JC004551

Banzon, Viva, Reynolds, Richard & National Centre for Atmospheric Research Staff (Eds). Last modified 25 June 2019. "The Climate Data Guide: SST data: NOAA High-resolution (0.25x0.25) Blended Analysis of Daily SST and Ice OISSTv2." Retrieved from https://climatedataguide.ucar.edu/climate-data/sst-data-noaa-high-resolution-025x025-blended-analysis-daily-sst-and-ice-oisstv2

Behrenfeld, M. J., O'Malley, R. T., Siegel, D. A., McClain, C. R., Sarmiento, J. L., Feldman, G. C., . . . Boss, E. S. (2006). Climate-driven trends in contemporary ocean productivity. *Nature, 444*(7120), 752-755. https://doi.org/10.1038/nature05317

Boyd, P.W., Watson, A. J., Law, C. S., Abraham, E. R., Trull, T., Murdoch, R., . . . Zeldis, J. (2000). A mesoscale phytoplankton bloom in the polar Southern Ocean stimulated by iron fertilization. *Nature, 407*(6805), 695-702. https://doi.org/10.1038/35037500

Brewin, R. J. W., Mélin, F., Sathyendranath, S., Steinmetz, F., Chuprin, A., & Grant, M. (2014). On the temporal consistency of chlorophyll products derived from three ocean-colour sensors. *ISPRS Journal of Photogrammetry and Remote Sensing, 97*, 171-184. https://doi.org/10.1016/j.isprsjprs.2014.08.013

Deppeler, S. L., & Davidson, A. T. (2017). Southern Ocean phytoplankton in a changing climate. *Frontiers in Marine Science, 4*(FEB). https://doi.org/10.3389/fmars.2017.00040

Dunstan, P. K., Foster, S. D., King, E., Risbey, J., O'Kane, T. J., Monselesan, D., . . . Thompson, P. A. (2018, 2018/10/02). Global patterns of change and variation in sea surface temperature and chlorophyll a. *Scientific Reports, 8*(1), 14624. https://doi.org/10.1038/s41598-018-33057-y

El Niño. (n.d.). In *Wikipedia.* Retrieved November 26, 2019, from https://en.wikipedia.org/wiki/El_Ni%C3%B1o

Feng, J., Durant, J. M., Stige, L. C., Hessen, D. O., Hjermann, D. Ø., Zhu, L., . . . Stenseth, N. C. (2015). Contrasting correlation patterns between environmental factors and chlorophyll levels in the global ocean. *Global Biogeochemical Cycles, 29*(12), 2095-2107. https://doi.org/10.1002/2015gb005216

Frenger, I., Münnich, M., & Gruber, N. (2018). Imprint of Southern Ocean mesoscale eddies on chlorophyll. *Biogeosciences, 15*(15), 4781-4798. https://doi.org/10.5194/bg-15-4781-2018

Hobday, A. J., Alexander, L. V., Perkins, S. E., Smale, D. A., Straub, S. C., Oliver, E. C. J., . . . Wernberg, T. (2016). A hierarchical approach to defining marine heatwaves. *Progress in Oceanography, 141*, 227-238. https://doi.org/10.1016/j.pocean.2015.12.014

Kitsiou, D., & Topouzelis, K. (2014, 01/01). Correlation between chlorophyll a concentration and sea surface temperature in the eastern mediterranean sea using gis and satellite data. *Fresenius Environmental Bulletin, 23*, 2919-2925.

Knox, G. A. (2007). *Biology of the Southern Ocean* (2nd ed.). Boca Raton: CRC Press/Taylor & Francis.

Li, W., El-Askary, H., Qurban, M. A., Proestakis, E., Garay, M. J., Kalashnikova, O. V., . . . Manikandan, K. P. (2018). An assessment of atmospheric and meteorological factors regulating Red Sea phytoplankton growth. *Remote Sensing, 10*(5). https://doi.org/10.3390/rs10050673

Liu, C., Sun, Q., Xing, Q., Wang, S., Tang, D., Zhu, D., & Xing, X. (2019). Variability in phytoplankton biomass and effects of sea surface temperature based on satellite data from the Yellow Sea, China. *PloS one, 14*(8), e0220058-e0220058. https://doi.org/10.1371/journal.pone.0220058

Macias, D., Stips, A., Garcia-Gorriz, E., & Dosio, A. (2018). Hydrological and biogeochemical response of the Mediterranean Sea to freshwater flow changes for the end of the 21st century. *PloS one, 13*(2), e0192174. https://doi.org/10.1371/journal.pone.0192174

Maranón, E., Cermeno, P., Latasa, M., & Tadonléké, R. D. (2012). Temperature, resources, and phytoplankton size structure in the ocean. *Limnology and Oceanography, 57*(5), 1266-1278.

NASA Goddard Space Flight Centre. *Moderate Resolution Imaging Spectroradiometer (MODIS).* Retrieved August 22, 2019, from https://modis.gsfc.nasa.gov/about/

NASA Goddard Space Flight Centre. *Ocean Colour Web: SeaWiFS.* Retrieved September 13, 2019, from https://oceancolor.gsfc.nasa.gov/data/seawifs/

Pinkerton, M. (2019). Change in environmental conditions of the Southern Ocean observed by satellites and data-assimilating models between 1981 and 2019. Report presented for consideration from CCAMLR. WG-EMM-2019/39.

Racault, M.-F., Sathyendranath, S., Brewin, R. J. W., Raitsos, D. E., Jackson, T., & Platt, T. (2017, 2017-May-08). Impact of El Niño Variability on Oceanic Phytoplankton. *Frontiers in Marine Science, 4*(133). https://doi.org/10.3389/fmars.2017.00133

Trainer, V. L., Moore, S. K., Hallegraeff, G., Kudela, R. M., Clement, A., Mardones, J. I., & Cochlan, W. P. (2019, 2019/05/03/). Pelagic harmful algal blooms and climate change: Lessons from nature's experiments with extremes. *Harmful Algae*. https://doi.org/https://doi.org/10.1016/j.hal.2019.03.009

Xue, C. J., Dong, Q., & Fan, X. (2014). Spatiotemporal association patterns of multiple parameters in the northwestern Pacific Ocean and their relationships with ENSO. *International Journal of Remote Sensing, 35*(11-12), 4467-4483. https://doi.org/10.1080/01431161.2014.916436

Zhang, H., Han, Z., Zhao, J., Yu, P., Hu, C., Sun, W., . . . Vetter, W. (2014, December 01). Phytoplankton and chlorophyll a relationships with ENSO in Prydz Bay, East Antarctica. *Science China Earth Sciences, 57*(12), 3073-3083. https://doi.org/10.1007/s11430-014-4939-8

Chapter Four

Marine Heatwave Remote Sensing Analysis

4.1. Introduction

Over the last few decades research has focused on impacts from gradual and slow increase in temperatures. However, extreme events, such as 'marine heatwaves' (MHWs) have recently been shown to drive sudden and dramatic shifts to the functioning and structure of ecosystems (Smale et al., 2019). Thus, the concept of MHWs has gained significant traction in both the scientific literature (Frölicher, Fischer, & Gruber, 2018; Holbrook et al., 2019; Oliver et al., 2018; Smale et al., 2019; Thomsen et al., 2019) as well as in the latest IPCC Special Report on the Oceans and Cryosphere (IPCC, 2019). Dramatic increases in short term oceanic warm anomalies, hereafter referred to as MHWs, are defined as anomalously warm events during which temperatures exceed the climatic 90th percentile persisting for >5 days. These events are likely caused by anthropogenic activities, in particular burning of fossil fuels (IPCC, 2019). Thus, MHWs cannot only be explained by natural climate variability and they are becoming more frequent, extensive and intense (Frölicher, Fischer, & Gruber, 2018; Oliver et al., 2018; Smale et al., 2019).

Phytoplankton are useful organisms to monitor to gauge the state of ocean biology. Most phytoplankton species have fast turnover rates (from hours to days) and can create extensive and dense blooms whenever light, nutrient and temperature conditions are optimal through rapid exponential growth. Spatio-temporal variability in phytoplankton blooms therefore largely reflects variability in their surrounding environment (Maranón, Cermeno, Latasa, & Tadonléké, 2012). Phytoplankton blooms can occur on a relatively small scale or extend over hundreds of square kilometres (Garrison, 2005) making observations from satellites possible.

Furthermore, it is essential that phytoplankton dynamics in response to physical variables are understood because they form the base of marine food-webs which sustain the diversity and wealth of iconic wildlife. For example, in the Southern Ocean (SO) krill, penguins, seabirds, seals and whales ultimately depend on these marine protists for their food (Deppeler & Davidson, 2017; Doney, 2010). It is of vital importance to consider the "unseen majority" in climate change research, as these microorganisms support humans, and every other life form as a direct food source or via trophic interactions and biogeochemical cycling (Cavicchioli et al., 2019). Any change in community composition, species type, phenology of blooms and the ecological boundaries of SO phytoplankton will in turn affect higher trophic levels if grazers and predators do not have time to adapt (Dutkiewicz et al., 2019; Li, Ji, Jenouvrier, Jin, & Stroeve, 2016).

Several other studies have analysed relationships between sea surface temperatures (SST) anomalies (and/ or MHWs) and oceanic chlorophyll concentrations. However, these studies are all from temperate, sub-tropical and tropical regions. For example, 2013-2016 SST anomalies have been shown to have negative effects on phytoplankton biomass and subsequently also on higher trophic levels off the California Current (Gómez-Ocampo, Gaxiola-Castro, Durazo, & Beier, 2018; Trainer et al., 2019). I hypothesised that

phytoplankton chl-a will increase (instead of decrease) in summer months in response to MHWs that are conceptually very similar to highly positive SST anomalies, because many polar phytoplankton species are temperature limited (Boyd, 2019). For example, physiological experiments on a key polar diatom, *Proboscia enermis*, showed a 25% increase in growth rate in response to 3°C of warming. Although if temperatures increased much beyond 3°C it may exceed their thermal maximum (Boyd et al., 2013). Furthermore, positive trends of increased phytoplankton biomass in response to increased SST have been reported from the Arctic (IPCC, 2019).

I tested two key questions in relation to MHWs and their influence on SO primary productivity: do extreme MHWs affect chlorophyll-a concentration in the SO - and if so, do effects vary among regions characterised by different sea surface temperatures and levels of winter ice covering? To address these questions, I applied the MHW definition of Hobday et al. (2016), as often done in recent literature (Frölicher, Fischer, & Gruber, 2018; Holbrook et al., 2019; Oliver et al., 2018; Smale et al., 2019; Thomsen et al., 2019). Chlorophyll-a (chl-a) concentrations were quantified in the SO from remote sensing techniques and ocean colour sensors, as done in many other studies (Alvain et al., 2013; Alvain, Moulin, Dandonneau, & Bréon, 2005; Alvain, Moulin, Dandonneau, & Loisel, 2008; Arrigo, van Dijken, & Bushinsky, 2008; Behrenfeld et al., 2006; Cape, Vernet, Kahru, & Spreen, 2014; Gregg & Rousseaux, 2014; McClain, 2009; Montes-Hugo et al., 2009; Moore & Abbott, 2000). This research is, to my knowledge, the first attempt to apply the MHW identification procedure (Hobday et al., 2016; Hobday et al., 2018) across the SO to gain insight into effects on primary production. Furthermore, this research addresses the "low confidence" conclusions on the influence of MHWs on phytoplankton in the SO highlighted in the latest IPCC Special Report (IPCC, 2019).

4.2. Methods and materials

First, 'extreme' MHWs (Hobday et al., 2018) were identified and grouped into four Southern Ocean zones; the sub-Antarctic zone (SAZ), the permanently open ocean (POOZ), seasonal sea ice zone (SSIZ) and the coastal zone (CZ) from the 'Marine Heatwave Tracker' (explained in detail below), where the two latter zones are more influenced by sea-ice and climatic temperature. Second, high-quality Aqua MODIS satellite imagery (i.e. images with low cloud- and ice-cover) that coincided in space and time with extreme MHWs were identified and analysed by comparing chl-a concentrations in impacted (by MHWs) to non-impacted control areas. When submerged in water, chlorophyll a and b pigments preferentially absorb red and blue light, whilst preferentially reflecting green light (Gordon, Brown, Brown, Evans, & Smith, 1988). Therefore, remote sensing satellite images can be used to measure the ratio of blue light to green light reflected from the ocean surface as a proxy for chl-a concentrations (and indirectly also as proxies for surface phytoplankton biomass and productivity) (see also Chapter 3 for more details about extracting chl-a data from satellite images).

This section outlines the procedures used to identify extreme MHWs in the SO using the online Marine Heatwave Tracker tool. It also describes the acquisition of appropriate Aqua MODIS satellite imagery, the control vs. impact design and analysis in ENVI 5.5. Finally, the statistical data analysis, using a standard Anova and correlation analysis, are described.

4.2.1. Marine heatwave tracker

Extreme marine heatwaves in the Southern Ocean were identified using the marine heatwave tracker (http://www.marineheatwaves.org/tracker.html). This digital tool uses 30 years of baseline data to determine moderate, strong, severe and extreme MHWs, as defined by Hobday et al. (2018), around the globe in near-real time. It hosts all the historic MHW records from 1st January 1982 to two weeks before present day. The tracker calculates MHWs based on the R version of the Hobday et al. (2016) marine heatwave definition. R data can be freely downloaded from https://robwschlegel.github.io/heatwaveR/articles/OISST_preparation.html and MHWs can be detected using this tutorial https://robwschlegel.github.io/heatwaveR/articles/gridded_event_detection.html. This method has been used in several recent studies (Oliver et al., 2018; Smale et al., 2019). Alternatively, it can be done in Python and MATLAB using the same algorithms. The reported MHWs are presented on an even ¼ degree grid over Earth's surface. Quarter degree grid cells divide the longitude and latitude degree square cells into smaller squares to form a system of nodes. Near the poles, these grid cells adopt an elongated trapeze shape. The conversion of decimal degrees coordinates from the marine heatwave tracker into geographical longitude latitude (degrees – minutes – seconds) coordinates in ENVI may cause some distortion due to proximity from the South Pole. The shape of the marine heatwave vector overlay may therefore not be entirely accurate when superimposed on the chl-a map. However, this vector overlay is only a visual guide showing the boundaries of the MHW with respect to the phytoplankton bloom, and it does not impact the analysis.

The global satellite product used in the MHW Tracker to detect temperature anomalies is the daily Optimally Interpolated Sea Surface Temperature (OISST) on board the NOAA satellites. These satellite data allows NOAA to monitor worldwide SST (Yang et al., 2013) and can be freely downloaded from https://www.ncdc.noaa.gov/oisst. Daily OSSIT is constructed by combining a series of platform observations, including satellites, ships and buoys, on a global grid. Interpolation methods create a spatially complete sea surface temperature map. A key limitation to this product is that in high latitudes *in situ* observations are sparse. The daily OSSIT data product has two data versions to reduce systematic error: 1) the Advanced Very High Resolution Radiometer (AVHRR) which is an infrared instrument that cannot see through clouds, and 2) the Advanced Microwave Scanning Radiometer on the Earth Observing System (AMSR-E) which is a microwave instrument that can measure SST during most weather conditions. These records began late 1981 and have continued to the present. In the Polar Regions satellite derived sea ice concentrations serve as the proxy for SST in the marginal ice zone (Banzon et al., 2019). An empirically derived linear regression equation with respect to SST observations allows for interpolation from the POOZ to the SSIZ.

The MHW Tracker has the capability to zoom in on specific regions as well as to specify the temporal range from January 1st, 1992 to the present day. The user can also filter out the different categories of MHWs from moderate to extreme events. Time series data are available for each pixel during a heatwave event. The information obtained provides the geographical location, duration, start date, peak date and end date of the MHW. Furthermore,

immediate feedback is provided on the climatology, threshold and current temperature for any given day during the heatwave (Schlegal, R. W., 2018).

This study focused on extreme MHWs that occurred across more than 5 pixels (>140 km^2) so that the defined MHWs were spatially large events, rather than small hotspots of increased SST. Additionally, data were only sourced in the summer months (November, December, January and February) from 1982 to 2018 because plankton will not be light limited and there is less sea ice coverage making ocean colour and SST measurements viable, as has been previously argued by Frölicher, Fischer, & Gruber (2018).

4.2.2. Aqua MODIS satellite data

The second stage of this study was to extract high quality Aqua MODIS satellite imagery which coincided with the identified extreme MHWs. Moderate Resolution Imaging Spectroradiometer (MODIS) is a sensor on the Aqua satellite that passes south to north over the equator in the afternoon. The Aqua satellite covers the entire Earth's surface every 1-2 days, acquiring data in 36 wavelength bands. MODIS is suitable for level-2 data (georeferenced and calibrated data with variables at the same resolution and location) and level-3 data (as level 2, but with variables mapped on uniform space-time grid scales for completeness and constancy). Level-2 Ocean Colour data was obtained from the NASA Ocean Colour Level 1 &2 Data Browser (https://oceancolor.gsfc.nasa.gov/cgi/browse.pl?sen=am) and processed using the ENVI Plugin for Ocean Colour (EPOC) extension (see section 4.2.3.1).

Aqua satellite data are available from 4th May 2002. Ocean colour data obtained from the Aqua MODIS sensor was used to determine the chl-a concentration of surface waters in cloud free areas at a spatial resolution of 1 km in near real time. Aqua MODIS have several data products which can be used to measure large-scale phytoplankton dynamics, including the MODIS Chlorophyll-a Concentration (chlor_a) product. The chlor_a product combines two algorithms: 1) the O'Reilly band ratio OC3/OC4 (OCx) algorithm, and 2) the Hu Colour Index (CI) algorithm. The chlor_a product returns the near-surface concentration of Chl-a in mg/m^3. This metric is calculated using an empirical relationship derived from *in situ* measurements of Chl-a and blue-to-green band ratios of *in situ* Remote Sensing Reflectance (RSR) (Blondeau-Patissier, Gower, Dekker, Phinn, & Brando, 2014). Implementation is contingent on the availability of three or more sensor bands spanning the 440-570 nm spectral regime. MODIS RSR is the ratio of upwelling radiance (light reflected by the ocean's surface) to downwelling irradiance (density flux of energy per unit area). Chl-a algorithms use RSR coupled with *in situ* measurements of chl-a to estimate concentrations in mg m^{-3} (Dutkiewicz et al., 2019; Werdell et al., 2018). The retrieved water-leaving radiance measured by each sensor is subsequently normalized to reduce effects of solar orientation and atmospheric attenuation of the down-welling radiation. This produces a normalized water-leaving radiance commonly expressed as radiance reflectance (Rsr). Information regarding the Aqua MODIS sensor and data product algorithms was accessed from the NASA MODIS website (https://modis.gsfc.nasa.gov/).

4.2.3. Data processing

The MHW Tracker was used to systematically identify extreme MHWs week by week starting January 1st, 2002 through to December 29th, 2018. A search was made for evidence of events on the 1st, 8th, 15th, 22nd and 29th (28th in the case of February) of November, December, January and February. For each identified extreme MHW, the time series tool was used to extract associated data related to (a) geographic location, (b) start date, (c) the average climatic temperature, (d) the temperature for the peak date and (e) duration, (f) accumulated intensity, (g) maximum intensity and (h) mean intensity of the MHW.

Similar to Arrigo, van Dijken & Bushinsky (2008) sea ice extent was used to assign each MHW to an ecological province, that is, zones were classified as: the Sub Antarctic Zone (SAZ), the Permanently Open Ocean Zone (POOZ), the Seasonal Sea Ice Zone (SSIZ) and the Coastal Zone (CZ). The National Snow and Ice Data Centre image archive (https://nsidc.org/data/seaice_index/archives) was used to determine province boundaries for the SSIZ and POOZ using maximum sea ice extents. The CZ was defined as being adjacent to land and the SAZ was defined as being between the Sub-Tropical Front and the Polar Front.

The central location and peak date derived for the identified extreme MHW, was used to identify corresponding chlorophyll satellite data that was downloaded in the Network Common Data Form (Net CDF) format (filename extension: .nc) from the NASA Ocean Colour Level 1 & 2 Data Browser. First, the correct date was allocated on the browser. Then, the visible region was specified to 'Antarctic' and the central coordinates were indicated. Appropriation of data was defined as being >80% cloud free across the location of a control vs. impact design experiment (see section 4.2.3.2). If chlorophyll images had high cloud or ice cover on the peak MHW date, the nearest date was chosen instead within five days of the peak with a high-quality image. The time series tool was then used to gather information on the average temperature, threshold temperature and extreme temperature for this new date.

4.2.3.1. ENVI Plugin for Ocean Colour extension

Aqua MODIS ocean products were analysed in ENVI 5.5 *(Exelis Visual Information Solutions, Boulder, Colorado)* using the ENVI Plugin for Ocean Colour (EPOC) extension. This plugin was downloaded from the GitHub toolbox (https://github.com/dawhite/ENVIPlugins) and contains the software package SeaDAS (https://seadas.gsfc.nasa.gov/). NASA SeaDAS aids in the processing, display, analysis and quality control of remote sensing Earth data. SeaDAS can correct for and calibrate atmospheric components to determine Earth/ocean surface level signals. Ultimately, EPOC is a Hierarchical Data Format (HDF) and NetCDF file conversion, re-projection and georeferencing utility for NASA ocean colour datasets such as the chlor_a product used in this study.

For EPOC to recognise the inputted Level-2 data file the first letter has to match the Aqua satellite, i.e. A - - .L2_LAC_OC.nc. Hereafter, EPOC will transfer the raw data into a

georeferenced .hdf file containing the chlor_a data product and modifications can be made to the image (see Figure 4.1).

4.2.3.2. Control vs. Impact analysis design

The primary goal was to test if phytoplankton abundance co-varied with extreme MHWs for surface waters of the SO, using chl-a concentration as a proxy. Chl-a within the spatial location of an extreme MHW (Impacted area) was therefore compared to an adjacent region with 'normal' SSTs (Control area). Following the pre-processing and image modifications in ENVI 5.5, the Aqua MODIS image could be analysed. First, a vector overlay was created using geographic latitude and longitude coordinates for the extreme MHWs. Vector overlays of the severe and strong MHWs were also included for reference of location. However, a vector overlay was not included for moderate heatwaves because their average size far exceeded the chipped view of MODIS images. As noted above, the shape of the MHW may contain minor distortions due to the ¼ degree grid used on the MHW Tracker website compared to the geographic projection in ENVI. It is not essential that the vector overlay is entirely accurate as this is only a general indication for where the extreme, severe and strong sea surface temperatures anomalies are positioned in comparison with normal SSTs. Once the general position of the marine heatwave was identified then impacted and control measurements could be extracted using the region of interest (ROI) tool (see Figure 4.2 for example).

From the spatial centre of the marine heatwave, 250 km and 500 km polylines were drawn along 16 equidistant directions. Control locations of 25 × 25 km ROIs were chosen at distances of 250 and 500 km along each of these lines only where each was >80% cloud-free. These distances were chosen to reflect regions not affected by the heatwave, analogous to Ortiz-Ahumada, Álvarez-Borrego, & Gómez-Valdés (2018) where two 300 km long transects off different coasts were sampled for SST, chl-a and primary production. Quadrants for measurements were also similar in size being 18 × 18 km (Ortiz-Ahumada, Álvarez-Borrego, & Gómez-Valdés, 2018). The impacted area was defined as a >80% cloud free, 25 × 25 km ROI. The ROI was taken at the centre of the MHW, as shown by the vector overlay. When the centre of the MHW exceeded 20% cloud cover the ROI was shifted to the closest region that was >80% cloud-free. The mean and standard deviation of chl-a (mg/m^{-3}) was recorded for the impacted region. The effects of the extreme temperatures at the centre of the heatwave are considered statistically independent from the controls due to their distance apart. The mean and standard deviation of chl-a (mg/m^{-3}) was recorded for each viable control region. Images of the control vs. impact design applied on each of the 19 MHWs are provided in Appendix 1. These images include outlines of the extreme, severe and strong MHWs drawn over chl-a concentration maps as well as polylines of distance and control and impacted ROIs.

4.2.4. Statistical analysis

Impacts of the MHWs on chl-a was analysed with standard Anova and correlation analysis.

Standard factorial Anova tested for individual and interactive effects of 'MHWs', 'Zone' and 'Sea temperature' on chl-a concentrations. Anovas were done separately on the

250 and 500 km control data, using the mean control chl-a level for each of the 19 identified extreme MHWs. I used a single mean control value per MHW because the many control values matching a single MHW event are non-independent. Data were Natural-log-transformed prior to analysis to remove (or in a single case strongly reduce) variance heterogeneity (Cochran's C tests; see Table 4.2).

In addition, correlation analyses were done to test whether the attributes of individual MHWs (see Table 4.1) modified effects. This analysis was done on the Log Response Ratio effect size, where LnRR = Ln (Chl-a impact/Chl-a control). LnRR is a standard effect size that often is used to tests ecological research questions. In this analysis, a positive LnRR value reflects that a MHW has higher chlorophyll concentrations than the corresponding mean control value. Correlation analyses were done for the 250 and 500 km chl-a data separately, with both linear ($r_{Pearson}$) and non-parametric ($r_{Spearman}$) coefficients, using as independent variables the (a) temperature at the impact site, (b) difference between the MHW and climatic mean temperature, as well as the (c) duration, (e) maximum intensity, (f) mean intensity and (g) cumulative intensity of each of the 19 MHWs.

Note finally that time series analyses of chl-a during individual MHWs was impossible to do in the SO because ice and cloud cover impose significant data discontinuity – even though time series of satellite data coupled with *in situ* measurements and modelling would provide stronger data (Ji, Edwards, MacKas, Runge, & Thomas, 2010) (see discussion for details).

4.3. Results

4.3.1. Exploratory, Anova and correlation analysis

Between 2002 and 2018, 19 extreme MHW events were identified in the SO; here, these are considered to be spatially and temporally independent events (see Figure 4.3 for their spatial location). The 19 MHWs varied dramatically with regard to their maximum temperature (-0.75 to 15.92 °C), duration (8-146 days), cumulative intensity (9.77-469 °C above 90% climatic record x days), maximum intensity (1.15-4.48 °C above 90% climatic record) and mean intensity (0.55-2.52 °C above 90% climatic record) (Table 4.1). Furthermore, the climatic temperatures were significantly ($p = 0.0004$) colder at the two zones that are more influenced by sea-ice (climatic mean of pooled CZ and SIZ sites = -0.27 °C ± 0.09 SE) compared to the two zones less influenced by sea ice (climatic mean of pooled POOZ and SAZ sites = 5.12 °C ± 1.72 SE).

The factorial Anovas demonstrated significant effects of both MHWs and sea temperature and with significant interaction effects of sea temperature and MHWs for both the 250 and 500 km control site distances ($p < 0.05$, Table 4.3). Chl-a concentration was significantly higher at the MHW-impacted sites (1.81 ± 0.49 mg m^{-3}) compared to control sites for both the 250 (0.44 ± 0.08 mg m^{-3}) and 500 (0.39 ± 0.14 mg m^{-3}) km distances (Figure 4.5). The effects of MHWs were also stronger at the colder sites (Figure 4.6); that is, mean chl-a levels were significantly greater in the centre of the MHW for the cold waters (2.76 ± 0.73 mg m^{-3}) compared to the centres of the MHWs occurring in warmer waters (0.51 ± 0.14) and the un-impacted control sites in the cold (0.55 ± 0.15 for 250 km; 0.56 ± 0.26 for 500 km) and warmer (0.30 ± 0.05 for 250 km; 0.21 ± 0.03 km) sites (Figure 4.6).

Finally, the correlation analyses revealed either no or negative associations between Ln RR values and temperature and MHW attributes (Fig. 4.7, Table 4.4). More specifically, there were significant negative spearman rank correlations between Ln RR and the temperature at the impacted site (at both the 250 and 500 km distances) and for delta temperature, MHW maximum intensity and MHW mean intensity (the latter four responses only for 250 km distances, Table 4.4). Note also that the correlation coefficients for the three MHW-related variables were all weak ($r < 0.17$).

4.4. Discussion

MHWs are becoming more frequent, extensive and intense (Frölicher, Fischer, & Gruber, 2018; Oliver et al., 2018; Smale et al., 2019) with potential major impacts on biodiversity, and ecosystem functioning. The objective of this chapter was to apply the MHW identification procedure (Hobday et al., 2018) across the SO to test if 19 extreme summer MHWs (where temperatures are four times the 90th percentile of climatic SST) affect primary production (Chlorophyll-a) of phytoplankton and if effects vary between regions characterised by different climatic temperatures and levels of winter ice covering.

I found strong positive effects of summer MHWs that increased chl-a concentration levels by ca. 76 and 78 percent compared to the 250 and 500 km controls, respectively. However, this positive effect was much stronger for the coldest regions (CZ and SSIZ), a finding that was supported by a correlation analysis that showed negative association between the effect size and the climatic sea surface temperature. These results add new insight to past studies from temperate to tropical latitudes that generally have shown negative impacts of warm sea surface anomalies and phytoplankton productivity (Gómez-Ocampo et al., 2018; Trainer et al., 2019). More generally, my results also highlight the importance of analysing MHWs in a specific spatio-temporal context, as exemplified here with a focus on summer months only and with different results for different regions. Furthermore, it is important that this definition of anomalously warm events, that is MHWs, is adopted in future comparable SO and global studies to ensure consistency within the literature.

To date, changes to long-term average temperature in the SO in particular has received much more research scrutiny compared to temperature anomalies, like MHWs (Deppeler & Davidson, 2017; Petrou et al., 2016; Tortell et al., 2008). However, my results support those of Dunstan et al. (2018) that argued, without the assessment of short-term variability and events such as MHWs, research is likely to fail to notice many impact on regional and local scales. Importantly, phytoplankton can respond rapidly to changes in the physical environment (including temperature) (Feng et al., 2015; Maranón, Cermeno, Latasa, & Tadonléké, 2012; Trainer et al., 2019) and short term extreme MHWs, superimposed on gradual climate changes, could therefore reach a tipping point where the SO would experience dramatic ecosystem shifts with changes to entire communities at the base of the food web. It therefore remains a fundamental challenge to understand and model variability in phytoplankton biomass while considering combined effects of long term climate change and MHWs in the SO within a regional context.

4.4.1. MHWs and Primary productivity in the SO

There were strong positive effects of MHWs on phytoplankton abundance, increasing surface concentrations by 2.1 mg/m^{-3} at sites with coldest climatic temperatures. These concentrations far exceed Moore & Abbott's (2000) threshold of '1 mg m^{-3}' to describe phytoplankton blooms in the SO. By contrast, Moore & Abbott (2000) also describe typical low SO chl-a concentrations of ca. 0.3-0.4 mg/m^{-3}. In the Ross Sea, Boyd (2000) describe typical low concentrations of ca. 0.25-0.3 mg/m^{-3}. The chl-a concentration results from control sites were generally within the higher range of these values (c. 0.5 mg m^{-3} for the cold sites (CZ and SSIZ) and 0.30-0.2 mg m^{-3} for the warm sites (POOZ and SAZ)). My results thereby generally align with the typical low SO chl-a concentrations reported in the SO by Moore & Abbott (2000) and Boyd (2000).

Although not specifically outlined as a key objective, it is of some interest to examine whether chl-a concentrations in control regions varied with distance from the extreme MHWs. Here, 250 km and 500 km were chosen as non-impacted controls; distances positioned in-between the 300 km transect distance used by Ortiz-Ahumada, Álvarez-Borrego, & Gómez-Valdés (2018) to measure SST, chl-a and primary production. Images of all the 19 MHWs are shown in Appendix 1 with control and impact regions superimposed on a chl-a map and showing the areal extent not only of the extreme, but also severe and strong MHWs. It is possible that control sites 250 km away from the extreme MHW centres could still be affected by the surrounding severe and strong MHWs. However, temperature in control regions that were 500 km away from the extreme MHW were likely more independent of MHW level influence (perhaps except MHWs 3 and 15). Concentrations within 500 km controls (0.39 mg m^{-3}) are therefore likely to be more indicative of typical SO chl-a concentrations than concentrations within the 250 km controls (0.44 mg m^{-3}) (Boyd, 2000; Moore & Abbott, 2000).

The Anova (Table 4.3) was used to test if extreme MHWs affects chl-a concentration in the SO - and if effects vary between regions characterised by different sea surface temperatures and levels of winter ice covering. I found significant effects for both MHWs and Sea Temperature and with significant interaction effects for both the 250 and 500 km control site distances (Table 4.3). These results confirm that MHWs significantly influence chl-a concentrations, a proxy for phytoplankton biomass, in the SO. These results, in agreement with Dunstan et al. (2018), confirm that the effect of a MHW differs between colder (CZ and SSIZ) and warmer (POOZ and SAZ) sites with higher chl-a in the centre of the MHWs for the cold sites (2.76 mg m^{-3}) compared to the centre of the MHWs at the warmer sites (0.51 mg m^{-3}, Figure 4.6).

Temperature change initiated by MHWs was found to be a principle physical driver in the SO. SO phytoplankton species are adapted to cold water environments allowing them to grow and reproduce at sub-zero temperatures (Boyd, 2019). However, predictions in the literature strongly suggest that all regions in the SO (CZ, SSIZ, POOZ and SAZ) will experience change in phytoplankton community composition and productivity with climate change (Deppeler & Davidson, 2017; Dutkiewicz et al., 2019; Dutkiewicz et al., 2013; Thomas et al., 2012) as SST in the SO could increase by 1.5°C by 2100 (Boyd, 2019). Considering the additional effect present day MHWs (mean SST increase ca. 2.61°C) have on SO phytoplankton, we can expect floristic shifts towards warmer water species over much of the

area of the SO (Boyd, 2019), whilst restricting the present dominant species to the furthest south waters (Petrou et al., 2016). My results coupled with results from Boyd et al. (2013, 2019), which assessed temperature tolerances of specific SO phytoplankton species, confirm these predictions. For example, a simulated increase in temperature of 3°C led to a 25% increase in growth of *Proboscia inermis*, although a further increase in temperature led to a rapid decline in productivity (Boyd et al., 2013). Ultimately, under the predicted 1.5°C increase in SST by 2100 scenario, the polar diatoms *Pseudonitzschia* sp., *Proboscia* sp. and *Nitzschia stellata,* and the picoplankton species *P. antarctica* will be close to, or exceed their thermal maximum during summer (Boyd, 2019) (Figure 2.11). With the added influence of MHWs, SST increases outside of the optimum growth range for SO phytoplankton species pose an imminent threat to the base of the SO food-web.

Finally, it is important to note the fundamental role sea ice has in controlling SST and phytoplankton dynamics. According to the latest NOAA Climate.gov (2019) records, sea ice extent in Antarctica can extend to 11.3 million km^2 in the winter and retreat to ca. 1.6 million km^2 in the summer. This highly dynamic process shapes the SO ecosystem. As sea ice forms in the winter on the surface ocean, dissolved salt is expelled ('brine rejection'), increasing the salinity of underlying waters. This process results in colder, denser water which sinks to the deep ocean. Conversely, sea ice creates an insulation cap on the surface ocean, thereby reducing heat loss and evaporation (Knox, 2007). Ultimately, the SST regime within sea ice is difficult to predict because these processes buffer temperature fluctuations. Sea ice also influences SO phytoplankton dynamics, providing a substratum for ice communities consisting mainly of phytoplankton and bacteria protozoa (Knox, 2007). These communities depend on the availability of sea ice in the sunlit surface layer to bloom. Furthermore, when sea ice is lost through melting or advection, nutrients are released into the surface waters. This process, combined with increases in thermal stratification and irradiance, initiates seasonal phytoplankton blooms (Arrigo et al., 2008; Ji et al., 2010), and highlight the importance of accounting for sea ice concentrations in response to MHWs in future SO studies (see section 4.4.3).

4.4.2. Remote sensing limitations

Satellite measurements of ocean colour are useful remote sensing techniques to estimate phytoplankton abundances on large scales (Behrenfeld et al., 2006), in part because of the much higher spatial and temporal resolution compared to *in situ* data collections from ships (Brewin et al., 2014). Today, remote sensing of ocean colour is therefore the principle source of data for assessing changes to phytoplankton biomass, especially in the SO that is remote, cold and characterized by extreme waves regimes (Alvain et al., 2013; Arrigo & van Dijken 2003; Arrigo et al., 2008; Montes-Hugo et al., 2009; Moore & Abbott, 2000; Rohr et al., 2017; Sallée et al., 2015; Sokolov, 2008; Zhang at al., 2014). However, remote sensing analysis has significant limitations.

First, the use of satellite data limits time series information which can restrict the reliable separation of long term trends from inter-annual variability (Yang et al., 2013). This study combined data from two satellites, of which, the NOAA satellite with OISST records that began late 1981 through present. However, of its two data versions, the AMSR-E (a microwave instrument that can measure SST during most weather conditions) was only functional from 2002-2011 (NOAA, 2019). Therefore, the overall time series of information

gathered for this research was restricted to 16 years (2002-2018). This meant that I could not reliably assess whether MHWs in the SO are increasing in frequency and intensity like they have been observed on the global scale (Frölicher et al., 2018; Oliver et al., 2018; Smale et al., 2019). Additionally, this limited time series of data alongside cloud cover, a common limitation in remote sensing, contributed to a small sample size of MHWs. Finally, the use of satellite remote sensing and lack of *in situ* observations in this research prevented me from taking into consideration additional physical variables that are known to significantly influence SO phytoplankton dynamics. For example, nutrient concentrations and salinity levels influenced by areas of upwelling (Boyce et al., 2010; Mann & Lazier, 2006; Moore & Abbott, 2000; Sokolov, 2008; Townsend, 2012), location of fronts and movement of currents (Arrigo et al., 2008; Boyd et al., 2000; Garrison et al., 2018; Knox, 2007; Landry et al., 2002; Mann & Lazier, 2006; Moore & Abbott, 2000; Sokolov, 2008; Thomas, 2012; Townsend, 2012; Tréguer at al., 2018; Williams & Follows, 2011) and impacts of mesoscale eddies (Deppeler & Davidson, 2017; Frenger et al., 2018; Garrison et al., 2018; Knox, 2007; Mann & Lazier, 2006; Williams & Follows, 2011).

4.4.3. Future research

MHWs are rapidly emerging as strong disturbances that has the capacity to restructure entire ecosystems. MHWs are becoming more frequent, extensive and intense with anthropogenic climate change (Frölicher, Fischer, & Gruber, 2018; Oliver et al., 2018; Smale et al., 2019) but no published research has, to my knowledge, quantified their impacts on polar phytoplankton primary production. Therefore, it is important that future research on MHWs in the SO build upon my findings and that the definition of MHWs (Hobday et al., 2016) is adopted in SO and global studies to ensure consistency within the literature. Furthermore, there are at least four areas where this study could be expanded. First, future research on SO MHWs should take into account the importance of sea ice, because sea ice can control SST and phytoplankton dynamics in the SO. For example, Polarview (https://www.polarview.aq/antarctic) provides a near-real-time sea ice concentration information service, primarily for ship operators (but data are only available 30 days from present). Alternative sea ice concentration records would be required to perform a multi-decadal study, which integrates data from several satellites and sensors. Second, it would be useful to take a multi-decadal approach. This would, however, require careful integration of data from several satellites and sensors to allow for a reliable assessment of whether MHWs in the SO are increasing in frequency and intensity. Third, future work should incorporate other variables, such as solar radiation, grazing pressure, eddies and fronts, known to affect SO phytoplankton growth and reproduction. Finally, more research should also focus on satellite validation using *in situ* observations and data collections.

4.4.4. Conclusions

Concerns have been raised that average SST in the SO could have increased by 1.5°C by 2100 (Boyd, 2019). This research found present day short term MHWs to be of similar concern because these events can raise SST by ca. 2.6°C and last for >100 days. These extreme events have been shown to drive sudden and dramatic shifts in the functioning and structure of ecosystems (Smale et al., 2019). Thus, the concept of MHWs has gained significant traction in both the research literature (Frölicher, Fischer, & Gruber, 2018;

Holbrook et al., 2019; Oliver et al., 2018; Smale et al., 2019; Thomsen et al., 2019) and in the latest IPCC Special Report on the Oceans and Cryosphere (IPCC, 2019). The present research is, to my knowledge, the first attempt to apply the MHW identification procedure (Hobday et al., 2016; Hobday et al., 2018) across the SO to gain insight into effects on primary production.

I tested two key questions in relation to MHWs and their influence on Southern Ocean (SO) primary productivity: do extreme MHWs affect chl-a concentration in the SO - and if so, do effects vary between regions characterised by different sea surface temperatures and levels of winter ice cover? The concentration of chl-a, a proxy for phytoplankton biomass, was significantly greater at the MHW-impacted sites compared to control sites at both 250 and 500 km distances. Therefore, extreme MHWs appear to have a strong effect on chl-a concentration. Furthermore, the effects of MHWs were stronger at colder sites suggesting that MHW effects can vary among regions characterised by different sea surface temperatures.

These results support Dunstan et al. (2018) who argued that without the assessment of short-term variability and events such as MHWs, research is likely to fail to notice many impacts on regional and local scales. Since phytoplankton can respond rapidly to changes in the physical environment (Feng et al., 2015; Maranón et al., 2012; Trainer et al., 2019) short term extreme MHWs, superimposed on gradual climate changes, could therefore reach a tipping point where the SO could experience dramatic ecosystem shifts at the base of the food web. Therefore, it remains a fundamental challenge to understand and model variability in phytoplankton biomass while considering combined effects of long-term climate change and MHWs.

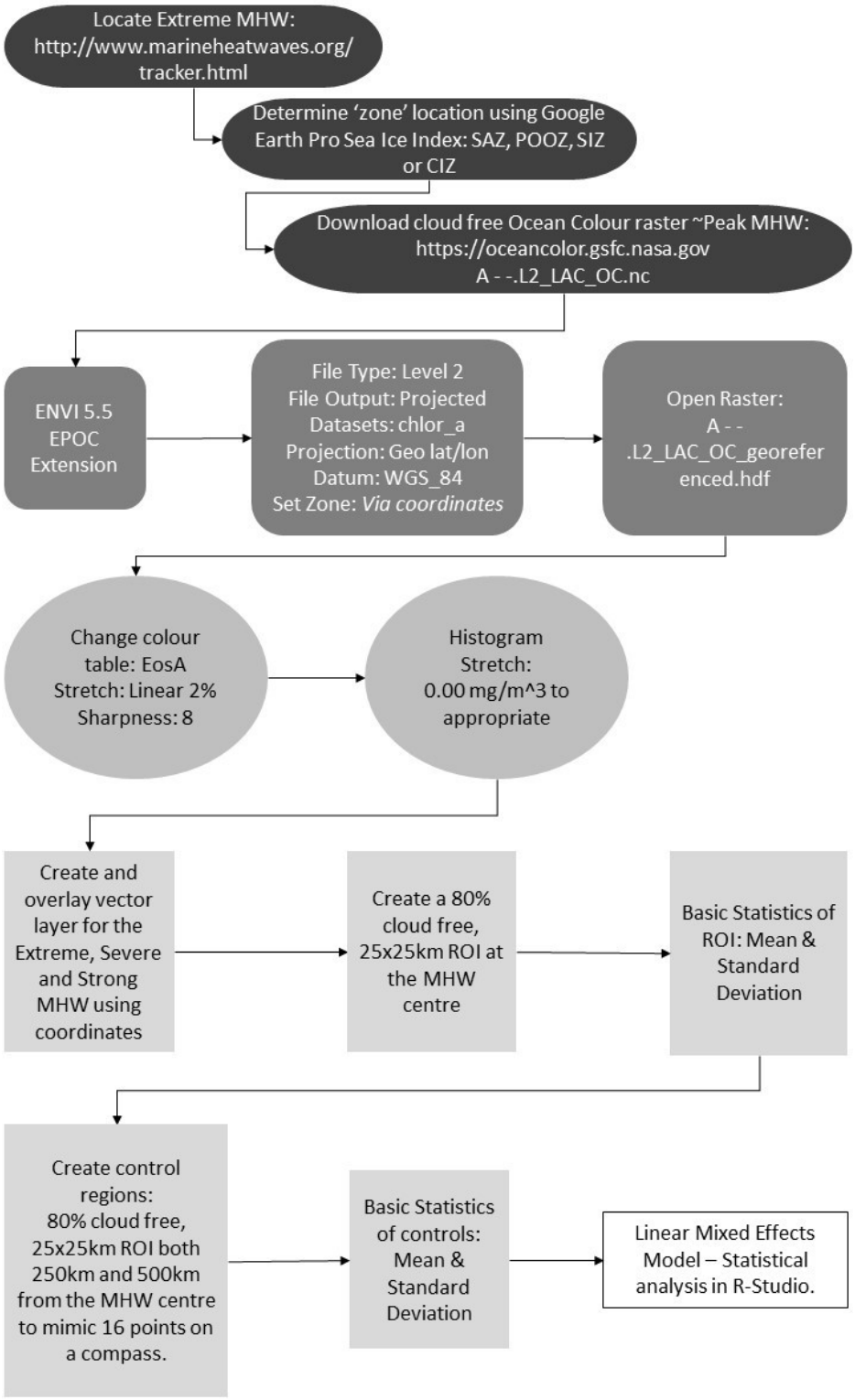

Figure 4.1. Processing summary for analysis in ENVI 5.5. Including the identification of an extreme marine heatwave event, determination of Southern Ocean location and raster image download (ovals), as well as the use of the EPOC extension (rounded rectangles), general image modifications (circles), experimental design (squares) and data collection (rectangle).

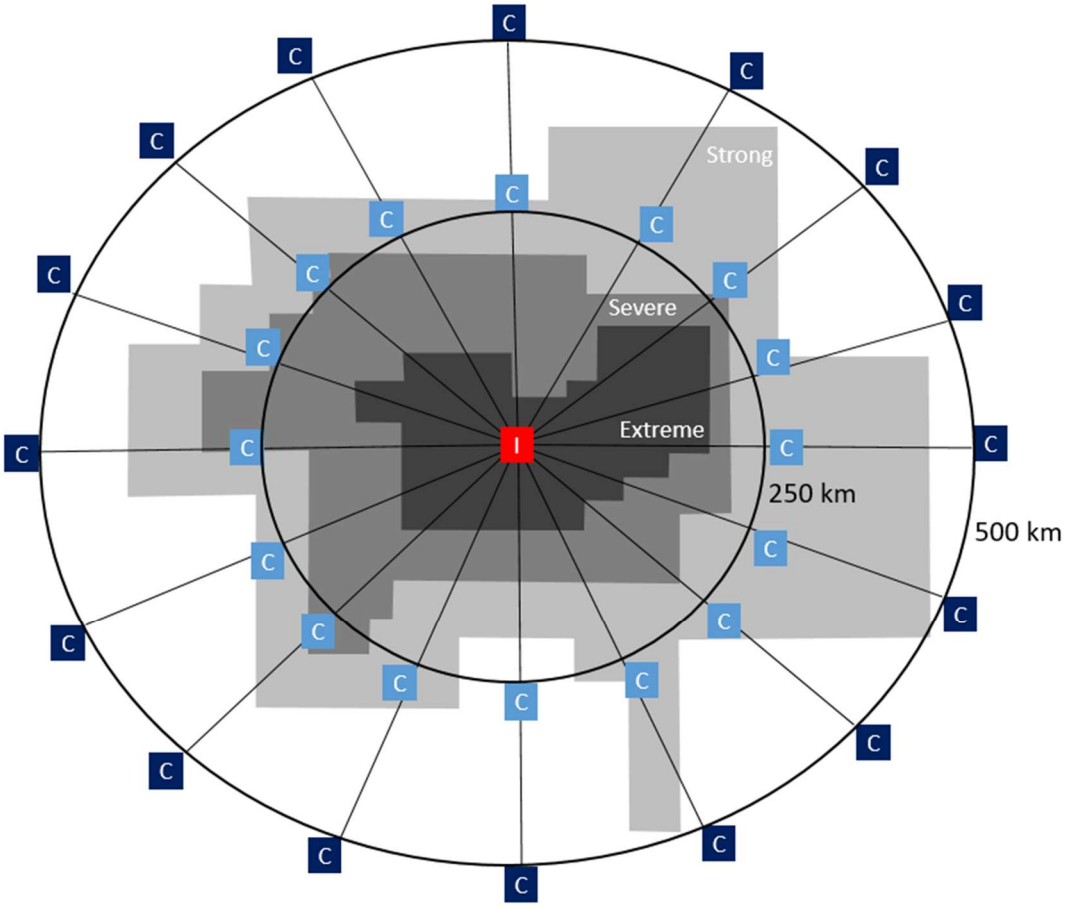

Figure 4.2. The design of a Control vs. Impact analysis. A hypothetical pixelated extreme MHW is shown with maximum intensity in the centre (red = I = impact site). This image would be superimposed on a chlorophyll-a map and if this was at least 80% cloud-free, data would be extracted from a single 25 x 25km area at the centre of an extreme MHW and from potentially up to 32 control regions (C). Controls were taken at 16 compass points at 250 km and 500 km distances from the heatwave centre. This figure shows an ideal example where all 32 potential control sites could be analysed but in reality this varied from 0 to 8 at each distance, due to high ice and/or cloud cover (see Table 4.1 for details).

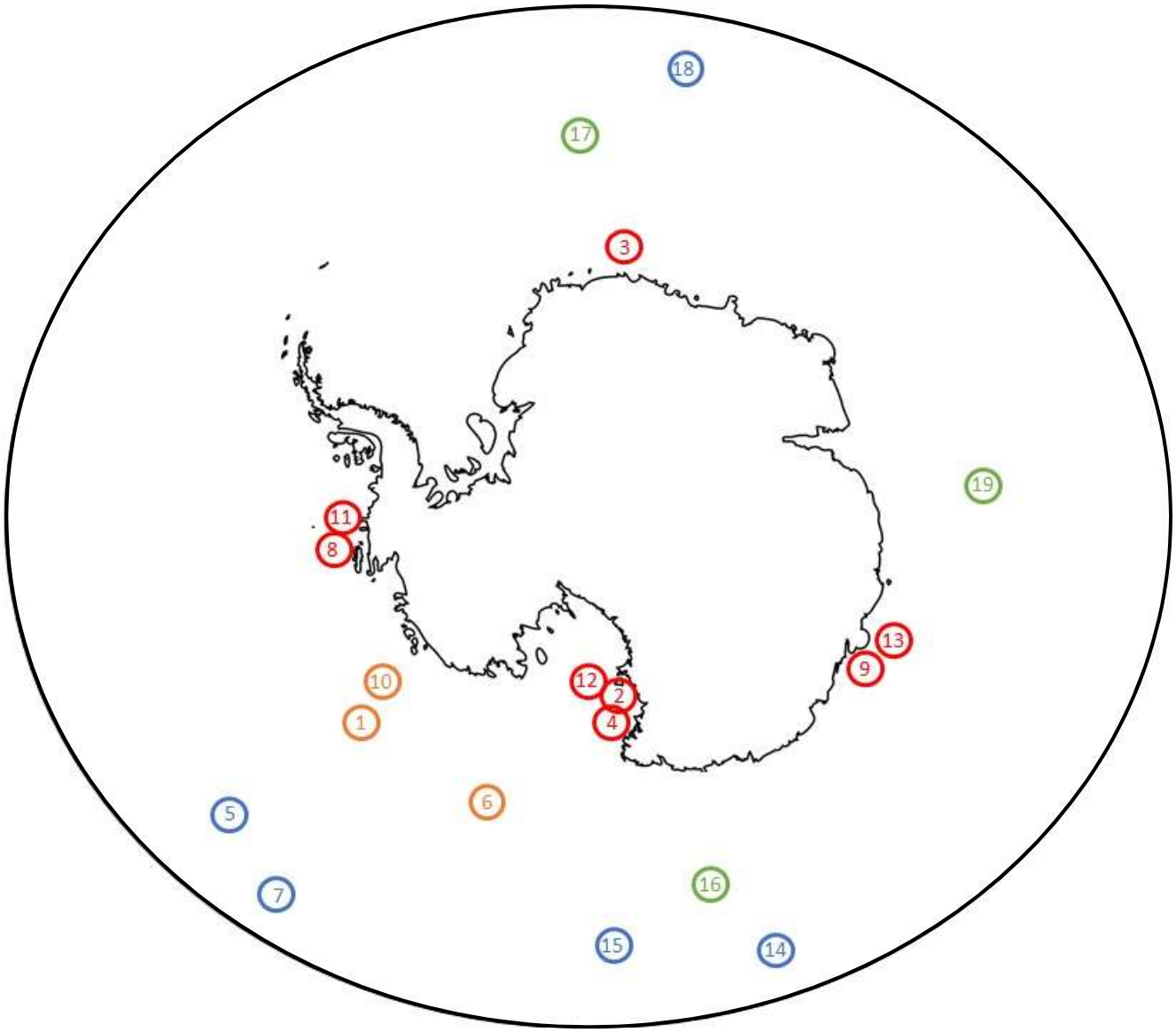

Figure 4.3. Location of 19 extreme summer MHWs during 2002-2018 classified into four different ocean regions: Coastal Zone (CZ, red), Seasonal Sea Ice Zone (SSIZ, orange), Permanently Open Ocean Zone (POOZ, green) and Sub-Antarctic Zone (SAZ, blue). See Table 4.1 for more details. In winter the CZ and SSIZ are covered by sea ice.

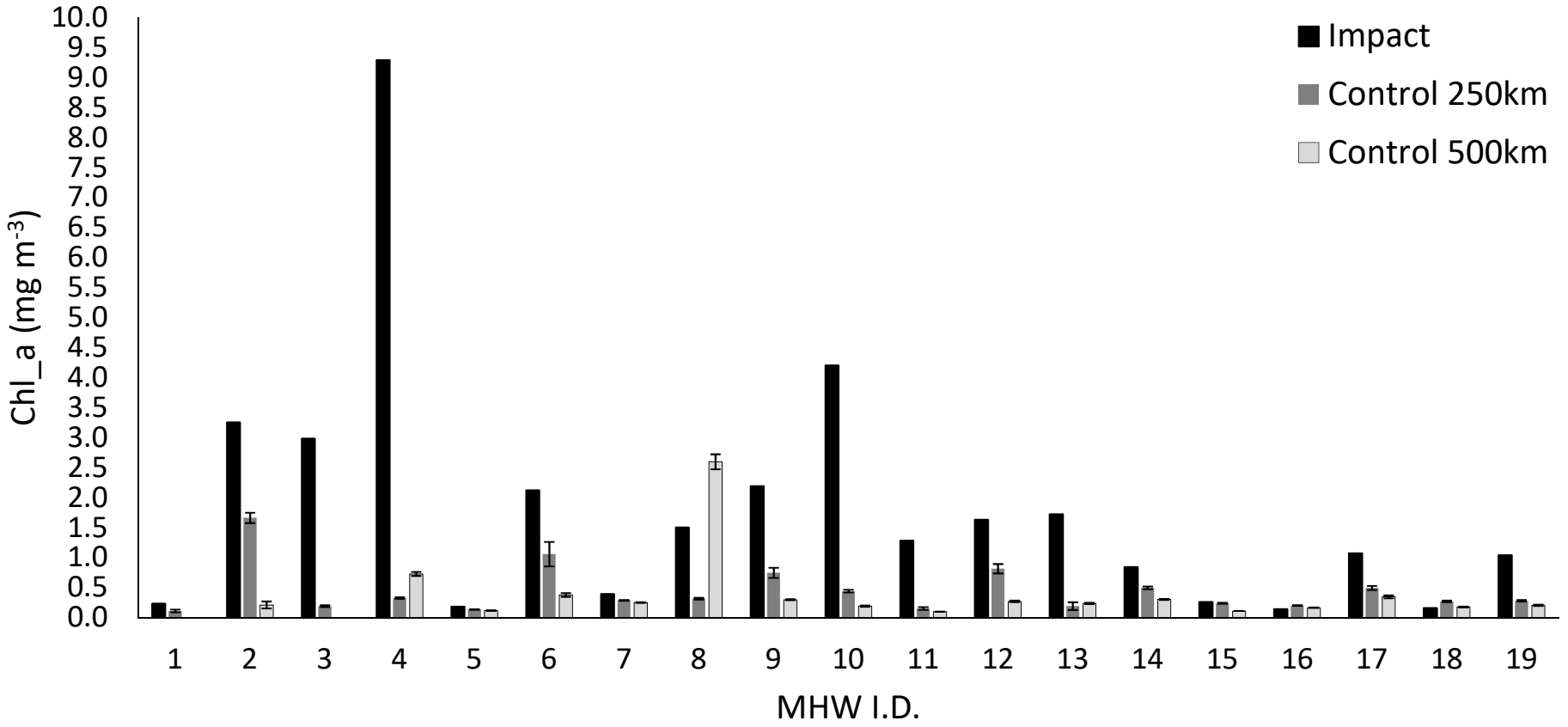

Figure 4.4. Bar plot showing the concentration of chl-a (mg m^{-3}) for impact (black) and control regions 250 km (white) and 500 km (grey) in 19 chronologically ordered MHWs in the SO. In 16 out of the 19 cases, the concentration of chl-a within the extreme MHWs is greater than the waters surrounding it.

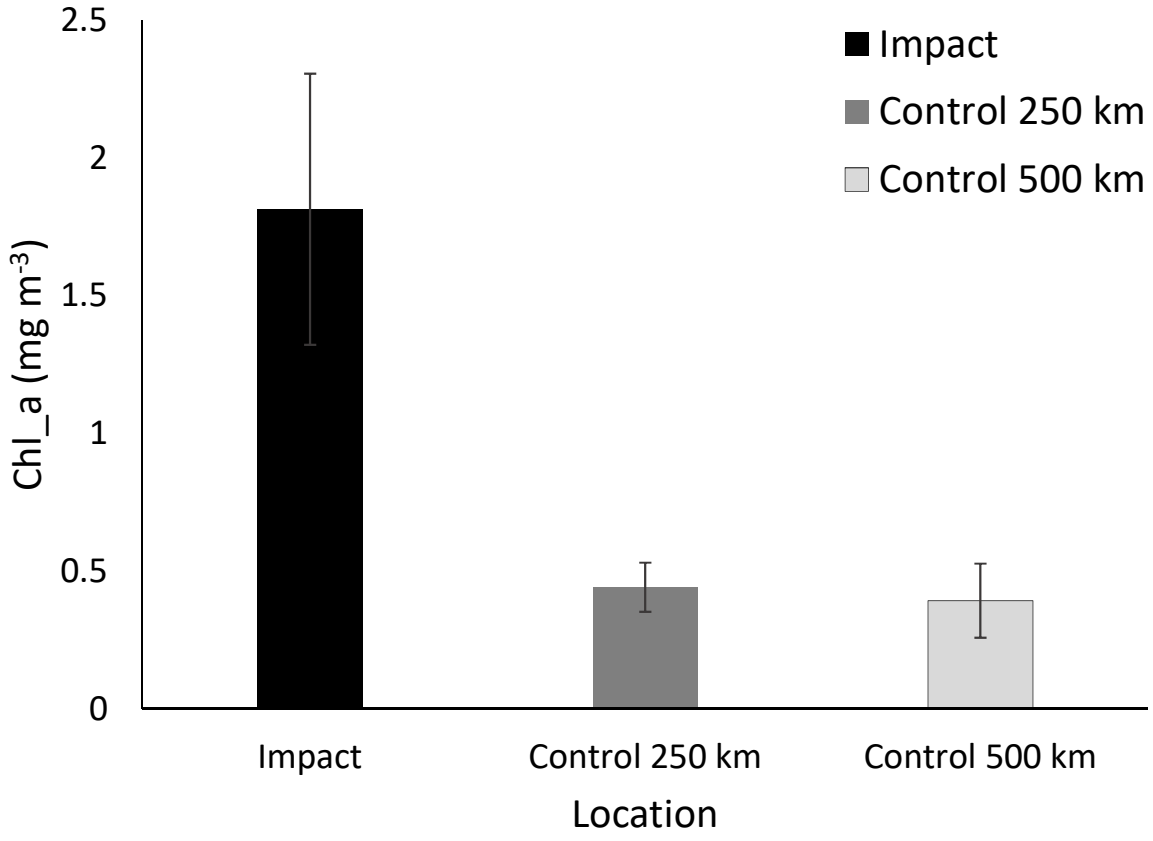

Figure 4.5. Bar plot showing the mean concentration of chl-a (mg m^{-3}) for impact (black) and control regions 250 km (white) and 500 km (grey).

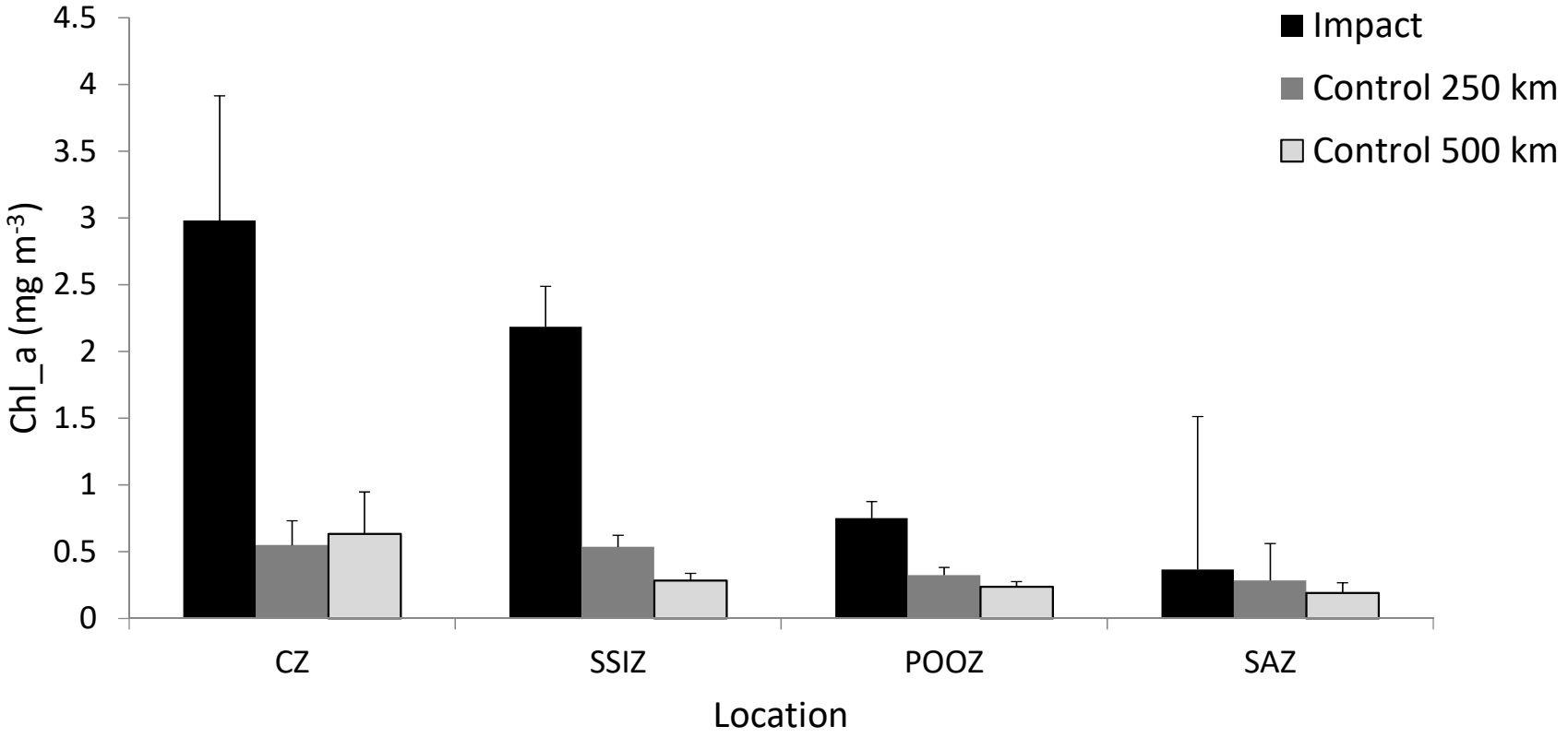

Figure 4.6. Bar plot showing the mean concentration of chl-a (mg m^{-3}) for impact (black) and control regions 250 km (dark grey) and 500 km (light grey) for four SO locations; coastal zone (CZ), seasonal sea ice zone (SSIZ), permanently open ocean zone (POOZ) and sub-Antarctic zone (SAZ). In winter, CZ and SSIZ are covered by sea ice.

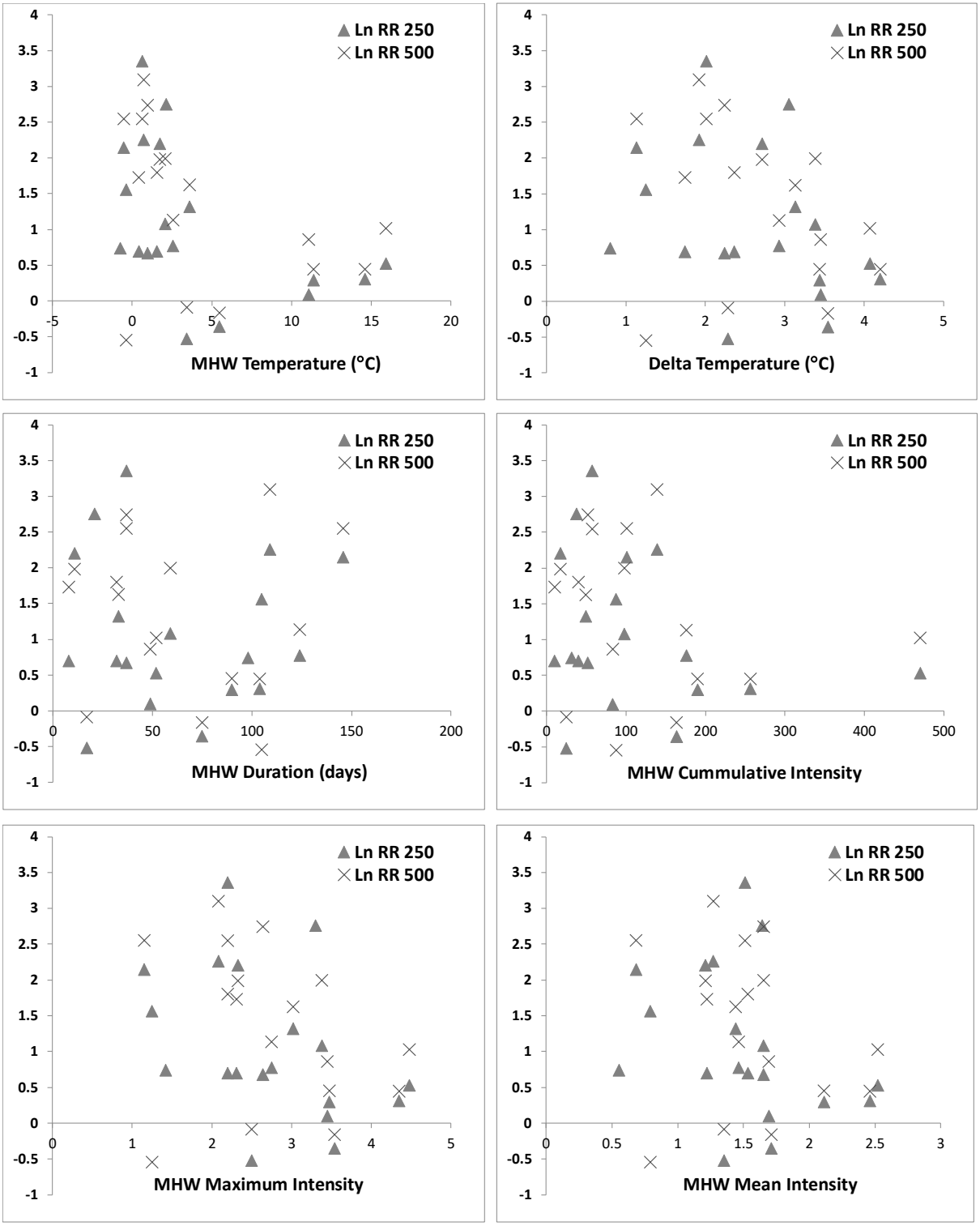

Figure 4.7. XY scatter plots of LnRR effect sizes vs. six MHW attributes (LnRR = Ln (Chl-a impact/Chl-a control)) calculated using control sites both 250 and 500 km away from the impact site).

Table 4.1. Attributes of 19 chronologically ordered extreme summer marine heatwaves (MHW) in the Southern Ocean observed from 2002 to 2018 in November to February. CZ = coastal zone, SSIZ = seasonal sea ice zone, POOZ = permanently open ocean zone and SAZ = sub-Antarctic zone. Temperature = °C, Duration = days, Intensity = °C, Chl-a concentration = mg/m^{-3}.

MHW I.D.	Zone	Latitude	Longitude	Image Acquisition Date	Climate Temperature	MHW Temperature	MHW Duration	MHW Cumulative Intensity	MHW Maximum Intensity	MHW Mean Intensity	MHW Impact Chl-a	Control 250 km Chl-a	Control 500 km Chl-a	N 250 km	N 500 km
1	SSIZ	-134.875	-66.375	26/11/2002	-1.55	-0.75	98	31.12	1.42	0.55	0.23	0.11	NA	1	0
2	CZ	166.875	-75.625	15/12/2004	-1.26	0.98	37	51.3	2.64	1.65	3.25	1.66	0.21	2	1
3	CZ	10.625	-68.875	8/01/2005	-0.92	2.13	21	37.65	3.3	1.64	2.98	0.19	NA	3	0
4	CZ	165.625	-74.375	12/01/2006	-1.37	0.64	37	57.31	2.2	1.51	9.29	0.325	0.728	4	4
5	SAZ	-131.625	-49.125	15/11/2009	7.93	11.37	90	189.9	3.47	2.11	0.18	0.134	0.115	5	2
6	SSIZ	-158.375	-66.625	13/12/2009	-1.33	0.41	8	9.77	2.31	1.22	2.12	1.057	0.377	3	3
7	SAZ	-139.625	-47.625	24/12/2009	10.39	14.59	104	256.22	4.35	2.46	0.39	0.286	0.25	8	2
8	CZ	-97.125	-71.375	5/02/2010	-1.62	-0.37	105	87.21	1.25	0.79	1.5	0.315	2.595	2	2
9	CZ	105.875	-65.625	30/01/2011	-1.32	2.06	59	97.61	3.38	1.65	2.19	0.746	0.298	5	4
10	SIZ	-129.125	-69.625	8/01/2013	-1.18	0.74	109	138.67	2.08	1.27	4.2	0.44	0.19	1	2
11	CZ	-95.375	-71.625	21/02/2013	-1.65	-0.52	146	100.39	1.15	0.68	1.28	0.15	0.1	1	1
12	CZ	169.375	-76.375	24/02/2013	-0.8	1.56	32	39.87	2.2	1.53	1.63	0.813	0.27	3	1
13	CZ	104.625	-64.625	28/12/2013	-0.96	1.75	11	17.05	2.33	1.21	1.72	0.19	0.237	1	3
14	SAZ	151.625	-46.375	15/12/2015	11.85	15.92	52	469.62	4.48	2.52	0.84	0.496	0.303	7	3
15	SAZ	-176.875	-51.625	7/11/2016	7.63	11.08	49	83.01	3.45	1.69	0.26	0.237	0.11	3	2
16	POOZ	159.875	-57.375	8/11/2016	1.92	5.46	75	163.06	3.54	1.71	0.14	0.2	0.165	6	2
17	POOZ	0.875	-58.875	2/01/2017	-0.38	2.55	124	175.62	2.75	1.46	1.07	0.494	0.345	5	2
18	SAZ	11.125	-53.625	20/02/2017	1.13	3.41	17	24.4	2.5	1.35	0.16	0.27	0.175	4	2
19	POOZ	83.125	-55.125	7/11/2017	0.46	3.59	33	49.12	3.02	1.44	1.04	0.278	0.205	5	2

Table 4.2. Cochran's tests for variance homogeneity.

Control distance	Tests factor	Test Statistic	P
250 km	MHW	0.736	**0.036**
	Zone	0.438	0.196
	Overall	0.330	0.172
500 Km	MHW	0.713	0.069
	Zone	0.406	0.331
	Overall	0.371	0.086

Table 4.3. Anova testing for effects of marine heatwaves (MHW; impacted site vs. control sites positioned either 250 or 500 km from the centre of the MHW) in two types of waters (cold and strongly influenced by sea ice vs. warmer and less influenced by sea ice) with two regions nested within each type of water (CZ and SIZ within the cold zone; POOZ and SAZ within the warmer zone, see Table 4.1 for details).

Control distance	Test factor	SS	DF	F-Stat	P
250 km	Sea temperature	9.443	1	14.042	**0.001**
	Zone(Sea temperature)	1.009	2	0.750	0.480
	MHW	11.150	1	16.581	**0.000**
	Sea temperature x MHW	4.190	1	6.231	**0.018**
	Total	47.311	37		
500 km	Sea temperature	11.567	1	17.210	**0.000**
	Zone(Sea temperature)	1.435	2	1.067	0.357
	MHW	15.036	1	22.372	**0.000**
	Sea temperature x MHW	2.949	1	4.387	**0.045**
	Total	52.253	35		

Table 4.4 Correlation analysis between Ln RR and six independent variables related to marine heat waves (MHW). Ln RR = Ln (chl-a concentrations at the impacted site/chl-a at the control sites), where control sites were evaluated from both 250 and 500 km distances away from the impact site. $N_{250\ km} = 19$, $N_{500\ km} = 17$, see Table 4.1 for details. Significant results are in bold.

Independent variable	Test type	r 250 Km	P 250 Km	r 500 Km	P 500Km
Temperature MHW impacted site	Pearson	-0.480	**0.038**	-0.439	0.078
	Spearman	-0.584	**0.009**	-0.525	**0.031**
Temp. diff. between MHW and	Pearson	-0.359	0.131	-0.338	0.184
Climatic mean	Spearman	-0.482	**0.036**	-0.453	0.068
MHW Duration	Pearson	0.005	0.983	-0.084	0.749
	Spearman	0.061	0.803	-0.056	0.830
MHW Cumulative intensity	Pearson	-0.258	0.286	-0.251	0.330
	Spearman	-0.212	0.383	-0.243	0.348
MHW Max Intensity	Pearson	-0.407	0.084	-0.313	0.222
	Spearman	-0.552	**0.014**	-0.462	0.062
MHW Mean Intensity	Pearson	-0.331	0.167	-0.229	0.376
	Spearman	-0.522	**0.022**	-0.296	0.249

References

Alvain, S., Le Quéré, C., Bopp, L., Racault, M. F., Beaugrand, G., Dessailly, D., &Buitenhuis, E. T. (2013). Rapid climatic driven shifts of diatoms at high latitudes. *Remote Sensing of Environment, 132*, 195-201. https://doi.org/10.1016/j.rse.2013.01.014

Alvain, S., Moulin, C., Dandonneau, Y., & Bréon, F. M. (2005). Remote sensing of phytoplankton groups in case 1 waters from global SeaWiFS imagery. *Deep-Sea Research Part I: Oceanographic Research Papers, 52*(11), 1989-2004. https://doi.org/10.1016/j.dsr.2005.06.015

Alvain, S., Moulin, C., Dandonneau, Y., & Loisel, H. (2008). Seasonal distribution and succession of dominant phytoplankton groups in the global ocean: A satellite view. *Global Biogeochemical Cycles, 22*(3). https://doi.org/10.1029/2007GB003154

Arrigo, K. R., van Dijken, G. L., & Bushinsky, S. (2008). Primary production in the Southern Ocean, 1997-2006. *Journal of Geophysical Research: Oceans, 113*(8). https://doi.org/10.1029/2007JC004551

Banzon, Viva, Reynolds, Richard & National Centre for Atmospheric Research Staff (Eds). Last modified 25 June 2019. "The Climate Data Guide: SST data: NOAA High-resolution (0.25x0.25) Blended Analysis of Daily SST and Ice OISSTv2." Retrieved from https://climatedataguide.ucar.edu/climate-data/sst-data-noaa-high-resolution-025x025-blended-analysis-daily-sst-and-ice-oisstv2

Behrenfeld, M. J., O'Malley, R. T., Siegel, D. A., McClain, C. R., Sarmiento, J. L., Feldman, G. C., . . . Boss, E. S. (2006). Climate-driven trends in contemporary ocean productivity. *Nature, 444*(7120), 752-755. https://doi.org/10.1038/nature05317

Blondeau-Patissier, D., Gower, J. F. R., Dekker, A. G., Phinn, S. R., & Brando, V. E. (2014, 2014/04/01/). A review of ocean color remote sensing methods and statistical techniques for the detection, mapping and analysis of phytoplankton blooms in coastal and open oceans. *Progress in Oceanography, 123*, 123-144. https://doi.org/https://doi.org/10.1016/j.pocean.2013.12.008

Boyce, D. G., Lewis, M. R., & Worm, B. (2010). Global phytoplankton decline over the past century. *Nature, 466*(7306), 591-596. https://doi.org/10.1038/nature09268

Boyd, P. W., Rynearson, T. A., Armstrong, E. A., Fu, F., Hayashi, K., Hu, Z., . . . Thomas, M. K. (2013). Marine phytoplankton temperature versus growth responses from polar to tropical waters--outcome of a scientific community-wide study. *PloS one, 8*(5), e63091-e63091. https://doi.org/10.1371/journal.pone.0063091

Brewin, R. J. W., Mélin, F., Sathyendranath, S., Steinmetz, F., Chuprin, A., & Grant, M. (2014). On the temporal consistency of chlorophyll products derived from three ocean-colour

sensors. *ISPRS Journal of Photogrammetry and Remote Sensing, 97*, 171-184. https://doi.org/10.1016/j.isprsjprs.2014.08.013

Campbell, J. W. (1995). The lognormal distribution as a model for bio-optical variability in the sea. *Journal of Geophysical Research: Oceans, 100*(C7), 13237-13254. https://doi.org/10.1029/95jc00458

Cape, M. R., Vernet, M., Kahru, M., & Spreen, G. (2014). Polynya dynamics drive primary production in the Larsen A and B embayments following ice shelf collapse. *Journal of Geophysical Research: Oceans, 119*(1), 572-594. https://doi.org/10.1002/2013JC009441

Crawley, M. J. (2007). *The R Book.* John Wiley & Sons, Ltd.

Deppeler, S. L., & Davidson, A. T. (2017). Southern Ocean phytoplankton in a changing climate. *Frontiers in Marine Science, 4*(FEB). https://doi.org/10.3389/fmars.2017.00040

Dunstan, P. K., Foster, S. D., King, E., Risbey, J., O'Kane, T. J., Monselesan, D., . . . Thompson, P. A. (2018, 2018/10/02). Global patterns of change and variation in sea surface temperature and chlorophyll a. *Scientific Reports, 8*(1), 14624. https://doi.org/10.1038/s41598-018-33057-y

Dutkiewicz, S., Hickman, A. E., Jahn, O., Henson, S., Beaulieu, C., & Monier, E. (2019). Ocean colour signature of climate change. *Nature Communications, 10*(1). https://doi.org/10.1038/s41467-019-08457-x

Dutkiewicz, S., Scott, J. R., & Follows, M. J. (2013). Winners and losers: Ecological and biogeochemical changes in a warming ocean. *Global Biogeochemical Cycles, 27*(2), 463-477. https://doi.org/10.1002/gbc.20042

Feng, J., Durant, J. M., Stige, L. C., Hessen, D. O., Hjermann, D. Ø., Zhu, L., . . . Stenseth, N. C. (2015). Contrasting correlation patterns between environmental factors and chlorophyll levels in the global ocean. *Global Biogeochemical Cycles, 29*(12), 2095-2107. https://doi.org/10.1002/2015gb005216

Frenger, I., Münnich, M., & Gruber, N. (2018). Imprint of Southern Ocean mesoscale eddies on chlorophyll. *Biogeosciences, 15*(15), 4781-4798. https://doi.org/10.5194/bg-15-4781-2018

Frölicher, T. L., Fischer, E. M., & Gruber, N. (2018). Marine heatwaves under global warming. *Nature, 560*(7718), 360-364. https://doi.org/10.1038/s41586-018-0383-9

Garrison, Tom. *Oceanography: An Invitation to Marine Science*. Belmont CA, 2005.
Spokes, L. Phytoplankton and nutrients in the oceans. *ESPERE*. (16-October 2003).
Miller, Charles. Biological

Gómez-Ocampo, E., Gaxiola-Castro, G., Durazo, R., & Beier, E. (2018). Effects of the 2013-2016 warm anomalies on the California Current phytoplankton. *Deep-Sea Research Part II: Topical Studies in Oceanography, 151*, 64-76. https://doi.org/10.1016/j.dsr2.2017.01.005

Gordon, H., Brown, J., Brown, O., Evans, R., & Smith, R. (1988, 10/20). A semianalytic radiance model of ocean color. *J. Geophys. Res., 93*. https://doi.org/10.1029/JD093iD09p10909

Gregg, W. W., & Rousseaux, C. S. (2014). Decadal trends in global pelagic ocean chlorophyll: A new assessment integrating multiple satellites, in situ data, and models. *Journal of Geophysical Research C: Oceans, 119*(9), 5921-5933. https://doi.org/10.1002/2014JC010158

Harrison, X. A., Donaldson, L., Correa-Cano, M. E., Evans, J., Fisher, D. N., Goodwin, C. E. D., . . . Inger, R. (2018). A brief introduction to mixed effects modelling and multi-model inference in ecology. *PeerJ, 6*, e4794. https://doi.org/10.7717/peerj.4794

Hobday, A. J., Alexander, L. V., Perkins, S. E., Smale, D. A., Straub, S. C., Oliver, E. C. J., . . . Wernberg, T. (2016). A hierarchical approach to defining marine heatwaves. *Progress in Oceanography, 141*, 227-238. https://doi.org/10.1016/j.pocean.2015.12.014

Hobday, A. J., Oliver, E. C. J., Gupta, A. S., Benthuysen, J. A., Burrows, M. T., Donat, M. G., . . . Smale, D. A. (2018). Categorizing and naming marine heatwaves. *Oceanography, 31*(2 Special Issue), 162-173. https://doi.org/10.5670/oceanog.2018.205

Holbrook, N. J., Scannell, H. A., Sen Gupta, A., Benthuysen, J. A., Feng, M., Oliver, E. C. J., . . . Wernberg, T. (2019, 2019/06/14). A global assessment of marine heatwaves and their drivers. *Nature Communications, 10*(1), 2624. https://doi.org/10.1038/s41467-019-10206-z

IPCC, 2019: IPCC Special Report on the Ocean and Cryosphere in a Changing Climate [H.-O. Pörtner, D.C. Roberts, V. Masson-Delmotte, P. Zhai, M. Tignor, E. Poloczanska, K. Mintenbeck, A. Alegría, M. Nicolai, A. Okem, J. Petzold, B. Rama, N.M. Weyer (eds.)]. In press.

Ji, R., Edwards, M., MacKas, D. L., Runge, J. A., & Thomas, A. C. (2010). Marine plankton phenology and life history in a changing climate: Current research and future directions. *Journal of Plankton Research, 32*(10), 1355-1368. https://doi.org/10.1093/plankt/fbq062

Knox, G. A. (2007). *Biology of the Southern Ocean* (2nd ed.). Boca Raton: CRC Press/Taylor & Francis.

Landry, M. R., Selph, K. E., Brown, S. L., Abbott, M. R., Measures, C. I., Vink, S., . . . Nolla, H. (2002, 2002/01/01/). Seasonal dynamics of phytoplankton in the Antarctic Polar Front region at 170°W. *Deep Sea Research Part II: Topical Studies in Oceanography, 49*(9), 1843-1865. https://doi.org/https://doi.org/10.1016/S0967-0645(02)00015-2

Mann, K. H., & Lazier, J. R. N. (2006). *Dynamics of marine ecosystems: biological-physical interactions in the oceans* (3rd ed.). Malden, MA: Blackwell Pub.

Maranón, E., Cermeno, P., Latasa, M., & Tadonléké, R. D. (2012). Temperature, resources, and phytoplankton size structure in the ocean. *Limnology and Oceanography, 57*(5), 1266-1278.

Marchant, H. J., Davidson, A. T., & Wright, S. W. (2001). Antarctic marine microorganisms and climate change: Impacts and feedbacks. *Ocean and Polar Research, 23*(4), 401-410.

McClain, C. R. (2009). A decade of satellite ocean color observations. *Annual Review of Marine Science, 1*, 19-42. https://doi.org/10.1146/annurev.marine.010908.163650

Montes-Hugo, M., Doney, S. C., Ducklow, H. W., Fraser, W., Martinson, D., Stammerjohn, S. E., & Schofield, O. (2009). Recent changes in phytoplankton communities associated with rapid regional climate change along the western Antarctic Peninsula. *Science, 323*(5920), 1470-1473. https://doi.org/10.1126/science.1164533

Moore, J. K., & Abbott, M. R. (2000). Phytoplankton chlorophyll distributions and primary production in the Southern Ocean. *Journal of Geophysical Research: Oceans, 105*(C12), 28709-28722.

NASA Goddard Space Flight Centre, Ocean Biology Processing Group. (2014). Moderate Resolution Imaging Spectroradiometer (MODIS) Ocean Colour Data, NASA OB.DAAC. Accessed June 6, 2019, from https://oceancolor.gsfc.nasa.gov/cgi/browse.pl?sen=am

NASA Goddard Space Flight Centre. *Moderate Resolution Imaging Spectroradiometer (MODIS).* Retrieved August 22, 2019, from https://modis.gsfc.nasa.gov/about/

NASA Goddard Space Flight Centre. *SeaDAS.* Retrieved August 22, 2019, from https://seadas.gsfc.nasa.gov/about/

National Snow & Ice Data Centre. (2019). *Sea Ice Index: Data Archive.* Retrieved June 6, 2019, from https://nsidc.org/data/seaice_index/archives

NASA Goddard Space Flight Centre. *Aqua Project Science.* Retrieved November 20, 2019, fromhttps://aqua.nasa.gov/

NOAA National Centers for Environmental Information. *Optimum Interpolation Sea Surface Temperature (OISST).* Retrieved November 20, 2019, from https://www.ncdc.noaa.gov/oisst

NOAA Climate.gov. *Understanding climate: Antarctic sea ice extent.* Retrieved November 21, 2019, from https://www.climate.gov

Oliver, E. C. J., Donat, M. G., Burrows, M. T., Moore, P. J., Smale, D. A., Alexander, L. V., . . . Wernberg, T. (2018). Longer and more frequent marine heatwaves over the past century. *Nature Communications, 9*(1). https://doi.org/10.1038/s41467-018-03732-9

Ortiz-Ahumada, J. C., Álvarez-Borrego, S., & Gómez-Valdés, J. (2018). Effects of seasonal and interannual events on satellite-derived phytoplankton biomass and production in the

southernmost part of the California Current System during 2003-2016. *Ciencias Marinas, 44*(1), 1-20. https://doi.org/10.7773/cm.v44i1.2743

Petrou, K., Kranz, S. A., Trimborn, S., Hassler, C. S., Ameijeiras, S. B., Sackett, O., . . . Davidson, A. T. (2016, 2016/09/20/). Southern Ocean phytoplankton physiology in a changing climate. *Journal of Plant Physiology, 203*, 135-150. https://doi.org/https://doi.org/10.1016/j.jplph.2016.05.004

Pinkerton, M. (2019). Change in environmental conditions of the Southern Ocean observed by satellites and data-assimilating models between 1981 and 2019. Report presented for consideration from CCAMLR. WG-EMM-2019/39.

Polarview. Retrieved November 21, 2019, from https://www.polarview.aq/antarctic

Rohr, T., Long, M. C., Kavanaugh, M. T., Lindsay, K., & Doney, S. C. (2017). Variability in the mechanisms controlling Southern Ocean phytoplankton bloom phenology in an ocean model and satellite observations. *Global Biogeochemical Cycles, 31*(5), 922-940. https://doi.org/10.1002/2016gb005615

Sallée, J.-B., Llort, J., Tagliabue, A., & Lévy, M. (2015). Characterization of distinct bloom phenology regimes in the Southern Ocean. *ICES Journal of Marine Science, 72*(6), 1985-1998. https://doi.org/10.1093/icesjms/fsv069

Smale, D. A., Wernberg, T., Oliver, E. C. J., Thomsen, M., Harvey, B. P., Straub, S. C., . . . Moore, P. J. (2019, 2019/03/04). Marine heatwaves threaten global biodiversity and the provision of ecosystem services. *Nature Climate Change*. https://doi.org/10.1038/s41558-019-0412-1

Sokolov, S. (2008). Chlorophyll blooms in the Antarctic Zone south of Australia and New Zealand in reference to the Antarctic Circumpolar Current fronts and sea ice forcing. *Journal of Geophysical Research: Oceans, 113*(3). https://doi.org/10.1029/2007JC004329

Thomas M. K., Kremer, C. T., Klausmeier, C. A., & Litchman, E. (2012). A global pattern of thermal adaptation in marine phytoplankton. *Science, 338*(6110), 1085-1088. https://doi.org/10.1126/science.1224836

Thomsen, M. S., Mondardini, L., Alestra, T., Gerrity, S., Tait, L., South, P. M., . . . Schiel, D. R. (2019, 2019-March-06). Local Extinction of Bull Kelp (Durvillaea spp.) Due to a Marine Heatwave. *Frontiers in Marine Science, 6*(84). https://doi.org/10.3389/fmars.2019.00084

Tortell, P. D., Payne, C. D., Li, Y., Trimborn, S., Rost, B., Smith, W. O., . . . DiTullio, G. R. (2008). CO<inf>2</inf> sensitivity of Southern Ocean phytoplankton. *Geophysical Research Letters, 35*(4). https://doi.org/10.1029/2007GL032583

Townsend, D. W. (2012). *Oceanography and marine biology: an introduction to marine science*. Sunderland, Mass: Sinauer Associates.

Trainer, V. L., Moore, S. K., Hallegraeff, G., Kudela, R. M., Clement, A., Mardones, J. I., & Cochlan, W. P. (2019, 2019/05/03/). Pelagic harmful algal blooms and climate change:

Lessons from nature's experiments with extremes. *Harmful Algae*. https://doi.org/https://doi.org/10.1016/j.hal.2019.03.009

Tréguer, P., Bowler, C., Moriceau, B., Dutkiewicz, S., Gehlen, M., Aumont, O., . . . Pondaven, P. (2018). Influence of diatom diversity on the ocean biological carbon pump. *Nature Geoscience, 11*(1), 27-37. https://doi.org/10.1038/s41561-017-0028-x

Werdell, P. J., McKinna, L. I. W., Boss, E., Ackleson, S. G., Craig, S. E., Gregg, W. W., . . . Zhang, X. (2018). An overview of approaches and challenges for retrieving marine inherent optical properties from ocean color remote sensing. *Progress in Oceanography, 160*, 186-212. https://doi.org/10.1016/j.pocean.2018.01.001

Williams, R. G., & Follows, M. J. (2011). *Ocean dynamics and the carbon cycle: principles and mechanisms*. Cambridge, UK;New York;: Cambridge University Press.

Yang, J., Gong, P., Fu, R., Zhang, M., Chen, J., Liang, S., . . . Dickinson, R. (2013, 09/15/online). The role of satellite remote sensing in climate change studies. *Nature Climate Change, 3*, 875. https://doi.org/10.1038/nclimate1908

Zhang, H., Han, Z., Zhao, J., Yu, P., Hu, C., Sun, W., . . . Vetter, W. (2014, December 01). Phytoplankton and chlorophyll a relationships with ENSO in Prydz Bay, East Antarctica. *Science China Earth Sciences, 57*(12), 3073-3083. https://doi.org/10.1007/s11430-014-4939-8

Chapter Five

Synthesis and conclusions

This study added new insights into the effects of increases in warm SST anomalies and MHWs on phytoplankton distribution and abundances in the SO. First, I reviewed the current literature on phytoplankton dynamics in the SO in a context of global warming, highlighting the expected increase in frequency and intensity of MHWs. This background knowledge provided the context for my two data chapters, where I analysed impacts on chl-a from monthly SST anomalies in the Ross Sea and extreme MHWs in the SO, respectively. The review chapter also included information on the importance of SO phytoplankton, the influence of physical variables, the observed effects of climate change on the SO and its sub-zones and an overview of the predicted impacts of MHWs and climate change on SO phytoplankton communities.

5.1. Correlation analysis of sea surface temperature and chlorophyll-a concentration anomalies in the Ross Sea

For the analysis of Ross Sea data (chapter three) I used a relatively common analytical approach (Behrenfeld et al., 2006; Kitsiou & Topouzelis, 2014; Li et al., 2018; Liu et al., 2019; Macias et al., 2018; Xue at al., 2014) to correlate SST anomalies and chl-a anomalies on a pixel-by-pixel scale. The Ross Sea region was chosen because it is the most productive coastal zone of Antarctica, accounting for ~30% of total annual primary production (Deppeler & Davidson, 2017). A recent study documenting decreases in chl-a in this region (Pinkerton, 2019) warranted further research scrutiny. Arrigo et al. methodology (2008) was followed using a pixel by pixel correlation analysis between monthly SST and chl-a concentration anomalies for each month from January 1998 to December 2018, to address the following three questions:

1) Do monthly SST anomalies from 1998-2018 correlate with chlorophyll-a concentration anomalies?
2) Do correlation levels vary between regions; more specifically between the coastal (>75°S), the transition (75°S - 70°S) and open ocean (70°S - 60°S) zones?
3) Do correlations for these three zones vary systematically across monthly, seasonal and annual time scales and between El Niño and non-El Niño years?

I found many small positive and negative correlations between SST anomalies and chl-a anomalies from 1998-2018 in the Ross Sea region. The largest positive correlation was in December for the coastal zone (0.09) and the largest negative correlation was in March in the open ocean zone (-0.04). These low correlation coefficients may be due to the relatively low spatial and temporal resolution of available remote sensing images, high ice and cloud cover, and lack of *in situ* ground truth observations. Furthermore, additional variables known to influence chl-a in the SO were not controlled for, in part due to the time constraint of this study, but, more importantly, also because data are unavailable (e.g. of top-down grazing effects).

In this analysis, there was no significant effect of 'zone', perhaps because I used latitude to define the zones within the Ross Sea. Future analyses should use more temporally dynamic boundaries by defining zones based on the location of fronts, currents and sea ice extent, as these fluctuating events can have strong impacts on phytoplankton dynamics in the SO (Boyd et al., 2000; Knox, 2007).

However, I did find that correlations varied systematically across different time scales. A highly significant difference in correlation coefficients ($p < 0.001$) occurred between March and December and between autumn and summer. Furthermore, a significant interaction effect was found between zone and years ($p = 0.030$) as well as a single factor effect of year ($p = 0.035$). However, even though past research have shown that El Niño years affect phytoplankton throughout most of the global ocean (Racault et al., 2017), I found no significant differences in correlation coefficients between El Niño and non-El Niño years in the Ross Sea.

The temporal (monthly) and spatial (9 km) resolution of this 20 year dataset could have masked short term spikes in SST if they were cancelled out by subsequent drops in SST during the same month (Hobday et al., 2016). This problem, combined with the high spatio-temporal variability of chl-a, suggest that monthly climatology data may not be adequate to address the three research questions listed above (Frenger et al., 2018). Furthermore, an 'anomaly' was here calculated by subtracting the climatological monthly mean from the observation in a given month for each pixel. In future analyses, an anomaly that accounts for more specific local and temporal ranges of SST could be applied instead to ensure that average SST and chl-a on smaller scales are not masked (Dunstan et al., 2018). These limitations suggest that standard remotely sensed data and analytical approaches used to correlate SST anomalies with chl-a anomalies in the Ross Sea region have important limitations.

5.2. Marine heatwave remote sensing analysis

For the broader analysis of impacts of MHWs on the entire Southern Ocean (chapter four), the limitations noted above were partly resolved. The 16 year data set was based on a higher resolution data set as the Aqua MODIS imagery report pixels on a 1 km grid with daily coverage. Furthermore, analysis of SST anomalies was refined in a context of MHWs as defined by Hobday et al. (2016) and further applied in the literature (Oliver et al., 2018; Smale et al., 2019). This MHW definition does not assume any particular drivers of chl-a and it accounts for specific regional and local SST variability. To my knowledge, this is a first attempt to apply the MHW approach across the entire SO to gain insight into effects on primary production. This research aimed to address two key questions in relation to MHWs and their influence on SO primary productivity: 1) do extreme MHWs affect chl-a concentration in the SO - and if so, 2) do effects vary between regions characterised by different sea surface temperatures and levels of winter ice cover?

The results from Anova and correlation analyses found significant differences between chl-a concentrations within the centre of MHWs compared to their surrounding 'control' regions 250 and 500 km away. Furthermore, these effects were stronger at colder sites (coastal and seasonal sea ice covered zones) compared to warmer sites (permanently open ocean and sub-Antarctic zones). These results conformed with previous studies (Boyd, 2000;

Moore & Abbott, 2000) and suggests that extreme MHWs can have important effects on chl-a concentrations in the SO.

Interestingly, my findings differed from results from temperate, subtropical and tropical regions where SST anomalies typically cause decreases in phytoplankton abundances (Gómez-Ocampo et al., 2018; Trainer et al., 2019). However, my results are in agreement with Feng et al. (2015) and align with positive effects of SST anomalies on chl-a as documented from the Arctic region (IPCC, 2019). Indeed, the positive effects of increased SST (here documented for extreme summertime MHWs) on phytoplankton abundance may exceed the negative effects of increased SST documented from temperate and tropical latitudes. Increasing SST may therefore be of particular importance in regulating phytoplankton biomass and production in the SO, perhaps until a tipping point is reached. For example, it is possible that extreme MHWs, when superimposed on slower and more gradual climate change, eventually exceed the thermal limit for growth and reproduction of the phytoplankton species that currently dominate SO communities.

5.3. General limitations of remote sensing

Limitations of remote sensing, relevant to my analyses, have been extensively covered in the literature. For example, remote sensing involving a single sensor on a single satellite increase the risk of sensor biases (Yang et al., 2013). More specifically, if data has not been compared across different instruments, biases can be difficult to detect. Furthermore, there can be uncertainties associated with retrieval algorithms (Blondeau-Patissier, Gower, Dekker, Phinn, & Brando, 2014; Yang et al., 2013), which convert the electromagnetic reflectance to variables such as chl-a concentration and SST (Yang et al., 2013). Currently, band-ratio algorithms are well-developed for open waters but are more limited in complex turbid coastal waters (Blondeau-Patissier et al., 2014). Therefore, data from my analyses should be interpreted cautiously as sensor measurements are constantly being improved. My research was based on current remote sensing techniques for both chl-a and SST data, but this type of analysis is nevertheless likely to be much improved in the near-future as sensors continue to become more advanced and spatio-temporal resolution continue to increase.

In addition to improvements in sensors and retrieval algorithms, high quality validation of data can also assist in instrument calibration, tuning of algorithms and decrease uncertainties (Yang et al., 2013). For example, the OISST data product used in my analyses is based on measurements across various platforms to retrieve SST, including satellites, ships and buoys from a global grid. Various interpolation methods are used to create spatially complete SST maps, although in the SO the underpinning *in situ* observations are very sparse and interpolated maps are therefore less reliable. Given that the SO remains an important region for climate change research with significant knowledge gaps in ocean colour research, more research effort should focus on satellite validation and *in situ* observations.

5.4. Final conclusion

This study aimed to improve knowledge of how warm SST anomalies and MHWs affects phytoplankton distribution and abundance in the SO. First, phytoplankton dynamics in the SO were reviewed based on the current literature, and possible impacts of MHWs on

phytoplankton communities were discussed. Two data chapters then analysed for impacts on warm SST anomalies and extreme MHWs on chl-a concentrations. First, a standard approach was used to correlate SST- and chl-a-anomalies on a pixel-by-pixel scale for the Ross Sea. Second, extreme summertime MHW events were identified throughout the SO and correlated to chl-a concentrations using a 'control vs. impact' experimental design.

I found that the traditional pixel-by-pixel correlation analysis, based on monthly images and low spatial resolution, had major limitations. For example, short term spikes in SST and the monthly temporal resolution in image acquisition, are likely to mask ecologically important short-term fluctuations in chl-a concentrations, a problem that is exaggerated when cloud or ice cover persisted for the majority of a month. This analytical method was adopted from various ocean colour studies in temperate, sub-tropical and tropical latitudes (Behrenfeld et al., 2006; Kitsiou & Topouzelis, 2014; Li et al., 2018; Liu et al., 2019; Macias, Stips, Garcia-Gorriz, & Dosio, 2018; Xue, Dong, & Fan, 2014) but appears to be less useful for the Ross Sea that often have high cloud and ice cover. However, the analysis based on higher resolution images and the MHW definition was more successful in identifying effects of short-term variability in SST on chl-a concentrations at the regional and local scale (Figure 5.1), highlighting that phytoplankton can respond rapidly to changes in the physical environment.

To maintain consistency, the MHW definition used here and in other studies worldwide (Oliver et al., 2018; Smale et al., 2019) should be adopted in future studies from the SO. Importantly, effects from short term and punctuated MHWs - when superimposed on effects from more gradual climate changes - could reach a critical tipping point in the SO. For example, if SO phytoplankton species reach their thermal maximum for growth and reproduction, dramatic changes could occur to the entire base of the Antarctic food web, with wide-ranging cascading effects on higher trophic levels. Therefore, it remains a fundamental challenge to study, understand and model the distribution and abundances of phytoplankton communities in the SO, in a context of long-term climate change and superimposed MHWs.

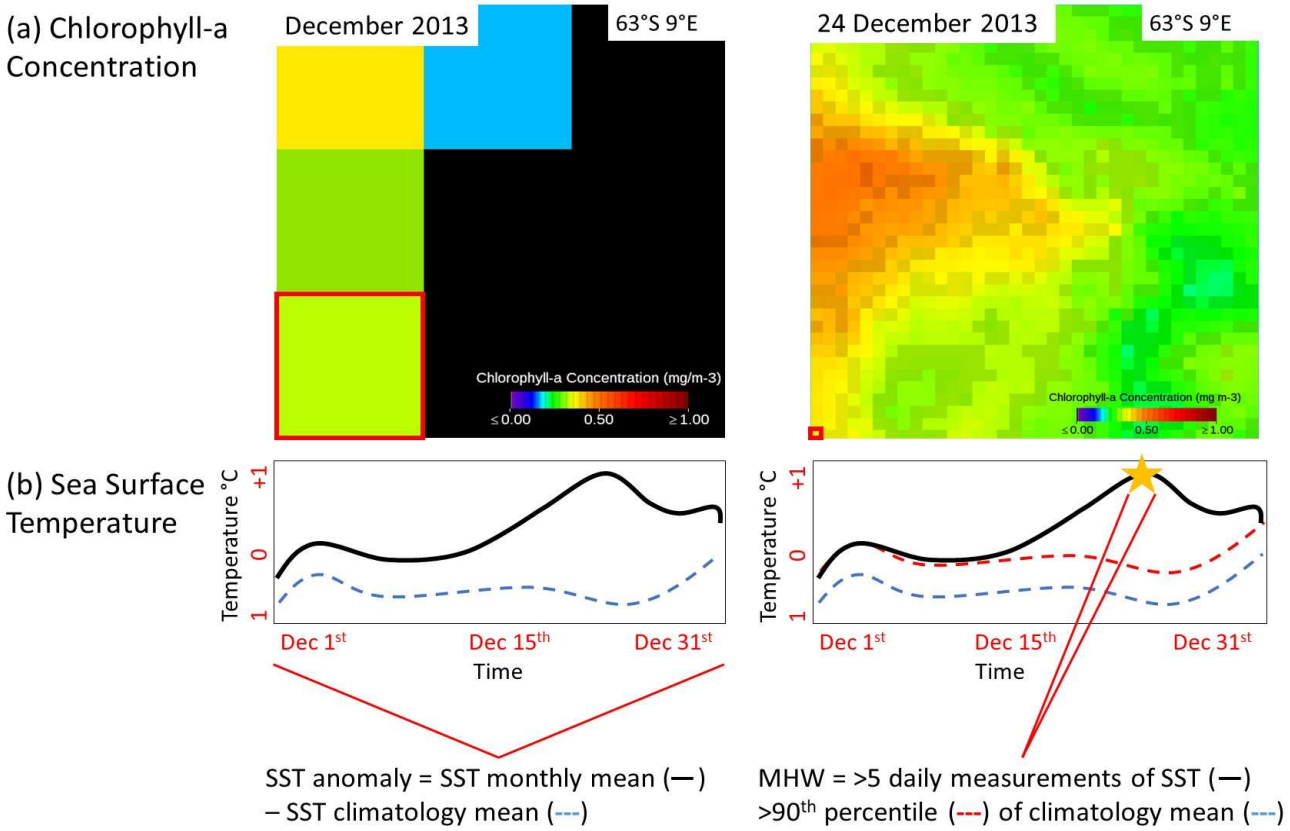

Figure 5.1. Comparison of the spatial and temporal resolution for data sets used in the Ross Sea analysis (Chapter three, left) and the broader Southern Ocean analysis (Chapter four, right). The top figures (a) shows the difference in spatial resolution of chlorophyll-a concentration. The combined SeaWiFS and MODIS imagery used in the Ross Sea analysis (top left) has a spatial resolution of 9 km where black pixels indicate lack of measurement due to cloud or ice cover (which typically occurred for the majority of the month). The MODIS imagery used in the broader Southern Ocean analysis (top right) has a spatial resolution of 1 km. The data set used in the broader Southern Ocean captures significantly more variability in chlorophyll-a concentration across the same area. The lower figures (b) shows the difference in temporal resolution in sea surface temperature. The Ross Sea analysis (lower left) uses mean monthly SST to determine presence or absence of an anomaly based on the mean climatology. The broader Southern Ocean analysis (lower right) uses daily SST measurements to determine the presence or absence of a MHW (identified by the 90th percentile threshold of SST being exceeded for >5 days). The data set used for analysis of MHW impacts captures significantly more intense short-term spikes in SST due to daily coverage.

References

Arrigo, K. R., van Dijken, G. L., & Bushinsky, S. (2008). Primary production in the Southern Ocean, 1997-2006. *Journal of Geophysical Research: Oceans, 113*(8). https://doi.org/10.1029/2007JC004551

Behrenfeld, M. J., O'Malley, R. T., Siegel, D. A., McClain, C. R., Sarmiento, J. L., Feldman, G. C., . . . Boss, E. S. (2006). Climate-driven trends in contemporary ocean productivity. *Nature, 444*(7120), 752-755. https://doi.org/10.1038/nature05317

Blondeau-Patissier, D., Gower, J. F. R., Dekker, A. G., Phinn, S. R., & Brando, V. E. (2014, 2014/04/01/). A review of ocean color remote sensing methods and statistical techniques for the detection, mapping and analysis of phytoplankton blooms in coastal and open oceans. *Progress in Oceanography, 123*, 123-144. https://doi.org/https://doi.org/10.1016/j.pocean.2013.12.008

Boyd, P.W., Watson, A. J., Law, C. S., Abraham, E. R., Trull, T., Murdoch, R., . . . Zeldis, J. (2000). A mesoscale phytoplankton bloom in the polar Southern Ocean stimulated by iron fertilization. *Nature, 407*(6805), 695-702. https://doi.org/10.1038/35037500

Deppeler, S. L., & Davidson, A. T. (2017). Southern Ocean phytoplankton in a changing climate. *Frontiers in Marine Science, 4*(FEB). https://doi.org/10.3389/fmars.2017.00040

Dunstan, P. K., Foster, S. D., King, E., Risbey, J., O'Kane, T. J., Monselesan, D., . . Thompson, P. A. (2018, 2018/10/02). Global patterns of change and variation in sea surface temperature and chlorophyll a. *Scientific Reports, 8*(1), 14624. https://doi.org/10.1038/s41598-018-33057-y

Feng, J., Durant, J. M., Stige, L. C., Hessen, D. O., Hjermann, D. Ø., Zhu, L., . . . Stenseth, N. C. (2015). Contrasting correlation patterns between environmental factors and chlorophyll levels in the global ocean. *Global Biogeochemical Cycles, 29*(12), 2095-2107. https://doi.org/10.1002/2015gb005216

Frenger, I., Münnich, M., & Gruber, N. (2018). Imprint of Southern Ocean mesoscale eddies on chlorophyll. *Biogeosciences, 15*(15), 4781-4798. https://doi.org/10.5194/bg-15-4781-2018

Frölicher, T. L., Fischer, E. M., & Gruber, N. (2018). Marine heatwaves under global warming. *Nature, 560*(7718), 360-364. https://doi.org/10.1038/s41586-018-0383-9

Gómez-Ocampo, E., Gaxiola-Castro, G., Durazo, R., & Beier, E. (2018). Effects of the 2013-2016 warm anomalies on the California Current phytoplankton. *Deep-Sea Research Part II: Topical Studies in Oceanography, 151*, 64-76. https://doi.org/10.1016/j.dsr2.2017.01.005

Hobday, A. J., Alexander, L. V., Perkins, S. E., Smale, D. A., Straub, S. C., Oliver, E. C. J., . . . Wernberg, T. (2016). A hierarchical approach to defining marine heatwaves. *Progress in Oceanography, 141*, 227-238. https://doi.org/10.1016/j.pocean.2015.12.014

Hobday, A. J., Oliver, E. C. J., Gupta, A. S., Benthuysen, J. A., Burrows, M. T., Donat, M. G., . . . Smale, D. A. (2018). Categorizing and naming marine heatwaves. *Oceanography, 31*(2 Special Issue), 162-173. https://doi.org/10.5670/oceanog.2018.205

Holbrook, N. J., Scannell, H. A., Sen Gupta, A., Benthuysen, J. A., Feng, M., Oliver, E. C. J., . . . Wernberg, T. (2019, 2019/06/14). A global assessment of marine heatwaves and their drivers. *Nature Communications, 10*(1), 2624. https://doi.org/10.1038/s41467-019-10206-z

IPCC, 2019: IPCC Special Report on the Ocean and Cryosphere in a Changing Climate [H.-O. Pörtner, D.C. Roberts, V. Masson-Delmotte, P. Zhai, M. Tignor, E. Poloczanska, K. Mintenbeck, A. Alegría, M. Nicolai, A. Okem, J. Petzold, B. Rama, N.M. Weyer (eds.)]. In press.

Kitsiou, D., & Topouzelis, K. (2014, 01/01). Correlation between chlorophyll a concentration and sea surface temperature in the eastern mediterranean sea using gis and satellite data. *Fresenius Environmental Bulletin, 23*, 2919-2925.

Knox, G. A. (2007). *Biology of the Southern Ocean* (2nd ed.). Boca Raton: CRC Press/Taylor & Francis.

Li, Y., Ji, R., Jenouvrier, S., Jin, M., & Stroeve, J. (2016). Synchronicity between ice retreat and phytoplankton bloom in circum-Antarctic polynyas. *Geophysical Research Letters, 43*(5), 2086-2093. https://doi.org/10.1002/2016GL067937

Liu, C., Sun, Q., Xing, Q., Wang, S., Tang, D., Zhu, D., & Xing, X. (2019). Variability in phytoplankton biomass and effects of sea surface temperature based on satellite data from the Yellow Sea, China. *PloS one, 14*(8), e0220058-e0220058. https://doi.org/10.1371/journal.pone.0220058

Macias, D., Stips, A., Garcia-Gorriz, E., & Dosio, A. (2018). Hydrological and biogeochemical response of the Mediterranean Sea to freshwater flow changes for the end of the 21st century. *PloS one, 13*(2), e0192174. https://doi.org/10.1371/journal.pone.0192174

Moore, J. K., & Abbott, M. R. (2000). Phytoplankton chlorophyll distributions and primary production in the Southern Ocean. *Journal of Geophysical Research: Oceans, 105*(C12), 28709-28722.

Oliver, E. C. J., Donat, M. G., Burrows, M. T., Moore, P. J., Smale, D. A., Alexander, L. V., . . . Wernberg, T. (2018). Longer and more frequent marine heatwaves over the past century. *Nature Communications, 9*(1). https://doi.org/10.1038/s41467-018-03732-9

Pinkerton, M. (2019). Change in environmental conditions of the Southern Ocean observed by satellites and data-assimilating models between 1981 and 2019. Report presented for consideration from CCAMLR. WG-EMM-2019/39.

Racault, M.-F., Sathyendranath, S., Brewin, R. J. W., Raitsos, D. E., Jackson, T., & Platt, T. (2017, 2017-May-08). Impact of El Niño Variability on Oceanic Phytoplankton. *Frontiers in Marine Science, 4*(133). https://doi.org/10.3389/fmars.2017.00133

Smale, D. A., Wernberg, T., Oliver, E. C. J., Thomsen, M., Harvey, B. P., Straub, S. C., . . . Moore, P. J. (2019, 2019/03/04). Marine heatwaves threaten global biodiversity and the provision of ecosystem services. *Nature Climate Change*. https://doi.org/10.1038/s41558-019-0412-1

Trainer, V. L., Moore, S. K., Hallegraeff, G., Kudela, R. M., Clement, A., Mardones, J. I., & Cochlan, W. P. (2019, 2019/05/03/). Pelagic harmful algal blooms and climate change: Lessons from nature's experiments with extremes. *Harmful Algae*. https://doi.org/https://doi.org/10.1016/j.hal.2019.03.009

Xue, C. J., Dong, Q., & Fan, X. (2014). Spatiotemporal association patterns of multiple parameters in the northwestern Pacific Ocean and their relationships with ENSO. *International Journal of Remote Sensing, 35*(11-12), 4467-4483. https://doi.org/10.1080/01431161.2014.916436

Yang, J., Gong, P., Fu, R., Zhang, M., Chen, J., Liang, S., . . . Dickinson, R. (2013, 09/15/online). The role of satellite remote sensing in climate change studies. *Nature Climate Change, 3*, 875. https://doi.org/10.1038/nclimate1908